Vol. 57 JUNE, 1953 No. 6

1543 3
5.00

THE JOURNAL OF PHYSICAL CHEMISTRY

(Registered in U. S. Patent Office)

Founded by Wilder D. Bancroft

Symposium on Liquid Ammonia Chemistry, Atlantic City, N. J., September, 1952

Founded by Wilder D. Bancroft

THE JOURNAL OF PHYSICAL CHEMISTRY

(Registered in U. S. Patent Office)

W. ALBERT NOYES, JR., EDITOR

ALLEN D. BLISS — ASSISTANT EDITORS — ARTHUR C. BOND

EDITORIAL BOARD

R. P. BELL
E. J. BOWEN
G. E. BOYD
MILTON BURTON
R. E. CONNICK
E. A. HAUSER
C. N. HINSHELWOOD
J. W. KENNEDY
S. C. LIND
W. O. MILLIGAN
E. A. MOELWYN-HUGHES

Published monthly (except July, August and September) by the American Chemical Society at 20th and Northampton Sts., Easton, Pa.

Entered as second-class matter at the Post Office at Easton, Pennsylvania.

The *Journal of Physical Chemistry* is devoted to the publication of selected symposia in the broad field of physical chemistry and to other contributed papers.

Manuscripts originating in the British Isles, Europe and Africa should be sent to F. C. Tompkins, The Faraday Society, 6 Gray's Inn Square, London W. C. 1, England.

Manuscripts originating elsewhere should be sent to W. Albert Noyes, Jr., Department of Chemistry, University of Rochester, Rochester 3, N. Y.

Correspondence regarding accepted copy, proofs and reprints should be directed to Assistant Editor, Allen D. Bliss, Department of Chemistry, Simmons College, 300 The Fenway, Boston 15, Mass.

Business Office: American Chemical Society, 1155 Sixteenth St., N. W., Washington 6, D. C.

Advertising Office: American Chemical Society, 332 West 42nd St., New York 36, N. Y.

Articles must be submitted in duplicate, typed and double spaced. They should have at the beginning a brief Abstract, in no case exceeding 300 words. Original drawings should accompany the manuscript. Lettering at the sides of graphs (black on white or blue) may be pencilled in, and will be typeset. Figures and tables should be held to a minimum consistent with adequate presentation of information. Photographs will not be printed on glossy paper except by special arrangement. All footnotes and references to the literature should be numbered consecutively and placed on the manuscript at the proper places. Initials of authors referred to in citations should be given. Nomenclature should conform to that used in *Chemical Abstracts*, mathematical characters marked for italic, Greek letters carefully made or annotated, and subscripts and superscripts clearly shown. Articles should be written as briefly as possible consistent with clarity and should avoid historical background unnecessary for specialists.

Symposium papers should be sent in all cases to Secretaries of Divisions sponsoring the symposium, who will be responsible for their transmittal to the Editor. The Secretary of the Division by agreement with the Editor will specify a time after which symposium papers cannot be accepted. The Editor reserves the right to refuse to publish symposium articles, for valid scientific reasons. Each symposium paper may not exceed four printed pages (about sixteen double spaced typewritten pages) in length except by prior arrangement with the Editor.

Remittances and orders for subscriptions and for single copies, notices of changes of address and new professional connections, and claims for missing numbers should be sent to the American Chemical Society, 1155 Sixteenth St., N. W., Washington 6, D. C. Changes of address for the *Journal of Physical Chemistry* must be received on or before the 30th of the preceding month.

Claims for missing numbers will not be allowed (1) if received more than sixty days from date of issue (because of delivery hazards, no claims can be honored from subscribers in Central Europe, Asia, or Pacific Islands other than Hawaii), (2) if loss was due to failure of notice of change of address to be received before the date specified in the preceding paragraph, or (3) if the reason for the claim is "missing from files."

Subscription Rates: to members of the American Chemical Society, $8.00 for 1 year, $15.00 for 2 years, $22.00 for 3 years; to nonmembers, $10.00 for 1 year, $18.00 for 2 years, $26.00 for 3 years. Postage free to countries in the Pan American Union; Canada, $0.40; all other countries, $1.20. Single copies, $1.25; foreign postage, $0.15; Canadian postage, $0.05.

The American Chemical Society and the Editors of the *Journal of Physical Chemistry* assume no responsibility for the statements and opinions advanced by contributors to THIS JOURNAL.

The American Chemical Society also publishes *Journal of the American Chemical Society, Chemical Abstracts, Industrial and Engineering Chemistry, Chemical and Engineering News, Analytical Chemistry*, and *Journal of Agricultural and Food Chemistry*. Rates on request.

THE JOURNAL OF
PHYSICAL CHEMISTRY

(Registered in U. S. Patent Office) (Copyright, 1953, by the American Chemical Society)

Founded by Wilder D. Bancroft

VOLUME 57 JUNE 30, 1953 NUMBER 6

SYMPOSIUM ON LIQUID AMMONIA CHEMISTRY. INTRODUCTORY REMARKS

BY JACOB KLEINBERG

Department of Chemistry, University of Kansas, Lawrence, Kansas

Received November 28, 1952

The last symposium dealing with liquid ammonia chemistry was held in Milwaukee, Wisconsin, in September, 1938. Three papers were presented at that meeting. The current symposium consists of eight papers on a wide variety of physical and inorganic aspects of the subject. Only the time limitation set by the Division has kept the contributions to this number, for there are at least a dozen laboratories over the country where these aspects of liquid ammonia chemistry are being vigorously and intelligently investigated.

In the opening paper Hutchison discusses the paramagnetic absorption resonance in liquid ammonia solutions of the alkali metals. This report is the first one concerned with the direct observation of the unpaired electrons in the alkali metal solutions and constitutes an important contribution to the elucidation of the nature of such solutions. The paper by Coulter on the thermochemistry of the alkali and alkaline earth metals and their halides in ammonia provides data useful in the interpretation of inorganic chemistry in this solvent. Ogg discusses the mechanism of amide formation in liquid ammonia solutions of alkali metals and also offers experimental evidence for the formation of atomic hydrogen as a transient intermediate in the reaction of such solutions with dissolved ammonium salts. The contribution by Evers and Finn deals with the electrolysis of alkali metal diphosphides and dihydrophosphides in liquid ammonia and particularly with the nature of the anode reactions. Scott reports the reactions of the unstable light metal carbonyls, which are prepared in liquid ammonia, with a variety of proton-donating reagents. A paper by Laitinen and McElroy extends previous work on polarography in liquid ammonia and reports the characteristics of the reduction of several other ions at the dropping mercury electrode. A continuation of the pioneer work of Watt and co-workers on potentiometric titrations with potassium in liquid ammonia describes experiments with metal ions of the aluminum family. The three distinct "end-points" obtained in the titration of aluminum(III) iodide are tentatively interpreted as evidence for the existence of lower oxidation states of aluminum in liquid ammonia, although other explanations are not excluded. The final paper by Davidson and Kleinberg emphasizes the usefulness of liquid ammonia as a medium for the preparation of compounds containing elements in unfamiliar oxidation states.

It is fitting that this symposium be dedicated to Professor Charles A. Kraus, the only surviving member of the triumvirate of Cady, Franklin and Kraus, the pioneers of liquid ammonia research in this country. It is primarily due to the investigations of these men and the inspiration they gave to succeeding workers that liquid ammonia has been the non-aqueous solvent most thoroughly studied by the physical and the inorganic chemist.

PARAMAGNETIC RESONANCE ABSORPTION IN SOLUTIONS OF POTASSIUM IN LIQUID AMMONIA*

BY CLYDE A. HUTCHISON, JR.

Institute for Nuclear Studies, and Department of Chemistry, University of Chicago, Chicago, Illinois

Received November 28, 1952

The application of the theory and techniques of electronic magnetic resonance to the study of the paramagnetism of solutions of K in liquid NH_3 is described.

1. Paramagnetic Resonance Absorption. 1.1. Description of the Phenomenon. 1.1.1. Spectroscopic Description.—Many of the forms of matter which are of interest to the chemist contain elemental magnets as fundamental units in their structure. These magnets may be molecules with unpaired electrons such as O_2 or NO or organic free radicals; magnetic ions such as praseodymium or uranium ions in crystals of salts of these elements; trapped electrons such as those produced by the irradiation of solids with γ-rays; or magnetic nuclei such as the protons in water. Whatever the nature of these magnets they have in common the property that they possess a rotating or spinning electric charge which produces a magnetic moment which may be oriented in various directions in a magnetic field. Associated with a given orientation in the magnetic field is the magnetic energy, $-\vec{\mu}\cdot\vec{H}$. $\vec{\mu}$ is the magnetic moment and $\vec{H}$ is the magnetic field. The angular momentum of such an electric charge can assume only a discrete set of orientations with respect to a preferred direction in space such as that of $\vec{H}$. Consequently, since it is the angular momentum of the charge that determines the moment, the moment can have only a finite set of orientations with respect to the magnetic field and a finite set of magnetic energy levels results. For orbital motion of an electron the energies are $M_L\beta H$ where M_L is zero or an integer + or − (quantum number), β is the Bohr magneton and H is the magnitude of $\vec{H}$. For electron spin the possible levels are $2M_s\beta H$ where M_s is the spin quantum number. For systems in which both orbital and spin angular momentum are present the situation may be quite complicated but in many cases the magnetic energy levels are given by $gM_J\beta H$ where M_J is a total angular momentum quantum number and g is the spectroscopic splitting factor which we have seen is 1 for purely orbital and 2 for purely spin angular momentum, and which may assume a variety of values for various combinations of the two. (If $Jh/2\pi$ is the total angular momentum then its component along the field may have $2J + 1$ values designated by $M_J = -J, -J + 1, \cdots, J$). Such magnetic energy levels are shown on the left side of Fig. 1 for a system with a magnetic degeneracy of 4.

The elemental magnets in a magnetic field distribute themselves in these magnetic energy levels according to a Boltzmann distribution and thus we have more magnets pointing one way than another with consequent magnetization of the substance. This produces a positive magnetic susceptibility in a static magnetic field. If now radiation is allowed to interact with the magnetized substance transitions may be induced between the magnetic levels. Selection rules allow M to change by only one unit. For example in an experiment in which the frequency, ν, of the radiation is kept constant and the magnetic field intensity is varied, when H reaches such a value that

$$h\nu = g\beta H \text{ or } \nu/H = g\beta/h$$

i.e., the quantum of radiation, $h\nu$, just matches the separation, $g\beta H$, between adjacent magnetic levels, then energy will be absorbed by the jumping of systems from lower to upper levels. Magnetic dipole transitions are induced by the alternating magnetic field of the radiation. This situation is shown graphically on the left side of Fig. 1. This phenomenon is known as magnetic resonance absorption. We will here restrict our attention to electronic magnetic resonance absorption in normal paramagnetic substances. We will also limit ourselves to a consideration of resonance in condensed phases.

1.1.2. **Classical Macroscopic Description.**—Descriptions of the paramagnetic resonance phenomenon other than the spectroscopic one just given may be offered. A classical macroscopic description gives considerable insight into the situation. If we have a magnetization, $\vec{M}$, associated with an angular momentum per unit volume, $\vec{J}$, we may write the equation of motion in a static magnetic field

$$\mathrm{d}\vec{J}/\mathrm{d}t = \vec{M} \times \vec{H}$$

which equates the time rate of change of the angular momentum to the torque exerted by the magnetic field. We may write $M/J = \gamma$ where γ is a constant, the gyromagnetic ratio. The equation of motion then becomes

$$\mathrm{d}\vec{M}/\mathrm{d}t = \gamma\vec{M} \times \vec{H}$$

whose steady state solutions give a precessional type motion as the normal mode. The frequency is found to be

$$2\pi\nu = \gamma H$$

Consequently if the precessing system is subjected simultaneously to an alternating magnetic field, when the normal frequency, $\nu = \gamma H/2\pi$, just matches the frequency of the alternating field the system will be resonant and large energy absorptions may occur. It is clear that from this viewpoint γ plays the same role as did $2\pi g\beta/h$ in the previous treatment.

1.1.3. **Description in Terms of Susceptibility.**—Also one may think of the paramagnetic resonance phenomenon in terms of a high frequency magnetic susceptibility. As is true of other a.c. quantities the magnetic susceptibility in an alternating field is best regarded as a sum of a real and an imaginary part. $\chi = \chi' - i\chi''$. The real part, χ', corresponds to the in phase component and the imaginary part,

(*) This work was assisted by the O. N. R.

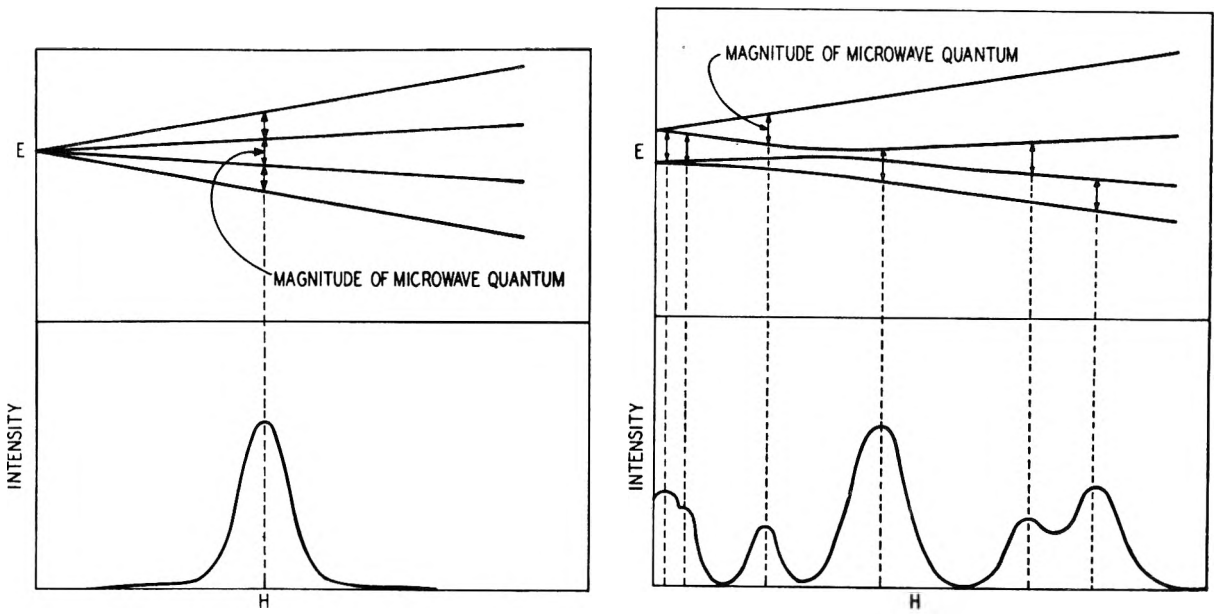

Fig. 1.—Energy and intensity of absorption as a function of magnetic field strength.

χ'', to the out of the phase component of the susceptibility. The magnetization lags the magnetizing field and the power loss or absorption of energy is proportional to χ''. In the vicinity of a resonant frequency χ' and χ'' may become very large and there are, just as in the case of the electric susceptibility or refractive index in the vicinity of an optical absorption, large dispersions and absorptions.

1.1.4. **Numerical Magnitudes.**—We have seen that the resonance condition exists when $\nu/H = g\beta/h$. For $g = 2$, as is the case for electron spin, $\nu/H = 2.800$ mc. sec.$^{-1}$ gauss^{-1}. For a field of the sort conveniently obtainable with a small iron electromagnet of say 3000 to 8000 gauss we therefore require frequencies of radiation roughly in the range of 9000 to 25,000 mc. sec.$^{-1}$. These are common radar frequencies and the apparatus needed for generating and using them is readily available. On the other hand for fields of a few gauss obtainable with small solenoids or Helmholtz coils the frequencies lie in the conventional short wave bands.

1.1.5. **Interactions.**—Since we are dealing with condensed phases the interactions of the elementary magnets with their surroundings in the structure in which they are imbedded are dominant in determining the general features of the paramagnetic resonance absorption other than the resonance position which we have already discussed. There are interactions which lead to broadening of the absorption line and there are interactions which lead to fine structure in the absorption line.

In the first place it is clear that the radiation will induce transitions from lower to upper levels (absorption) with the same probability as transitions from upper to lower levels (emission). Initially there is a net absorption of energy because the Boltzmann distribution places more systems in the lower than the upper levels. This condition cannot be maintained, however, unless there is available some non-radiative relaxation mechanism to return magnetically excited systems to their ground state, *i.e.*, to convert the magnetic energy to thermal vibrations of the structure. If such an interaction with the surroundings does not exist the resonance will be unobservable due to the fact that the levels will very quickly become equally populated. On the other hand, if the relaxation mechanism is too efficient the situation may be compared with a strongly damped oscillator in which the resonance becomes very broad. In the extreme case the resonance may become too broad for observation. In many cases of electronic resonance the relaxation mechanism is such as to permit observation of the resonance without undue broadening.

Also it must be remembered that the elementary magnets will interact magnetically with their magnetic neighbors in the structure. The external field necessary to produce resonance in a given elementary magnet will depend on the local magnetic field present in its vicinity. Since there is a Boltzmann distribution in the alignment of neighbors there will be a variety of external fields which will produce resonance conditions at some points in the substance. This dipole–dipole width is of the order of the magnitude of the local fields which may amount to several hundred or several thousand gauss.

There are also interactions which lead to fine structure and multiple absorptions. One of these is due to the electric fields which exist because of neighboring ions or water dipoles. Such a situation is described in the right side of Fig. 1. Degeneracy may be removed at zero magnetic field strength by these electric fields. (If there is an odd number of electrons in the magnetic system then the electric field alone can never remove all the degeneracy. In the system depicted for example which may be regarded as one with spin of 3/2 there is twofold degeneracy remaining for each level.) When the magnetic field is added the behavior of the magnetic levels is in general no longer linear and the selection rules do not hold. There may consequently be a variety of field strengths at which the quantum of radiation matches the separation between levels and paramagnetic resonance absorption occurs.

Other interactions leading to fine structure are the magnetic interactions with the magnetic nuclei in the structure containing the electronic magnets.

There may also exist various effects which tend to minimize the results of the perturbations by the local fields and thus make the absorption peaks narrower than would otherwise be expected. One of these is the quantum mechanical exchange interaction between neighboring electronic systems. Another is motion of the elementary magnets through the structure. Both of these effects tend to expose a given magnet to fields which vary in time in such a way as to average out or partially cancel each other's effects. The resonances in crystals may be hundreds of gauss wide at half-height. When, however, motion of the elemental magnets becomes possible as, for example, when the crystal is dissolved in water the peaks may be only tens of gauss wide.

1.2. Comparison with Magnetic Measurements in Static Fields.—It is interesting to compare the types of information on chemical systems obtainable by means of paramagnetic resonance absorption and by more conventional magnetic techniques using only static fields. Two important differences may be noted.

Firstly it will be seen that whereas conventional measurements of magnetic susceptibility give statistically averaged information on systems in a variety of energy states the resonance phenomenon

gives detailed information on the individual states. One may for example by the latter method determine in detail the effects of the electrostatic field in the crystal on the electronic states of paramagnetic species. Or one may by observing the magnetic interactions of the odd electron in a free radical with magnetic nuclei in the radical get a detailed insight into the behavior of the electron. This information would be gained only indirectly on the basis of a statistical model from static susceptibility data.

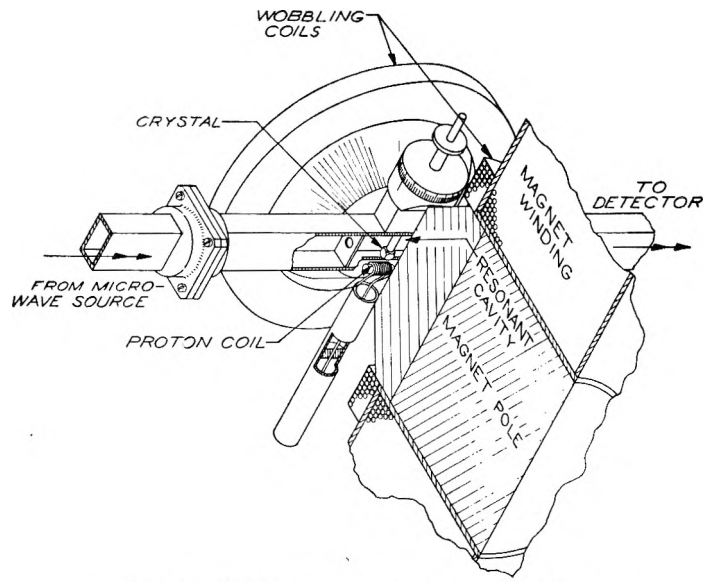

Fig. 2.—High frequency microwave apparatus.

Secondly since the electronic paramagnetic resonance absorption is peculiar to the unpaired electrons in a substance one may measure the paramagnetism of such a system exclusive of its diamagnetism. In a conventional measurement of magnetic susceptibilities one measures the sum of the oppositely directed forces arising from the diamagnetic and paramagnetic susceptibilities. The difficulties encountered in many systems of chemical interest are twofold: (1) relatively very large amounts of diamagnetic material are usually present and this may largely obscure the paramagnetism; (2) the diamagnetism of the paramagnetic species itself must be known and there is usually no reliable method of estimating or measuring its value. Difficulty (1) may frequently be eliminated by proper design of experiment but difficulty (2) is more fundamental. The method of paramagnetic resonance absorption avoids this difficulty and enables one to observe and count the paramagnetic absorbers directly. Also comparison of the results of the high frequency and of the static measurements enables one to know the amount of diamagnetism. The fundamental relationship involved is the general Kronig-Kramers relation.

$$\chi = \frac{2}{\pi}\int_0^\infty \frac{\chi''(\nu)}{\nu}d\nu$$

in which χ is the paramagnetic part of the static susceptibility. This is the relation between the static susceptibility and the integral of the power absorbed in a resonance absorption. Actually our experiments are carried out at constant ν and variable H but the relationship may be transformed so as to be suitable for describing such an experiment and shows that the paramagnetic part of the static susceptibility is proportional to the area under the curve of absorption *versus* field strength. Hence these areas are a direct measure of the number of paramagnetic absorbers.

1.3. **Experimental Methods.**—In the case of a magnetic resonance in a crystalline paramagnetic salt in which the resonance may be several hundreds of gauss wide and in which the electrostatic fields may result in peaks ranging over several thousand gauss it is necessary to make observations at microwave frequencies. It is also clear that the intensity of the resonance will be greater at the higher frequencies. For two magnetic energy levels separated by $g\beta H$ the Boltzmann distribution requires the ratio of the numbers of systems in the two states to be $e^{-g\beta H/kT}$. Even at fields of 10^4 gauss $g\beta H/k$ is only about 1°K. It is therefore clear that for a T of 300°K. we may write the difference in the population of the two states as $g\beta H/kT$. It is this difference which determines the net absorption of power. Hence one desires large H and hence large ν for the detection of small amounts of paramagnetic species.

In Fig. 2 a microwave apparatus that has been used in our laboratory is shown schematically. The sample is placed in a resonant cavity through which passes the radiation. The wobbling coils serve the purpose of modulating the magnetic field, thereby giving an alternating component to the magnetic signal so that a.c. amplifiers may be used. The proton coil is part of a system which measures the magnetic field strength making use of the nuclear magnetic resonance of the protons in water.

If one is examining a narrow resonance and is not interested in the greatest sensitivity he may use the low field of a solenoid or Helmholtz coils to remove the magnetic degeneracy since he may quite easily obtain great homogeneity in this case. This will enable him to make observations of the details of the line shape which otherwise might be obscured by field inhomogeneities.

An apparatus for low field and low frequency measurements is shown schematically in Fig. 3. This is the apparatus which we have employed for our measurements on solutions of K in liquid NH_3. H is the static field and H_1 the *rf* field. The solenoid may be oriented so that it makes a known angle, usually zero, with the earth's field which is an appreciable fraction of the static field in which the sample is immersed. The sample is placed in a coil which is the tank coil of a resonant circuit and which supplies the radiation which induces the magnetic transitions. A regenerative oscillator detector is employed to drive the coil and detect the magnetic signal which appears when the static magnetic field reaches the resonant value. Frequencies in the range of 5.5 to 8.2 mc. sec.$^{-1}$ corresponding to field strengths in the range of 2.0 to 2.9 gauss were employed. The auxiliary coil inside the solenoid provided modulation of the field at 40 cycle sec.$^{-1}$ producing a corresponding a.c. component in the magnetic signal which was convenient for amplification. The amplitude of the modulation was sufficiently small to ensure a magnetic signal proportional to the first derivative of the resonance absorption. The static magnetic field of the solenoid was varied linearly with time by an electronic current supply with a mechanically driven scanning potentiometer. After suitable amplification the first derivative of the magnetic signal and the current through the solenoid were both plotted by a recording potentiometer.

A Watkins-Pound[1] calibrator circuit was employed for determining signal intensities. With this device one may simulate the change in coil resistance produced by the magnetic signal by means of a changing plate resistance in a thermionic tube. One then employs the regenerative oscillator-detector-amplifier-recorder system to compare the magnetic signal with the calibrator signal produced when a

(1) G. D. Watkins and R. V. Pound, *Phys. Rev.*, **82**, 343 (1951).

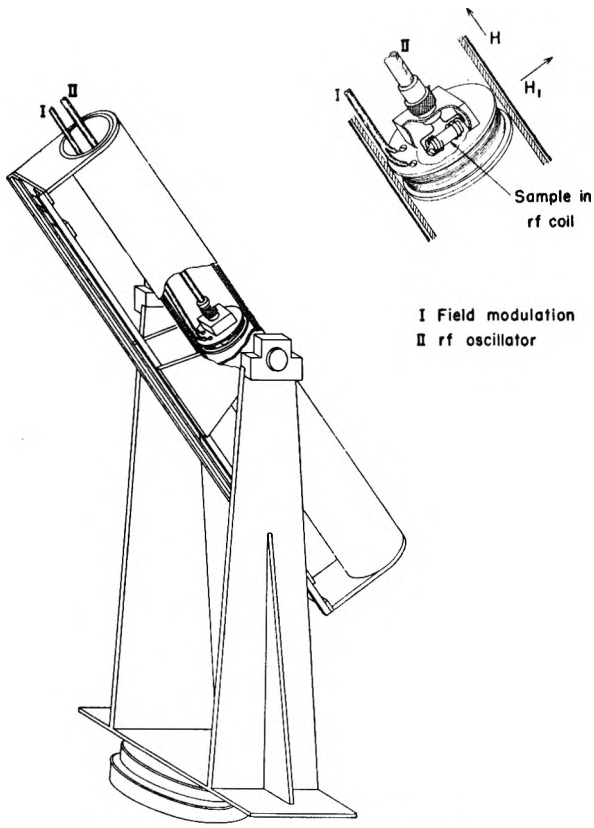

Fig. 3.—Low frequency apparatus.

40 cycle sec.$^{-1}$ signal is placed on the grid of the calibrator tube at known fixed plate current.

The areas under the curves drawn by the recording potentiometer were obtained by numerical integration. Since the derivative is plotted by the recording potentiometer, the integral up to a given H plotted against H gives a curve proportional to the absorption provided the scale is linear in magnetic signal. The scale on the field strength axis was quite linear as determined from the current recording. The scale on the magnetic signal axis was quite linear in calibrator grid voltage. Moreover it was found that the grid voltage at constant plate current was very close to being proportional to magnetic signal over the range employed in the experiments. This last was determined by comparing calibrator signals with magnetic signals of various sizes produced with an organic free radical by field modulation amplitudes of various sizes. It was consequently a simple matter to obtain the absorption curves with errors not greater than probably 5%. Some absorption curves were also determined using the Watkins–Pound RF Spectrometer.[1] The results were indistinguishable from those obtained with the regenerative oscillator–detector. The regenerative oscillator–detector was employed in our investigations because of its much more favorable signal-to-noise ratio.

The integrated intensity under the absorption curve may then be obtained from a second numerical integration. The relation between the area under the absorption and the paramagnetic part of the static susceptibility is given by the following equation (derivable from the Kronig–Kramers relation)

$$\chi = \frac{2\beta}{\pi\xi\omega^2 C h}\int_0^\infty \frac{\Delta R}{R^2}\,dH$$

where χ is the paramagnetic part of the static susceptibility, β is the Bohr magneton, ξ is the fraction of the energy of the *rf* field which is stored within the volume of the sample, ω is the angular frequency, C is the capacity across the coil, h is the Planck constant, R is the *rf* resistance of the coil and H is the field strength.

The first integral of the magnetic signal expressed in terms of calibrator grid voltage is proportional to $\Delta R/R^2$. Hence we replaced $\int_0^\infty (\Delta R/R^2)\,dH$ with the second integral of the recorder curves and employed a standard substance with known number of paramagnetic absorbers to eliminate the proportionality constant. The standard substance employed was tris-*p*-nitrophenylmethyl, a completely dissociated free radical in which resonance was first observed by Pake, Weissman and Townsend,[2] at Washington University. A sample of this material was prepared and later assayed chemically (by means of measuring the amount of O_2 required to react with the radical) for us by Professor Weissman. We carried out scannings of the resonance of this material. The comparison of the second integrals of the curves so obtained with the similar ones for the K in liquid NH_3 enabled us to calculate the paramagnetic part of the static susceptibilities of the solutions relative to that of the organic compound. The free radical was assumed to have the static susceptibility of 1 mole of spins at 28° per mole of free radical. The number of moles in the sample of organic free radical was known to approximately 5%.

2. Solutions of Metals in Liquid NH_3.—The alkali metals and the alkaline earth metals dissolve readily in liquid NH_3.[3-7] The solubilities[6] of Na and K at the boiling point of NH_3, −33.4°, are about 5.4 and 4.9 mole l.$^{-1}$, respectively, and the solubility changes very little with temperature. The concentrated solutions have the color of bronze and a metallic luster. The more dilute solutions are blue, the absorption spectrum of the dilute solutions of all the alkali metals being identical.[8] When the solvent is evaporated the pure alkali metals remain as residues. (Reaction of the metal with the solvent will occur at varying rates depending upon temperature, impurities, etc. but in the absence of impurities the solutions contained in Pyrex glass at room temperature are quite stable enough to make possible a variety of measurements of physical properties.) A study of the vapor pressure[9] as a function of concentration shows the non-existence of compounds in the freshly prepared solutions of the alkali metals.

One of the striking properties of such solutions is their electrical conductivity.[10-13] The conductivity is shown in Fig. 4. At all concentrations the equivalent conductivity is greater than that of any known salt in any known solvent. In the most dilute solutions the equivalent conductance reaches a limiting value of approximately 1000 ohm^{-1} cm.^{2} mole^{-1} which is three times that of the best conducting salts

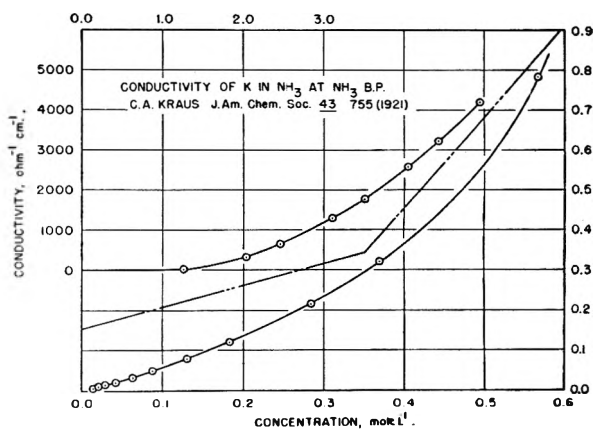

Fig. 4.—Conductivity of K in NH_3 at its boiling point.

(2) G. E. Pake, S. Weissman and J. Townsend, personal communication.

(3) C. A. Kraus, *J. Franklin Inst.*, **212**, 537 (1931).

(4) C. A. Kraus, "The Properties of Electrically Conducting Systems," (Chemical Catalog Co.) Reinhold Publ. Corp., New York, N. Y., 1922.

(5) Yost and Russell, "Systematic Inorganic Chemistry," Prentice-Hall, Inc., New York, N. Y., 1944, p. 136.

(6) W. C. Johnson and A. W. Meyer, *Chem. Revs.*, **8**, 273 (1931).

(7) W. C. Fernelius and G. W. Watt, *ibid.*, **20**, 195 (1937).

(8) G. E. Gibson and W. L. Argo, *J. Am. Chem. Soc.*, **40**, 1327 (1918).

(9) C. A. Kraus, E. S. Carney and W. C. Johnson, *ibid.*, **49**, 2206 (1927).

(10) C. A. Kraus, *ibid.*, **43**, 749 (1921).

(11) C. A. Kraus and W. W. Lucasse, *ibid.*, **43**, 2529 (1921).

(12) C. A. Kraus and W. W. Lucasse, *ibid.*, **45**, 2551 (1923).

(13) G. E. Gibson and T. E. Phipps, *ibid.*, **48**, 312 (1926).

in liquid NH_3. Even more remarkable is the behavior of the conductivity at the higher concentrations. A saturated solution of K in NH_3 has a conductivity of approximately 4500 ohm^{-1} $cm.^{-1}$. This may be compared with the conductivity of Hg at 20° which is 10,400 and it is seen that these solutions have a conductivity of the same order as that of metals. The conductances of the solutions of the various alkali metals in liquid NH_3 agree very closely at all concentrations. Both electromotive force and conductance studies lead to the conclusion that in the most dilute solutions of Na the speed of the negative charge carrier is about 7 times that of the positive charge carrier. When the concentration is increased the equivalent conductance decreases, passes through a minimum at about 0.04 *M* and then increases to the enormous values already mentioned. In the concentrated solutions the speeds of the negative carriers approach those of the electrons in metals.

One is led to the conclusion that when any of the alkali metals is dissolved in NH_3 there is a dissociation into positive alkali metal ions and electrons. The negative charge carrier is apparently the electron in each case. In the dilute solutions the electrons behave as though they were bound not too tightly in some way to the solvent molecules. In the concentrated solutions the electrons are much less tightly bound and move in much the same manner as in metals. In such solutions we have the possibility of examining the properties of electrons over a range of concentrations varying by a factor of 10^4 to 10^5.

The behavior of the conductivity with concentration was interpreted by Kraus and his co-workers in terms of equilibria between Na atoms, Na ions, free electrons and solvated electrons. Several lines of evidence lead to the discarding of such models. One of the clearest reasons for rejecting models involving the existence of large concentrations of alkali metal atoms or solvated electrons is a consideration of the results of studies of the static magnetic susceptibilities

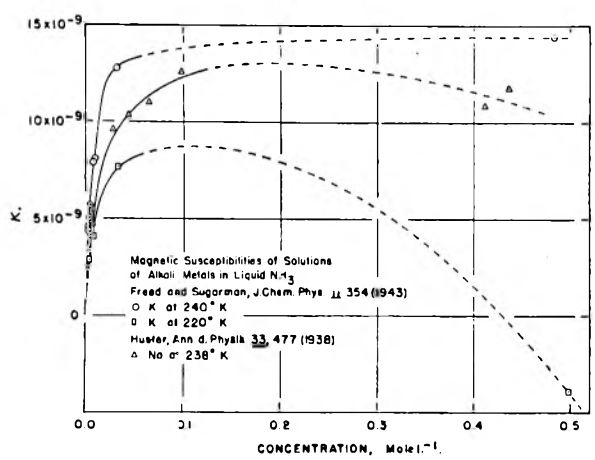

Fig. 5.—Magnetic susceptibilities of solutions of alkali metals in liquid NH_3.

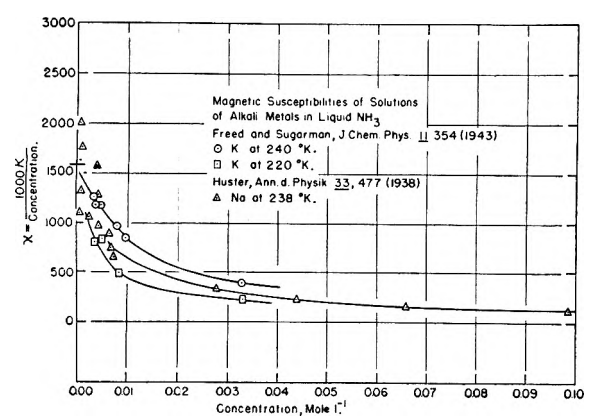

Fig. 6.—Magnetic susceptibilities of solutions of alkali metals in liquid NH_3.

of such solutions.[14,15] If such species existed in large numbers the solutions would be paramagnetic and their susceptibilities would obey Curie's law with respect to variation of temperature and concentration. This type of behavior is not observed. The experimental measurements of the static susceptibilities are shown in Figs. 5 and 6. In the very concentrated solutions and down to a few tenths normal the susceptibility is quite small of the order found in the metal and has a very small temperature coefficient. As the concentration is lowered the molar susceptibility increases rapidly and approaches in the most dilute solutions the value for one mole of spins. This is the general qualitative type of behavior to be expected if the electrons are free or in a periodic potential as in a metal. Under such conditions they would at high concentrations form a degenerate Fermi gas with most of the electrons paired and not contributing to the paramagnetism. At the lower concentrations however the degeneracy would be removed and the susceptibility would be of the order of that of a mole of spins. Hence in this particular respect the solutions behave much as would be expected for a metal in which the concentrations of electrons could be varied over a very wide range.

With respect to both conductivity and magnetic susceptibility the behavior is not in detail like that of metals. For example the temperature coefficient of the conductivity is positive at all concentrations.[12,13] Also the magnetic susceptibility is considerably lower than that calculated for a free electron gas[16] and at all concentrations investigated the susceptibility increases with increasing temperature.[14] Various attempts have been made to account for this behavior of the susceptibility. Huster[15] suggested an equilibrium between on the one hand electrons and Na ions and on the other diatomic molecules. The necessary molecular concentrations are however in disagreement with the apparent molecular weight measurements of Kraus.[17] Freed and Sugarman[14] have proposed a decrease of density of energy levels near the top of the Fermi distribution because of the binding of the electron in a variety of resonance structures involving NH_3 molecules and solvated metal ions. This would result in a reduction of the magnitude of the susceptibility. They also proposed that there are pairwise interactions between electrons similar to those which lead to the F′ centers in crystals in which two electrons are trapped in a single vacancy.[18] These pairs would be expected to be diamagnetic and would thus lead to lowered susceptibilities. In particular they might be responsible for the increase of susceptibility with increasing temperature. Ogg[19–21] has discussed in some detail the formation of F′-like centers. He proposes that individual electrons are trapped in cavities which they create in the solution and are in equilibrium with pairs of electrons similarly trapped. He believes that he can account for the behavior of several physical properties including the magnetic susceptibility on the basis of such an equilibrium. Moreover, he believes that the cavities are very large and that as a consequence of this there is an extraordinarily large diamagnetic contribution to the susceptibility.

3. Paramagnetic Resonance Absorption in Solutions of K in Liquid NH_3. 3.1. Preliminary Measurements.—Some time ago Pastor and Hutchison reported observations on the paramagnetic resonance absorption in solutions of K in liquid NH_3 at microwave frequencies.[22] Observations of the resonance have also been made by Garstens and Ryan[23] and by Levinthal, Rogers and Ogg.[24] The most striking feature of the reso-

(14) S. Freed and N. Sugarman, *J. Chem. Phys.*, **11**, 354 (1943).
(15) E. Huster, *Ann. Physik*, **33**, 477 (1938).
(16) N. F. Mott and H. Jones, "Theory of Properties of Metals and Alloys," The Clarendon Press, Oxford, 1936, p. 184.
(17) C. A. Kraus, *J. Am. Chem. Soc.*, **30**, 1197 (1908).
(18) F. Seitz, *Rev. Mod. Phys.*, **18**, 384 (1946).
(19) R. A. Ogg, Jr., *J. Chem. Phys.*, **14**, 114 (1946).
(20) R. A. Ogg, Jr., *ibid.*, **14**, 295 (1946).
(21) R. A. Ogg, Jr., *J. Am. Chem. Soc.*, **68**, 155 (1946).
(22) C. A. Hutchison, Jr., and R. C. Pastor, *Phys. Rev.*, **81**, 282 (1951).
(23) M. A. Garstens and A. H. Ryan, *ibid.*, **81**, 888 (1951).
(24) E. C. Levinthal, E. H. Rogers and R. A. Ogg, Jr., *ibid.*, **83**, 182 (1951).

nance was its extreme sharpness. As we have pointed out previously the resonances in crystalline salts of the transition elements, for example, may be hundreds of gauss wide. This resonance proved to be only a few tens of milligauss wide. It was apparent that a relatively very complete averaging out of local fields was being produced by the very rapid motion of the electrons in this system. Due to the extreme sharpness of this resonance it was of course extraordinarily intense. The width of 0.1 gauss which we initially reported turned out to be caused largely by inhomogeneities in our magnetic field. We consequently have used the small fields and low frequencies previously described. The following results were obtained in coöperation with Mr. Pastor.

3.2. Samples.—The samples of K in liquid NH_3 were prepared by distilling K several times in high vacuum and finally distilling it into Pyrex glass capsules. Then NH_3 dried by addition of K and subsequent distillation was added and the capsule sealed. The amount of K in these solutions was determined after completion of magnetic investigation by dissolving in H_2O and boiling to remove the NH_3. The resulting solution was titrated with standard acid. The weight of NH_3 + K was determined by weighing the capsule before and after opening it.

Measurements were made at a room temperature of 28° and at the boiling point of liquid NH_3 which is −33°. For the low temperature runs the sample was immersed in a Dewar filled with liquid NH_3.

3.3. Spectroscopic Splitting Factor.—The spectroscopic splitting factors, g, in the relation $\nu/H = g\beta/h$, for the solutions of K in liquid NH_3 were compared with the factor for 2,2-diphenyl-1-picrylhydrazyl[22,25] at approximately 8.2 mc. sec.$^{-1}$. In the case of the solution of K in NH_3 the *rf* coil field strength was 0.0023 gauss r.m.s. The shift of the center of the resonance under these conditions due to the Block–Siegert[26] effect is by the factor, $[1 - (2H_1)^2/16H_0^2] = 1 - 1.6 \times 10^{-7}$, and is consequently small enough to be neglected. Assuming the splitting factor for 2,2-diphenyl-1-picrylhydrazyl to be 2.0037[19,23] (the microwave value) we find the factor at room temperature for K in NH_3 to be 2.0010 ± 0.0002 at 0.425 mole l.$^{-1}$ and 2.0011 ± 0.0002 at 0.0365 mole l.$^{-1}$. This is the same as the value 2.0012 ± 0.0002 found at 23,500 mc. sec.$^{-1}$.[22] This factor is considerably lower than the value of the g-factor, 2.0023, for a free electron spin. However, it is not nearly so low as the value, 1.995,[27] which we have observed for additively colored crystals of KCl. Recent calculations by Yafet and Kittel[28] have shown that the g for Na metal should be 2.0019. According to Kittel[28] the g for a diluted metal should be still lower than this figure for the pure substance.

3.4. Width.—The width of the resonance between the points of maximum slope was determined by measuring the distance between the maximum and minimum on the recorder chart which when combined with the current record on the same chart gave the width.

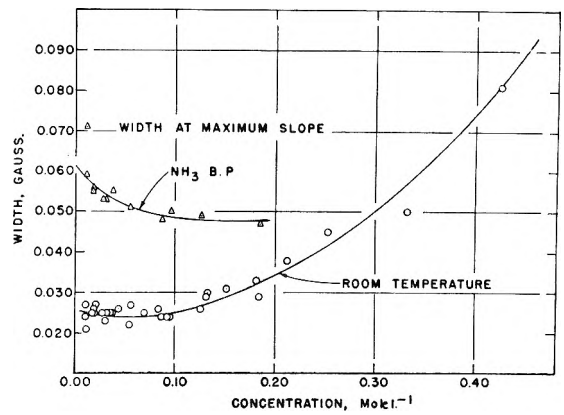

Fig. 7.—Width of resonance at maximum slope *vs.* concentration.

The results are shown in Fig. 7. The width was measured at room temperature from a concentration of 0.425 down to 0.011 mole l.$^{-1}$ and at the boiling point of NH_3 from 0.185 to 0.011 mole l.$^{-1}$. It is clear that this resonance is by far the sharpest electronic resonance so far observed in a condensed phase. In the case of a resonance as sharp as this, one must consider the Rabi[29] width associated with the flipping of the spin by the perturbing *rf* magnetic field. This is approximated by

$$\Delta H/H = 4 \sin \theta/2$$

where ΔH is the width at half-height and where θ is given by

$$\theta = \tan^{-1} \frac{rf \text{ field strength}^*}{\sqrt{2}H}$$

(* This is the r.m.s. field strength.)

When θ is very small as in our case

$$\Delta H = \sqrt{2} rf \text{ field strength}$$

For a sample whose concentration was 0.152 mole l.$^{-1}$ the variation of width with *rf* field strength was investigated with the results tabulated:

$\sqrt{2}$ *rf* field strength, gauss	Width at max. slope, gauss
0.0032	0.0311
.0081	.0327
.0163	.0335
.0324	.0388

It is clear that at the higher coil voltages the Rabi width is seriously interfering with observation of the true width. Consequently all scannings of the resonance absorption were made at coil voltages corresponding approximately to the smallest *rf* field listed above or about 0.05 volt. In the case of an organic free radical which is much wider than the K resonance there is of course no observable change of width with coil voltage.

The width of this resonance is several orders of magnitude less than that observed in aqueous solution of paramagnetic salts of about the same concentrations. It is also much narrower than the

(25) A. N. Holden, C. Kittel, F. R. Merritt and W. A. Yager, *Phys. Rev.*, **77**, 147 (1950).

(26) F. Block and A. Siegert, *ibid.*, **57**, 522 (1940).

(27) C. A. Hutchison, Jr., and G. A. Noble, *ibid.*, **87**, 1125 (1952).

(28) C. Kittel, private communication.

(29) I. I. Rabi, *Phys. Rev.*, **51**, 652 (1937).

widths of order of one gauss reported for certain organic free radicals. There is evidently an extraordinarily large narrowing associated with the great mobility of the electrons in these solutions.[30] The average value of β/r^3 (r is the distance between electrons) ranges from 0.06 to 2.6 gauss. The broadening by magnetic nuclei would normally be expected to be several gauss. At room temperature there is perhaps a slight increase in the width at the lowest concentrations and the increase is marked at the lower temperature. This increase becomes pronounced in the vicinity of the region in which the susceptibility begins to rise rapidly with dilution. The room temperature measurements were extended to considerably higher concentrations than at the lower temperature and there is apparently quite a large increase of width at the higher concentrations.

3.5. Line Shape.—The absorption curves were obtained by numerical integration of the recorder curves as previously described. In Fig. 8 are shown the line shapes at two temperatures and three concentrations. The points are taken from the experimental curves and are compared with a Lorentzian and with a Gaussian curve. In the case of a Lorentzian or "resonance" type curve the absorption is given by $1/(1 + (H - H_0)^2)$ when the curves are normalized to unit height at maximum absorption and to unit half-width at half-maximum absorption. For the same normalization the Gaussian shape is given by $e^{-(H - H_0)^2 \ln 2}$. H is the field strength and H_0 is the resonance field strength. It is clear that the experimental curves follow the Lorentzian much more closely than the Gaussian throughout the central portion of the resonance but drop toward the Gaussian in the wings of the curve. Anderson and Weiss[30] have recently shown that this is the qualitative behavior to be expected in cases in which there is rapid motion of the spin systems.

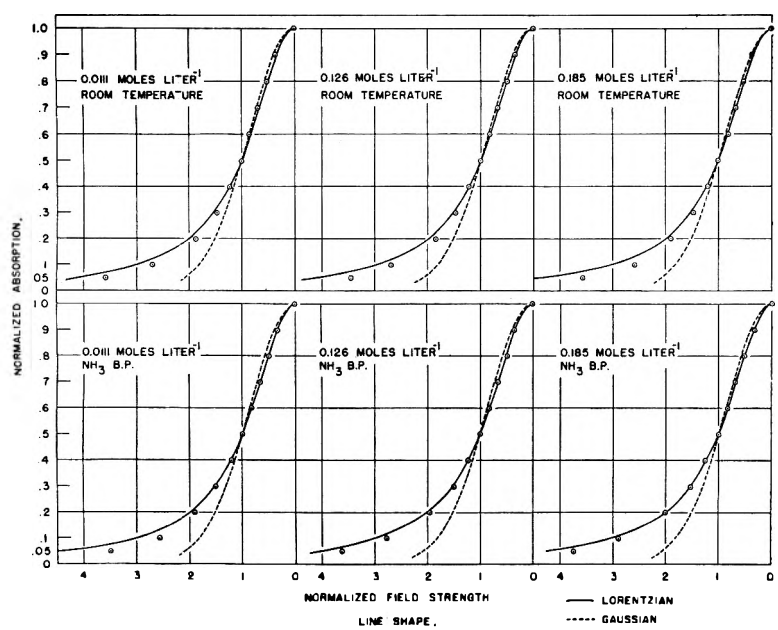

Fig. 8.—Line shape.

(30) P. W. Anderson and P. R. Weiss, Washington Conference on Magnetism, *Rev. Mod. Phys.*, Jan. 1953.

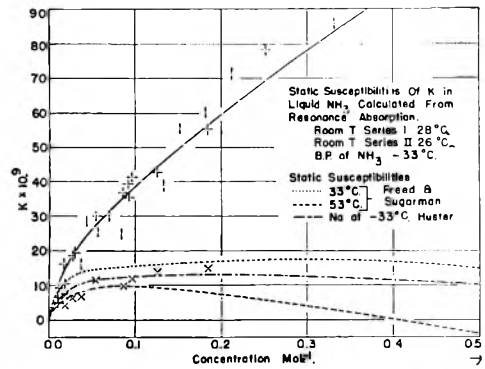

Fig. 9.—Static susceptibilities of K in liquid NH_3 calculated from resonance absorptions.

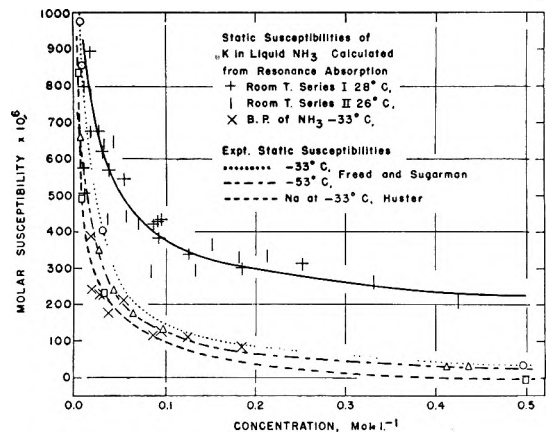

Fig. 10.—Static susceptibilities of K in liquid NH_3 calculated from resonance absorptions.

3.6. Intensity.—A second numerical integration yielded, in the manner previously described, a comparison of the paramagnetic part of the static susceptibility with that of the standard organic free radical, tris-*p*-nitrophenylmethyl.

The results of the susceptibility determinations are shown in Figs. 9 and 10. At room temperature the calculated static susceptibility is seen to follow the same sort of pattern as determined in static field experiments at low temperatures. The susceptibilities are considerably higher than those of the static experiments at the boiling point. Like the latter they rise sharply with dilution at about the same concentration. The low temperature runs were made some time subsequent to the high temperature runs and two points have been omitted for the two lowest concentrations where some decomposition is known to have occurred. These two samples also give obviously low results at the higher temperature. Some of the other points at the lower concentrations are probably suspect for the same reason. The points for the molar susceptibility at the higher concentrations at the lower temperature are in reasonably good agreement with the static

field measurements. As we have previously pointed out the resonance phenomenon is peculiar to the paramagnetic spins and is relatively unaffected by the diamagnetism. Consequently such a comparison of static field measurements with static susceptibilities calculated from *rf* measurements enables one to detect the presence of any abnormal diamagnetic susceptibilities. It is clear that no abnormally large diamagnetism exists in these solutions at the boiling point of NH_3 at the concentrations investigated by both methods. Such determinations of static susceptibilities from *rf* measurements afford a powerful tool for a number of problems of chemical and physical interest where large amounts of diamagnetic material or abnormally large diamagnetisms of the paramagnetic species itself may obscure the primary effect. We have discussed this problem recently for the case of the detection of organic free radicals in solution.[31]

Acknowledgments.—The experiments on the solutions of K in NH_3 were carried out with Ricardo C. Pastor. We wish to thank Clarence Arnow for the design and construction of the electronic equipment used in these experiments; Jack Boardman for the numerical integrations and other computations; and Edward Bartal for the construction of the solenoid, low temperature apparatus and other machine work.

(31) C. A. Hutchison, Jr., A. Kowalsky, R. C. Pastor and G. W. Wheland, *J. Chem. Phys.*, **20**, 1485 (1952).

THE THERMOCHEMISTRY OF THE ALKALI AND ALKALINE EARTH METALS AND HALIDES IN LIQUID AMMONIA AT −33°

By Lowell V. Coulter

Department of Chemistry, Boston University, Boston, Mass.

Received November 28, 1952

The thermochemistry of the alkali and alkaline earth metals and their salts in liquid ammonia has been employed in the interpretation of certain aspects of inorganic chemistry in this solvent. Ionic entropies have been calculated from heats of reaction of the metals with NH_4^+(am), the heats of solution of salts in liquid ammonia, the corresponding free energy changes and appropriate entropy data. For both alkali and alkaline earth metal solutions a common heat of reaction has been obtained for the reaction: $^1/_2e_2^-$(am) + NH_4^+(am) = $^1/_2H_2$(g) + NH_3(l), per equivalent of metal which indicates one and two electron ionization of the alkali and alkaline earth metals, respectively, in liquid ammonia. The experimental heats of ammonation of gas ion pairs have been interpreted with the aid of a crude model for the process of solvation. Heats of ammonation of the alkali and alkaline earth chlorides, bromides and iodides are larger than the corresponding heats of hydration. This appears to result from a smaller energy consumption in depolymerization and reorientation processes in ammonia than in water. The heat of ammonation of the electron has been calculated and is in qualitative agreement with other theoretical and experimental conclusions.

The interpretation of inorganic chemistry in non-aqueous polar solvents and the understanding of the process of solvation of electrolytes are greatly facilitated by a knowledge of the thermodynamic properties of the various ions in the solvent of interest. Although much information has been available for aqueous systems and considerable attention has been directed toward the process of hydration of ions, relatively little advance has been made in non-aqueous media along these lines. With this situation in mind, we have recently undertaken the further thermochemical study of ammonia solutions of electrolytes. For the first step, we have directed our attention to the thermochemistry of the alkali and alkaline earth metals and their halides.

Heats of the reaction

$$\text{M(etal)(s)} + NH_4^+(\text{am}) = M^+(\text{am}) + NH_3(l) + {}^1/_2H_2(g)$$
$$\text{or} \qquad (1)$$
$$\text{M(etal)(s)} + H^+(\text{am}) = M^+(\text{am}) + {}^1/_2H_2(g)$$

and the corresponding free energy changes, now known only approximately, permit evaluation of relative ionic entropies as well as free energies of the ions. In addition, combination of the heats of reaction 1 with the heats of solution of metals in liquid ammonia

$$\text{M(etal)(s)} = M^+(\text{am}) + {}^1/_2e_2^-(\text{am}) \qquad (2)$$

gives the heat of reaction of the ammonated electron with NH_4^+ (am)

$$^1/_2e_2^-(\text{am}) + NH_4^+(\text{am}) = NH_3(l) + {}^1/_2H_2(g) \qquad (3)$$

and provides a method for comparison of the state of the solvated electron for the various metal ammonia solutions.

Heats of solution of salts in liquid ammonia also provide a path for the calculation of ionic entropies if the corresponding free-energy changes are calculable from known solubilities and activity coefficient data. Unfortunately, few activity coefficients are known and we are compelled for the moment to limit application of heat of solution data primarily to the elucidation of the energy changes of the ammonation of ions.

Experimental Procedure.—The measurement of these reaction heats has been accomplished with a calorimeter previously described.[1] The observed heat effects of the reactions at −33° have been calculated from the heat effect accompanying the vaporization of ammonia from the calorimeter at constant pressure and the measured temperature change and known heat capacity of the calorimeter. Depending upon the vigor of the reaction, an accuracy of 1 to 3% appears to be possible. For well controlled solution reactions, agreement within these limits between researchers using different calorimeters of this type also appears possible as indicated by our confirmation within these limits of the heat of solution of NH_4Br previously reported by Schmidt[2] who used a calorimeter having approximately $^1/_4$ the capacity of the instrument employed in this work.

Experimental Results.—The results of the calorimetric

(1) L. V. Coulter and R. H. Maybury, *J. Am. Chem. Soc.*, **71**, 3394 (1949).

(2) F. C. Schmidt, J. Sottysiak and H. D. Kluge, *ibid.*, **58**, 2509 (1936).

measurements for the reaction of the alkali metals and calcium, strontium and barium with ammonium ion are presented in column 2 of Table I. In the succeeding column are listed our observed heats of solution of lithium, calcium, strontium and barium metals in liquid ammonia. In addition are tabulated the observed heats of solution of sodium, potassium, rubidium and cesium reported by Kraus, Schmidt and co-workers.[3] The heat of reaction of the solvated electron pair with NH_4^+(am), eq. (3), has been obtained by subtracting the heat of reaction for eq. (2) from the heat of reaction for eq. (1). The values obtained, ΔH_3, for each metal solution are tabulated in column 4 of Table I. For the moderately dilute solution (1500 moles NH_3/equiv. of metal) for which these heat effects (ΔH_3) hold, we have represented the electron in a paired state in view of its magnetic and thermal properties. On the basis of current measurements in our laboratory, it appears that some unpairing has occurred at this concentration in view of an observable heat of dilution. The relative magnitude of the effect is not sufficient, however, to regard the majority of electrons in an unpaired state at this concentration.

TABLE I

SUMMARY OF HEATS OF REACTION OF THE ALKALI AND ALKALINE EARTH METALS AT −33°

Reactants	ΔH_1, kcal./g. atom	ΔH_2, kcal./g. atom	ΔH_3, kcal./equiv.
Li and NH_4Br	− 50.5[a]	− 9.7[d]	−40.8[d]
Na and NH_4Br	− 38.5[a]	+ 1.4[e]	−39.9[a]
Na and NH_4Cl	− 38.8[a]	+ 1.4[e]	−40.2[a]
K and NH_4Br	− 39.7[a]	0.0[f]	−39.7[a]
Cs and NH_4Br	− 41.6[a]	0.0[f]	−41.6[a]
Ca and NH_4I	− 99.2[b]	−19.7[b]	−39.8[b]
Sr and NH_4I	−100.7[c]	−20.7[c]	−40.0[c]
Ba and NH_4I	−104.0[c]	−19.0[c]	−42.5[c]

[a] L. V. Coulter and R. H. Maybury, *J. Am. Chem. Soc.*, **71**, 3394 (1949). [b] S. P. Wolsky, E. J. Zdanuk and L. V. Coulter, *ibid.*, **74**, 6196 (1952). [c] S. P. Wolsky, Thesis, Boston University, Boston, Mass., 1952. [d] L. V. Coulter and L. Monchick, *J. Am. Chem. Soc.*, **73**, 5867 (1951). [e] C. A. Kraus and F. C. Schmidt, *ibid.*, **56**, 2298 (1934). [f] F. C. Schmidt, F. J. Studer and J. Sottysiak, *ibid.*, **60**, 2780 (1938).

Comparison of the ΔH_3 values in Table I indicates essentially a common heat effect for eq. (3) per equivalent of metal as is to be expected if the nature of the solvated electron is independent of the cation present. Excluding cesium and barium in which a few tenths per cent. of impurity of lighter metals would introduce considerable error in the heat of reaction, we have obtained −40.1 kcal. per equivalent for ΔH_3 of eq. (3). It is to be noted that the equivalent heat of reaction 3 for calcium is entirely normal and thereby indicates two electron ionization of calcium metal in liquid ammonia rather than $Ca(s) = {}^1/_2\ Ca_2^{++}(am) + {}^1/_2\ e_2^{=}(am)$, previously proposed by Yost and Russell[4] to account for the low magnetic susceptibility measurements of Freed and Sugarman.[5]

For the heats of solution of lithium, calcium, strontium and barium eq. (2), we have not obtained agreement with the previously determined heats by Schmidt and co-workers,[3] who have reported 7.96, 9.76, 17.35 and 11.02 kcal., respectively, at somewhat higher concentrations. Although their observations indicate some concentration dependence of the heat of solution, we have not noted any effect beyond experimental error. In view of the fact that this large discrepancy cannot be due to instrumental differences or concentration dependence, we are inclined to account for the differences on the basis of impurities in the metals used by previous workers. Considerable care was taken in our laboratories to use metals 99+% free metal by analysis. For example, the calcium employed was 100.0 ± 0.2% for selected samples.

(3) C. A. Kraus and F. C. Schmidt, *J. Am. Chem. Soc.*, **56**, 2298 (1934); F. C. Schmidt, F. J. Studer and J. Sottysiak, *ibid.*, **60**, 2780 (1938).

(4) Don. M. Yost and Horace Russell, Jr., "Systematic Inorganic Chemistry," Prentice-Hall, Inc., New York, N. Y., 1944, p. 148.

(5) S. Freed and N. Sugarman, *J. Chem. Phys.*, **11**, 354 (1943).

Ionic Entropies.—The heats of reaction for eq. (1) now provide a means for the calculation of the entropies of the alkali ions and Ca^{++} in liquid ammonia since approximate free energy changes are available. We have chosen to make the calculation at −33° rather than at 25°, which Jolly[6] has recently selected for a compilation of the thermodynamic properties of the ions, since the greater proportion of information is furnished and will probably be employed by inorganic chemists in the vicinity of −33°. This selection seems further justified in view of the fact that the theoretical aspects of ammonation of ions will be more pertinent for liquid ammonia near or below its normal boiling point, thereby giving a better comparison of the process of ammonation with other types of solvation such as hydration. For the standard heat content change, $\Delta H^\circ_{240^\circ}$, we have used directly the observed heats of reaction of eq. (1) which appear to be independent of concentration. The corresponding standard free energy changes at 240°K. have been calculated from the cell potential data reported by Pleskov and Monoszon[7] which have been corrected to 240°K. with the aid of the observed heats of reaction. Ionic entropies have been calculated relative to $\bar{S}^\circ_{H^+(am)} = 0$ and $\Delta S^\circ = 0$ for the reaction $H^+(am) + NH_3(l) = NH_4^+(am)$. Tabulation of these calculations for each of the metals has been made in Table II.

The evaluation of ionic entropies from solution reactions of salts is limited at the present because of the paucity of activity data and the insufficiency of information regarding the nature and thermodynamic properties of the solid phases in equilibrium with the saturated ammonia solutions. It has been possible, however, to make what appear to be reliable calculations for Cl^- based on the solution reaction

$$NH_4Cl\cdot 6NH_3(s) = NH_4^+(am) + Cl^-(am) + 6NH_3(l)$$

The $\Delta H^\circ_{240^\circ}$ for this reaction has been obtained from the sum of the heat of dissociation,[8] $\Delta H^\circ_{240^\circ} = 43.1$ kcal., of the hexammonate: $NH_4Cl\cdot 6NH_3(s) = NH_4Cl(s) + 6NH_3(g)$, the heat of liquefaction of six moles of gaseous ammonia,[9] $\Delta H^\circ_{240^\circ} = -33.5$ kcal., and the heat of solution of NH_4Cl[2] $\Delta H^\circ_{240^\circ} = -6.8$ kcal., in liquid ammonia at infinite dilution. At equilibrium the saturated solution is 3.0 molal[10] for which we estimate $\gamma_\pm = 0.017$ from the activity coefficient data reported by Ritchey and Hunt at 25°.[11] For the activity of the solvent in the saturated solution, 0.9 appears to be a reasonable estimate as indicated by the decomposition pressure of the hexammonate[8] and the vapor pressure of ammonia solutions of NH_4Cl at 25°.[12] For the free energy of solution of the hexammonate to give the hypothetical 1 molal solution, we find $\Delta F^\circ_{240^\circ} = 3.14$ kcal. From the heat and free energy of dissociation of the hexammonate and the entropies of NH_4Cl and NH_3 at 240°K., we obtain $S^\circ_{240^\circ}(NH_4Cl\cdot 6NH_3) = 115.2$ e.u. From these data we obtain $\bar{S}^\circ_{240^\circ}(Cl^-) = -31.8$ e.u. which now provides a path for the calculation of ionic entropies of the alkali ions through similar solution reactions illustrated by KCl in Table II.

The heat of solution of KCl has not been experimentally determined. For this calculation it has been possible, however, to estimate it from the temperature dependence of the free energy of solution since activity coefficients at −36°[13] and the solubility of KCl between +44 and −77° are known.[14]

By interpolation, $\Delta F^\circ_{240^\circ} = 4.55$ kcal. for the solution reaction to give the hypothetical 1 molal solution and $\Delta H^\circ_{240^\circ} = -1.45$ kcal. For K^+, $\bar{S}^\circ_{240^\circ}(K^+) = 24.0$ e.u. based on −31.8 for the entropy of Cl^-. We observe that good agreement is obtained in this case between the entropies of K^+ calculated from two different reactions. Extension of this procedure to the other alkali ions at 240° K. is, at the moment, impossible because of the insufficiency of reliable data.

(6) W. L. Jolly, *Chem. Revs.*, **50**, 351 (1952).

(7) V. A. Pleskov and A. M. Monoszon, *Acta Physicochim.* (*U.R.S.S.*), **2**, 615 (1935); V. A. Pleskov, *ibid.*, **6**, 1 (1937).

(8) Calculated from the temperature dependence of the dissociation pressure, M. L. Troost, *Compt. rend.*, **88**, 578 (1879).

(9) National Bureau of Standards, Circular 500, "Selected Values of Chemical Thermodynamic Properties," U. S. Govt. Printing Office, Washington, D. C. (1952).

(10) G. Patscheke and C. Tanne, *Z. physik. Chem.*, **174**, 135 (1935); J. Kendall and J. G. Davidson, *J. Am. Chem. Soc.*, **42**, 1141 (1920).

(11) H. W. Ritchey and H. Hunt, THIS JOURNAL, **43**, 407 (1939).

(12) W. E. Larsen and H. Hunt, *ibid.*, **39**, 877 (1935).

(13) J. Sedlet and T. DeVries, *J. Am. Chem. Soc.*, **73**, 5808 (1951).

(14) G. Patscheke and C. Tanne, *Z. physik. Chem.*, **174**, 135 (1935).

TABLE II

ENTROPY CALCULATIONS

Free energies and heats in kcal.; entropies in cal. per degree per mole

Reaction	$\Delta H°_{240°}$	$\Delta F°_{240°}$	$\Delta S°_{240°}$	$\bar{S}°_{240°}$	Ion	$\bar{S}°_{240°}$ [a]
$NH_4Cl \cdot 6NH_3(s) = NH_4^+(am) + Cl^-(am) + 6NH_3(l)$	2.8	3.14	− 1.4	− 31.8	Cl^-	−33.5
$Li(s) + H^+(am) = Li^+(am) + {}^1/_2H_2(g)$	−50.6	−51.4	3.3	− 6.1	Li^+	...
$Na(s) + H^+(am) = Na^+(am) + {}^1/_2H_2(g)$	−38.7	−42.7	16.7	12.6	Na^+	12
$K(s) + H^+(am) = K^+(am) + {}^1/_2H_2(g)$	−39.7	−46.1	26.7	25.3	K^+	19
$KCl(s) = K^+(am) + Cl^-(am)$	− 1.45	4.55	− 25.0	24.0	K^+	
$Rb(s) + H^+(am) = Rb^+(am) + {}^1/_2H_2(g)$	−40.0 [b]	−44.7	19.6	19.8	Rb^+	29
$Cs(s) + H^+(am) = Cs^+(am) + {}^1/_2H_2(g)$	−41.6	−45.2	15.0	18.0	Cs^+	30
$Ca(s) + 2H^+(am) = Ca^{++}(am) + H_2(g)$	−99.3	−73.4	−108	−129	Ca^{++}	...

[a] Calculated from the compilation by W. L. Jolly[6] at 298°K. [b] Estimated from heat of solution of Rb and heat of reaction of eq. (3).

Jolly[6] has recently calculated and compiled the thermodynamic properties of a number of ions in liquid ammonia at 25° which have been based, in part, on estimated activity coefficients and assumed solid phases for the equilibrium solution reactions of salts. For comparison purposes, we have corrected his results to 240°K. and have listed the resulting ionic entropies in column 7 of Table II. Although reasonably good agreement is observed for Cl^-, K^+ and Na^+, poor agreement is obtained for Rb^+ and Cs^+. Whether or not the disagreement in the latter cases is a result of the assumptions involved in the calculation based on the solution reaction or is caused by the errors in the cell potential data, cannot be stated. By analogy with aqueous systems, the increasing trend in the values of the ionic entropies calculated by Jolly appears to be more acceptable for Rb^+ and Cs^+. Nevertheless, it would not be entirely unexpected to find the entropies of K^+, Rb^+ and Cs^+ essentially the same, as column 5 suggests within experimental error, since a somewhat analogous effect has been observed previously by Latimer and Slansky[15] for Na^+ and K^+ in methyl alcohol in which both ions display the same solvation entropy. This has been explained by them as an indication of the presence of holes in the methyl alcohol complexes into which the ions fit with essentially the same entropy effect regardless of radius. Eley and Pepper[16] regard the same entropy effect to result from a "seeding" effect of the first solvent shell on the adjacent solvent resulting in an ordering of the solvent essentially independent of ionic radius, but with little change in heat content of the solvating shells beyond the primary layer. It will be of interest to ascertain the reality of this observation when reliable free energy data become available. It is to be expected that ammonia might follow this behavior in view of the difference in structures of liquid ammonia and water.

The large negative entropy, −129, exhibited by Ca^{++} is indicative of a pronounced net ordering effect of the ion on the solvent ammonia to an extent not observed in water in which $\bar{S}°_{Ca^{++}(aq)} = -13$ relative to $\bar{S}°_{H^+(aq)} = 0$. Although this large discrepancy is probably to be explained in part by a rather large negative absolute value for the entropy of $H^+(am)$, it does not appear reasonable to account for the observed difference on this basis completely. The reality of this large negative entropy for Ca^{++} is supported qualitatively by the observed larger energy of solvation of Ca^{++} by ammonia than by water, a point further discussed in the following section.

Heats of Ammonation of Ions.—The greater solvation heats of ions in liquid ammonia are evident from the greater heats of solution of salts in liquid ammonia in comparison with water as demonstrated in Table III. The large heat of ammonation of Ca^{++} is also apparent in the ammonation of CaI_2 in the solid state when compared with hydration. For the reactions

$$CaI_2(s) + 8H_2O(l) = CaI_2 \cdot 8H_2O(s)$$
$$CaI_2(s) + 8NH_3(l) = CaI_2 \cdot 8NH_3(s)$$

$\Delta H_{291°} = -26.8$ and -70.7 kcal., respectively.[17] Assuming that the interaction energy of the solvated Ca^{++} and close neighbors is essentially the same for both solvates, the difference is to be ascribed to the greater heat of ammonation of Ca^{++} and is consistent with our greater observed heat of CaI_2 in ammonia compared with water.

To account for the heats of ammonation of ions as well as to interpret the differences in the thermochemistry of salts in liquid ammonia and in water, a

TABLE III

COMPARISON OF HEATS OF SOLUTION IN AMMONIA AND WATER, KCAL.

Salt	$\Delta H°$ (aq)[a] 25°	ΔH(am) −33°	NH_3/Salt
LiBr	−11.7	−19.7[b]	233
LiI	−15.1	−18.1[b]	213
NaCl	+ 0.9	− 1.5[c]	200
NaBr	− 0.2	−10.4[d]	∞
NaI	− 1.9	−13.9[c]	733
KBr	+ 4.8	− 2.9[e]	170
KI	+ 4.9	− 5.9[e]	171
RbBr	+ 5.2	− 0.4[b]	385
AgI	+26.9	− 7.4[f]	484
CaI_2	−28.7	−62.8[g]	∞
PbI_2	+15.5	−27.4[b]	869
HgI_2	+40.0	−20.1[b]	329
NH_4Cl	+ 3.6	− 6.8[b]	∞
NH_4Br	+ 3.9	−10.5[b]	∞
NH_4I	+ 3.2	−13.0[c]	727
NH_4NO_3	+ 6.2	− 5.7[e]	271
$C_2H_5NH_3Cl$	+ 2.2	− 3.6[b]	270
KNO_3	+ 8.4	+ 0.4[e]	168
$NaNO_3$	+ 4.9	− 4.0[c]	∞
$LiNO_3$	− 0.7	−10.8[e]	170
KCl	+ 4.1	− 1.5[h]	

[a] F. D. Rossini, D. D. Wagman, W. H. Evans, S. Levin and I. Jaffe, "Selected Values of Chemical Thermodynamic Properties," Circular of the National Bureau of Standards 500, U. S. Govt. Printing Office, Washington, D. C. (1952). F. R. Bichowsky and F. D. Rossini, "The Thermochemistry of Chemical Substances," Reinhold Publ. Corp., New York, N. Y., 1936. [b] F. C. Schmidt, J. Sottysiak and H. D. Kluge, *J. Am. Chem. Soc.* 58, 2509 (1936). [c] F. C. Schmidt, J. Sottysiak, E. Tajkowski and W. A. Denison, *ibid.*, 63, 2669 (1941). [d] C. A. Kraus and F. C. Schmidt, *ibid.*, 56, 2298 (1934). [e] C. A. Kraus and J. A. Ridderhof, *ibid.*, 56, 79 (1934). [f] E. Hennelly, D. K. Stevens, M. Warren, H. Zuhr and J. Sottysiak with F. C. Schmidt, *ibid.*, 69, 1025 (1947). [g] S. P. Wolsky, E. J. Zdanuk and L. V. Coulter, *ibid.*, 74, 6193 (1952). [h] Table II.

(15) W. M. Latimer and C. Slansky, *J. Am. Chem. Soc.*, **62**, 2019 (1940).

(16) D. D. Eley and D. C. Pepper, *Trans. Faraday Soc.*, **37**, 581 (1941).

(17) F. R. Bichowsky and F. D. Rossini, "The Thermochemistry of the Chemical Substances," Reinhold Publ. Corp., New York, N. Y., 1936.

calculation of the electrostatic energy of interaction of the ions with ammonia as the solvent has been attempted. For this calculation the Bernal–Fowler and Eley–Evans[18] approach has been utilized along with certain modifications introduced more recently by Eley and Pepper,[16] and by Verwey.[19] In accordance with the criticism of the Bernal–Fowler model by Verwey, it has been assumed that orientation of the ammonia molecules composing the primary solvation shell requires negligible work in changing the structure of the solvent when the ammonia molecules coördinated by the ions are brought into their new positions. This assumption appears to be justified in the case of ionic solvation by methyl alcohol[16] and would seem to be more acceptable in the case of ammonia which is capable of forming only weak hydrogen bonds. The coördination number and charge distribution employed have been selected to give as much conformity as possible of the calculated heats of ammonation of the alkali and halide ions with experimental data. These assignments must, as a consequence, be regarded as tentative until further opportunity permits comparisons to be made with more extensive data of appropriate accuracy. It has been assumed that the net energy effects resulting from van der Waals and repulsive forces are negligibly small for the crude model assumed.

It is convenient to itemize ionic ammonation as follows: (a) creation of a hole in the solvent for the ion; (b) electrostatic interaction of ± 1 ions with four molecules of ammonia in the primary solvation shell (six molecules for ± 2 ions); (c) interaction of the ions with the dielectric beyond the primary solvation shell. For step (a) the energy, ΔE, required to create the hole has been obtained from the expression $\Delta H = \Delta E + RT$ where ΔH is the heat of vaporization of ammonia. Although the size of the cavity required depends upon ionic radius and consequently affects ΔE to some extent, we have not taken this factor into account in the calculations. For each mole of ions we have required the vaporization of one mole of ammonia for which $\Delta E = 5$ kcal.

The second energy term, the energy of interaction of the ions with the primary solvent shell, has been calculated from the sum of electrostatic terms, $\Sigma \frac{\alpha e \cdot ze \cdot N}{r}$, where αe and ze are the charges on the hydrogen or nitrogen atoms of the ammonia molecule, and the ion, respectively; and r is the distance between the center of the ion and the N or H atoms of the ammonia molecules. Ionic radii, the van der Waals radius and the structure of ammonia given by Pauling[20] have been employed in the calculations. The ammonia molecule in the primary shell has been regarded as a spherical molecule with the nitrogen atom at the center. For positive ion orientation of the ammonia molecules in the solvation shell at equilibrium, all hydrogens are at equivalent maximum distances from the ion. For negative ion orientation, one hydrogen of the ammonia molecule is located on the straight line connecting centers of the ion and nitrogen atom. In order to account for the observed heat of solvation of the alkali halide gas ion pairs, $+0.4e$ and $-1.2e$ charges have been assigned to the hydrogen and nitrogen atoms, respectively, of the ammonia molecules in the primary shell. As will be seen later, this assignment accounts for the solvation heat of $Ca^{++}(g)$ and is consistent by analogy with the assignment made for the hydration process.[18] The dependence of the coulombic energy of interaction of ± 1 ions with one mole of solvent ammonia in the primary shell is presented graphically in Fig. 1 as a function of the ionic radius. For comparison purposes, the same energy term has been plotted for water[18b] and for methyl alcohol as calculated by Eley and Pepper.[16] It is to be noted that the ammonation and hydration energies of positive ions are essentially the same for the primary shell. Negative ions in ammonia interact with much less energy than in water or methyl alcohol.

Term (c) has been calculated from the Born expression[21]

$$\Delta E_{B.C} = \frac{Nz^2e^2}{2(r_i + 2r_a)}\left(1 - \frac{1}{D}\right)$$

where r_i and r_a are the crystal radius of the ion and the van der Waals radius of the ammonia molecule, respectively. The results of these calculations are summarized in Table IV in which the energy of interaction of the ion with the first solvent shell, 4P, is presented in column 3 and the energy of Born charging follows in column 4. Employing these values as approximate changes in heat content along with the energy required to create the ion cavity, the final values for the solvation heat, ΔH_s, have been obtained and listed in the final column of Table IV. For divalent ions six molecules of ammonia have been assumed to be in the primary shell.

TABLE IV

CALCULATED HEATS OF AMMONATION OF IONS IN LIQUID AMMONIA, KCAL.

	r, Å.	$-4P$	$-\Delta E_{B.C.}$	$-\Delta H_s$
Li^+	0.60	130.8	40.0	166
Na^+	0.95	98.0	36.7	130
K^+	1.33	75.2	33.8	104
Rb^+	1.48	68.0	32.8	96
Cs^+	1.69	58.8	31.5	85
$Ca^{++}(6P)$	0.99	286.8	145.6	427
$Sr^{++}(6P)$	1.13	258.0	141.0	394
$Ba^{++}(6P)$	1.35	222.0	134.5	352
Ag^+	1.26	78.8	34.2	108
$Hg^{++}(6P)$	1.10	264	142	401
$F-$	1.36	42.4	33.5	71
$Cl-$	1.81	29.2	30.7	55
$Br-$	1.95	26.0	29.9	51
$I-$	2.16	22.4	28.7	46

To provide a direct comparison with the hydration process, the hydration energies of the same ions have been recalculated using the molecular and ionic data given by Pauling[20] and the charge dis-

(18) (a) J. D. Bernal and R. H. Fowler, *J. Chem. Phys.*, **1**, 515 (1933); (b) D. D. Eley and M. G. Evans, *Trans. Faraday Soc.*, **34**, 1093 (1938).

(19) E. J. W. Verwey, *Rec. trav. chim.*, **61**, 127 (1942).

(20) Linus Pauling, "The Nature of the Chemical Bond," Cornell University Press, Ithaca, N. Y., 1940.

(21) M. Born, *Z. Physik*, **1**, 45 (1920).

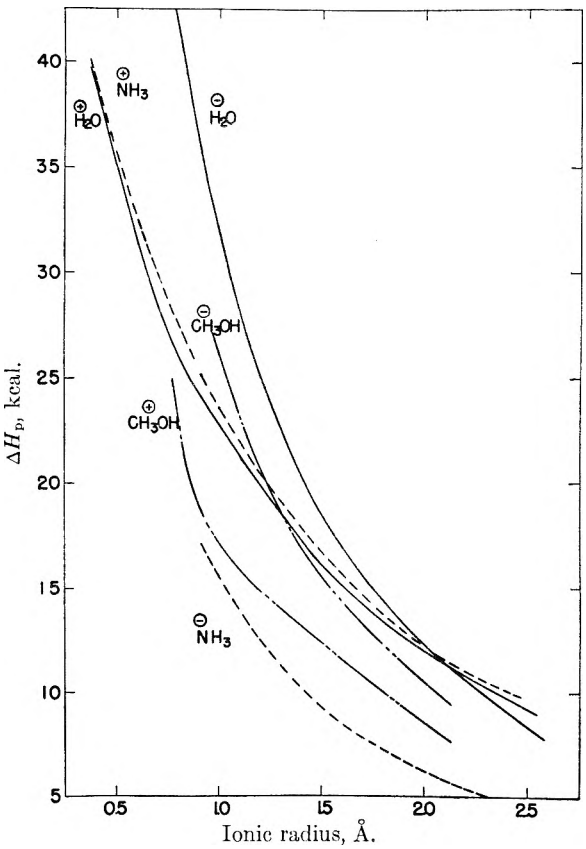

Fig. 1.—Electrostatic energy of interaction of one mole of ±1 ions with one mole of solvent in the primary solvation shell.

tribution employed by Eley and Evans.[18b] These values, which are essentially the same as those calculated by Eley and Evans,[18b] are summarized in column 3 of Table V. The results obtained are presented graphically as a function of ionic radius in Fig. 2 along with the energies of solvation by ammonia and methyl alcohol.

TABLE V

COMPARISON OF HEATS OF SOLVATION OF IONS, KCAL.

Ion	Hydration at 298°K. $\Delta H°$(exp.)	$\Delta H°$(calc.)	Ammonation at 240° $\Delta H°$(exp.)	$\Delta H°$(calc.)
Li^+	145	157	155	166
Na^+	119	119	134	130
K^+	99	94	111	104
Rb^+	93	85	103	96
Cs^+	85	75	...	...
Ag^+	136	106	172	108
Ca^{++}	426	432	459	427
Sr^{++}	391	402	429	394
Ba^{++}	357	357	400	352
Hg^{++}	480	408	544	401
F^-	84	94	...	71
Cl^-	66	62	56	55
Br^-	58	55	53	51
I^-	47	46	45	46

Comparison of the theoretical values for the heats of solvation of ions with experimental data can be made on the basis of ion pairs or on an individual basis if a method for division of the solvation heat is available. It has appeared desirable to make the comparison on the latter

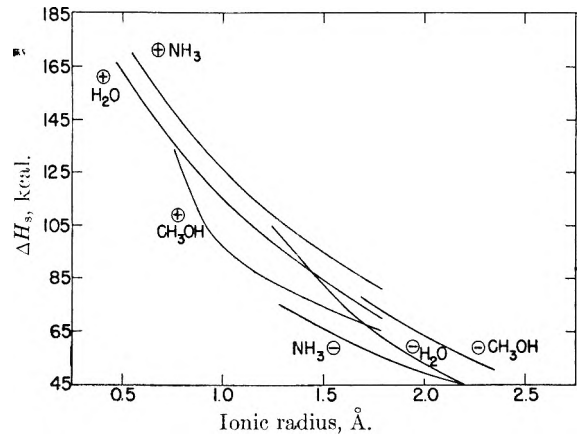

Fig. 2.—Heats of solvation of gas ions (±1).

basis so that comparison with other procedures can be accomplished. For the hydration process, the experimental heat of solvation of the K–Br pair has been divided according to the ratio 94/55 predicted by the theoretical calculations. The values thereby obtained for the hydration heats of $K^+(g)$ and $Br^-(g)$ (99 and 58 kcal., respectively) have then been subtracted from the measured hydration heats of the other gas ion pairs to obtain the individual experimental hydration heats of the ions tabulated in column 2 of Table V.

For the ammonation process the assignment of experimental solvation heats to the various ions has been made in a similar manner with the exception that the division of the experimental heat of ammonation of the Na–Br gas ion pair has been made according to the corresponding theoretical ratio 130/51 since the heat of solution is known with greater certainty in this case. Individual solvation heats in ammonia have been calculated from the thermal data compiled by the Bureau of Standards,[9] the heats of solution in ammonia summarized in Table III and the compilation by Bichowsky and Rossini.[17]

Comparison of the calculated values of the hydration and ammonation energies of ions with the experimental values, obtained in the manner just described, is made in Table V. As is to be seen, the crude model assumed leads to heats of solvation of the alkali metal and halide ions in reasonably good agreement with the observed quantities; and, within 6 to 11%, accounts for the large heats of solvation of Ca^{++}, Sr^{++} and Ba^{++} in liquid ammonia. Although the agreement is not as satisfactory as for the hydration process, it does not appear likely that covalent bond interaction is required to account for the heat of ammonation of the alkaline earth ions. In contrast with this conclusion, we observe that the calculated heats of solvation of Ag^+ and Hg^{++} in ammonia are only 63 and 74%, respectively, of the observed energy effect. This is not surprising in view of the well-known covalent nature of the complexes of these two ions with ammonia which would contribute further stabilization to the solvated ion. The same behavior is also displayed by these ions in water but to a lesser degree.

With the aid of the theoretical curves of Fig. 2 for the simplified model of solvation of ions, a

partial interpretation of the greater heats of solution of monovalent electrolytes in ammonia than in water is possible. For the negative ions, Cl^- and Br^-, the ammonation energies of the gas ions are 7 and 4 kcal. less than the corresponding hydration energies; whereas the solvation energies of I^- in water and ammonia are identical. This smaller energy effect for these halide ions in ammonia is, however, more than compensated for by the greater energy of ammonation of the alkali cations which exceeds the corresponding hydration energies by 10 to 12 kcal. As a consequence, the heats of solution of the alkali chlorides, bromides and iodies are more exothermic in ammonia than in water. This behavior results from the relatively small endothermic energy of vaporization and reorientation in ammonia since all the other exothermic energy terms in the ammonation process are essentially the same as or less than the corresponding terms in the hydration process. This, of course, is to be expected in view of the small energy of the N–H·N hydrogen bond in ammonia which is insufficient to give rise to the structural characteristics of water at 25°. As a consequence of the small interaction energy between liquid ammonia molecules, orientation of solvent molecules around ions in ammonia takes place with essentially no absorption of energy because of hydrogen bond disruption within the solvent.

Heats of solution or precipitation of the sparingly soluble fluorides have not been determined in ammonia and, as a consequence, comparison of solvation heats cannot be made with the calculated values. It is to be expected, however, that heats of solution of the alkali fluorides will be smaller in ammonia than in water since the ammonation energy of $F^-(g)$ is about 23 kcal. less exothermic than the corresponding hydration energy.

An explanation of the differences in the thermochemistry of salts in water and ammonia was also sought with the aid of the model proposed by Verwey for ionic solvation. Solvation heats calculated by this approach did not, however, account for the observed differences in as satisfactory a manner.

Heats of Ammonation of e^- Gas.—The assignment of heats of solvation in ammonia to the alkali and alkaline earth ions in the manner just described now makes possible the calculation of the heat of ammonation of the unpaired gaseous electron. Heats of ammonation of the gas ion pairs, M^+(etal) (g) and $e^-(g)$, are readily calculated from the following equations for which heat content changes are known

$$M^+(g) + e^-(g) = M(s)^9$$

$$M(s) = M^+(am) + {}^1/_2e_2^=(am)^{3,22}$$

$${}^1/_2e_2^=(am) = e^-(am) \quad \Delta H_{240}^\circ \sim 3 \text{ kcal.}^{23}$$

$$M^+(g) + e^-(g) = M^+(am) + e^-(am)$$

Subtraction of the experimental heat of ammonation of the corresponding +1 or +2 cation listed in Table V gives the ΔH for the reaction

$$e^-(g) = e^-(am)$$

On the basis of the thermochemistry of the alkali metals, we obtain for this reaction $\Delta H = -11 \pm 4$ kcal. This value is in poor agreement with the heat of ammonation, −39 kcal., recently calculated by Jolly[6] which has been based on the absolute potential of the calomel electrode, the absolute entropy of chloride ion in aqueous solution and the assumption that the ions Rb^+ and Br^- have equal heats of ammonation. As we have seen from the above considerations, the latter assumption may be questionable on the basis of the model employed in this research which leads to an experimental heat of ammonation of 103 and 53 kcal., respectively, for Rb^+ and Br^-. Correcting for this factor alone, however, does not lead to agreement between the two methods.

The energy of solvation of the "trapped" electron in ammonia has been calculated theoretically by Ogg[24] to be approximately 8 kcal. which is in rough agreement with an upper limit of 18 kcal. experimentally observed by him in photo emission measurements. Although the agreement between these values and the heat of electron solvation obtained in this research still leaves much to be desired, it is encouraging that the various approaches to this problem lead to the approximate agreement observed.

Acknowledgment.—The author and co-workers are indebted to the Research Corporation for a grant-in-aid-of-research that has made this investigation possible. The author expresses thanks to Professor William Argersinger for his helpful suggestions in the preparation of this paper.

(22) S. P. Wolsky, Thesis, Boston University, Mass. (1952).

(23) G. Candela, Thesis, Boston University, Mass. (1952).

(24) R. A. Ogg, O. N. R. Report, "Electronic Processes in Liquid Dielectric Media," Stanford University, Calif., April 11, 1947.

THE ALKALI METAL PHOSPHIDES. III. ELECTROLYSIS STUDIES IN LIQUID AMMONIA[1,2]

BY E. CHARLES EVERS AND JOHN M. FINN, JR.

Department of Chemistry, University of Pennsylvania, Philadelphia, Pa.

Received November 28, 1952

The electrolysis of sodium and potassium dihydrophosphides and of tetrasodium diphosphide has been studied in liquid ammonia. With the former, the anode reaction is given by the equation: $6PH_2^- + 2NH_3 = N_2 + 6PH_3 + 6e^-$, but a more complicated reaction was found to occur in the case of the diphosphide salt. With the latter the ratio of nitrogen evolved to current passed is the same as with the dihydrophosphides, but no large amount of phosphine is produced until electrolysis is approximately 50% completed; then, almost immediately, 50 to 60% of the phosphorus is evolved as phosphine. These results may be accounted for satisfactorily by assuming that the primary anode process involves the oxidation of solvent, namely $8NH_3 = N_2 + 6NH_4^+ + 6e^-$. The protons liberated in this oxidation then become available for reaction with the protophilic diphosphide ion, leading in stages to the several species, P_2H^{-3}, $P_2H_2^{-2}$ and $P_2H_3^-$. A chain mechanism, involving the reaction of solvent with the species $P_2H_3^-$, is postulated to account for the high yield of phosphine, at the point of 50% electrolysis.

Introduction

The present paper[3] describes the results of further investigations relating to the properties of certain alkali metal phosphides and is concerned specifically with the electrolysis of sodium and potassium dihydrophosphides, MPH_2, and of tetrasodium diphosphide, M_4P_2, in liquid ammonia.

As might be expected, these substances are extremely protophilic. When treated with ammonium bromide in liquid ammonia the dihydrophosphides evolve phosphine quantitatively. But with tetrasodium diphosphide a more complicated reaction ensues in which only part of the phosphorus is evolved as phosphine; and the evolution of phosphine only occurs appreciably after approximately two equivalents of ammonium ion are added per mole of salt.

In an earlier study[3b] we obtained indirect evidence indicating that protons apparently may add to the diphosphide ion stepwise in liquid ammonia forming partially hydrogenated species and probably eventually biphosphine, H_4P_2, on complete protonation. However, it was not found practical to carry out a detailed study of this protonation process by treating solutions of the diphosphide with ammonium bromide for at least two reasons: (1) experimentally it was difficult to add small increments of ammonium bromide quantitatively and obtain interpretable results; (2) biphosphine itself was found to decompose in liquid ammonia yielding a substantial part of its phosphorus as phosphine. As a result, it could only be inferred that biphosphine was a likely end-product of the protonation, and that its decomposition was responsible for the evolution of phosphine when the diphosphide salt was treated with an excess of ammonium bromide.

In searching for another attack on the problem it occurred to us that the protonation reaction might be followed effectively by electrolyzing solutions of the salts in liquid ammonia provided the process could be carried out under such conditions that protons together with nitrogen might be produced at the anode, *i.e.*, under conditions involving the oxidation of solvent. In this way protons produced by the oxidation could become available for reaction with the protophilic anions.

A study, such as that outlined above, has been the object of the present investigation and the data secured serve to demonstrate that protonation does in fact take place at the anode under our experimental conditions.

Experimental

1. **Apparatus and Procedure.**—Electrolyses were carried out at the boiling point of liquid ammonia using a cell similar to that described by Foster and Hooper[4] with electrodes approximately 2 cm. apart. The anode (1 cm.^{2}) was of platinum while the cathode (7 cm.^{2}) was of mercury, which was forced into the cell from a reservoir just prior to electrolysis; the mercury served to absorb alkali metal produced at this electrode. The electrolysis current was maintained at some predetermined constant value ranging between 10 and 20 ma. by means of a suitable variable resistance which was inserted in series with a 120-v. d.c. supply line. The current was measured within an accuracy of $\pm 0.25\%$ by means of a calibrated ammeter, and the product of current and time served to measure the quantity of electricity used in electrolysis.

The alkali metal phosphides were prepared *in situ* using samples of metal ranging in size from 2.5 to 7.5 milliatoms, which were weighed accurately. The dihydrophosphides were prepared by passing a gaseous mixture of ammonia and phosphine through a solution of the appropriate metal in liquid ammonia; tetrasodium diphosphide was prepared according to the method described earlier.[3a] Electrolyses of the dihydrophosphides were commenced immediately after purging the system of excess phosphine and hydrogen. With tetrasodium diphosphide it was first necessary to remove the mixture of ammonia and toluene which had been introduced during the preparation of the salt; then the diphosphide was redissolved in approximately 75 cc. of liquid ammonia. In all operations strict precautions were observed to prevent the solutions from coming in contact with the atmosphere.

In carrying out the electrolyses, current was permitted to flow until a predetermined ratio of electricity to starting material was reached. With the dihydrophosphides a steady increase in the voltage was necessary in order to maintain a constant current and a full value of 120 v. was needed as the electrolysis approached completion. With the diphosphide, however, the electrolysis current could be maintained constant with but little adjustment of voltage, and the solutions were fairly good conductors even after the passage of a quantity of current equivalent to the sodium content of the salt. With both systems hydrogen commenced to evolve at the cathode when electrolysis was approximately 80% completed. Evolution of gas began immediately at the anode and continued throughout the electrolysis.

(1) This paper is based on research supported by the Office of Naval Research under contracts N8onr-74200 and Nonr-598(00).

(2) From a thesis by John M. Finn, Jr., submitted in partial fulfillment of the requirements for the Ph.D. degree, 1953.

(3) Previous papers in this series are: (a) E. C. Evers, *J. Am. Chem. Soc.*, **73**, 2038 (1951); (b) E. C. Evers, E. H. Street, Jr., and S. L. Jung, *ibid.*, **73**, 5088 (1951).

(4) L. S. Foster and G. S. Hooper, *ibid.*, **57**, 76 (1935).

After turning off the current substantially all the liquid ammonia, together with gaseous products, was transferred by distillation from the cell into an evacuated flask containing sodium iodide cooled with ice-water. The sodium iodide served to absorb most of the ammonia and caused the gaseous products to concentrate largely in the vapor phase.[3b] Thereafter residual ammonia was separated from other gases using essentially the procedure of Johnson and Pechukas.[5] Finally the products were separated into fractions which were condensable and non-condensable by liquid air. These were measured and then characterized as phosphine and nitrogen, respectively, using standard procedures.

2. **Results.**—In several experiments the cathode mercury was analyzed for total sodium to check the effectiveness of the cathode process. The sodium was extracted with hydrochloric acid and the extract was evaporated to dryness in a platinum vessel. Ammonium chloride was sublimed away and the residue of sodium chloride was weighed. Results of two experiments follow: expt. 21: 1.84 millifaradays electricity, 1.85 milliatoms sodium; expt. 22: 1.85, 1.86, respectively. These results also confirmed the effectiveness of the procedure used in measuring current and time. While analyses were not carried out in most cases, it was assumed that the amount of alkali metal deposited was equivalent to the quantity of electricity employed. Without doubt this assumption was justifiable so long as no cathode gassing was observed, and this took place only after electrolysis was 80% or more completed. When hydrogen did evolve it was necessary to apply a correction to the nitrogen value. This was done within the accuracy of our results by measuring the density of the gas mixtures and computing the percentage of nitrogen.

Molecular weight data were employed almost exclusively to identify the liquid air condensable and non-condensable fractions. The following typical data are presented to indicate the reliability of the results. **Non-condensable**: expt. 6: 1.33 mmoles gas, 37.9 wt. mg., 28.5 mol. wt. found; expt. 13: 0.733, 20.8, 28.4; expt. 16: 0.352, 10.1, 28.7, respectively. Mol. wt. N_2, calcd., 28.0. **Condensable**: expt. 16: 0.318 mmole gas, 10.8 wt. mg., 33.8 mol. wt. found; expt. 18: 0.411, 14.1, 34.3, respectively; mol. wt. PH_3 calcd., 34.1.

In view of the large amount of data collected and that their primary function was to indicate the course of the anode reaction, it has seemed most expedient to present the significant results graphically as shown in Figs. 1 and 2. Since the samples of starting materials varied considerably in size, it has been convenient in presenting these data to divide the variable on both ordinate and abscissa axes, *i.e.*, the yields of products and quantity of electricity passed, respectively, by the number of gram-atoms of phosphorus employed in making up the several alkali metal phosphides. In effect this places all the results on an equivalent basis.

While it is intended to discuss the significance of these plots in detail in the sections to follow, it seems appropriate here to emphasize an extremely important feature of these results, namely, that the ratio of the yield of nitrogen obtained to current passed was constant within experimental error and independent of the nature of the solute being studied. For example, in the case of tetrasodium diphosphide, a value of 0.165 was found as an average taken over some twenty-one experiments in which the quantity of electricity passed ranged from approximately 25 to 100% of equivalence, based on the quantity of sodium used in the preparation of the salt. The maximum deviation from the mean was 0.012 unit or 7%, and it showed no trend with the extent of electrolysis. In the last five experiments, using perfected techniques, it was 3%. As typical examples we submit the following data: expt. 41: 2.04 millifaradays electricity, 0.338 mmole N_2, 0.166 ratio N_2 to electricity; expt. 42: 3.61, 0.610, 0.169; expt. 43: 3.15, 0.517, 0.164, respectively. The agreement in the case of the dihydrophosphides was even better, being less than 2%. This is brought out in Fig. 1, where the yield of nitrogen plotted against the extent of electrolysis results in a straight line of slope 0.167, which signifies that the ratio of moles of nitrogen formed to faradays of electricity passed is 1:6.

Whereas the production of nitrogen at the anode is evidently independent of the salt type, the yield of phosphine is very much a function of the nature of the anion which is present in solution. In the case of the dihydrophosphides (Fig. 1) we obtain a linear relation on plotting moles of phosphine evolved against faradays of electricity; in fact, the resulting curve has a slope of unity, signifying that one mole of phosphine is obtained per equivalent of electricity. But in the case of solutions of tetrasodium diphosphide, a sigmoidal type of curve results, as shown by Fig. 2; and the curve rises almost vertically when electrolysis is approximately 50% completed, *i.e.*, at a value of unity on the abscissa axis. It may be pointed out that although the yield of phosphorus as phosphine was usually determined directly, in a few cases the residue was analyzed for total phosphorus and the volatilized phosphorus was computed by difference; these data are represented by solid circles in Fig. 2. Such a procedure was usually legitimate since in those cases when both phosphine and residual phosphorus were determined the material balance was entirely satisfactory.

One other point bears emphasis in order that a correct interpretation may be given these data. First of all it must be realized that each datum shown in Figs. 1 and 2 represents a complete and independent experiment with electrolysis carried to the value given by the abscissa before the products were quantitatively removed for analyses. In this connection it was found unnecessary completely to evaporate our solutions after electrolysis in order to obtain quantitative recovery of volatile products. This is significant since it indicates that any reaction which produces phosphine or nitrogen is completed once the electrolysis is stopped. Thus the data do not refer to equilibrium quantities of volatile products but rather to quantities produced in completed reactions. Furthermore, secondary reactions, which conceivably might have also given rise to these products, apparently do not occur as the residues are taken to dryness.

Electrolysis of Alkali Metal Dihydrophosphides

The over-all reaction at the anode during the electrolysis of the alkali metal dihydrophosphides may be represented by the equation

$$6PH_2^- + 2NH_3 = 6PH_3 + N_2 + 6e^- \qquad (1)$$

where six equivalents of electricity serve to liberate one mole of nitrogen and six moles of phosphine. As may be seen by reference to Fig. 1, the experimental data are in good accord with this equation. The solid lines were computed according to the above expression; the points are experimental. As noted above, the slopes of the lines establish the values of the coefficients for phosphine and nitrogen, respectively, in equation (1).

An entirely analogous result has been obtained by Teal and Kraus,[6] who found, on electrolyzing solutions of sodium germanyl, that the anode reaction could be expressed by the equation

$$6GeH_3^- + 2NH_3 = 6GeH_4 + N_2 + 6e^- \qquad (2)$$

It is evident that solvent must be involved intimately in these reactions since, effectively, for every six equivalents of electricity passed two moles of solvent are completely stripped of their hydrogen. While the complexity of the processes leading to this end result cannot be underemphasized, this behavior, *i.e.*, the oxidation of solvent, is not unique. In aqueous systems, for example, whenever conditions are favorable (high discharge potential for the anion, low concentration of solute, etc.) electrolysis very often leads to the evolution of oxygen and accumulation of hydrogen ions at the anode. Consequently, in liquid ammonia under suitable circumstances, the evolution of nitrogen is not unexpected.

However, an outstanding feature of the present study, as well as that on sodium germanyl, lies in

(5) W. C. Johnson and A. Pechukas, *J. Am. Chem. Soc.*, **59**, 2065 (1937).

(6) G. K. Teal and C. A. Kraus, *ibid.*, **72**, 4706 (1950).

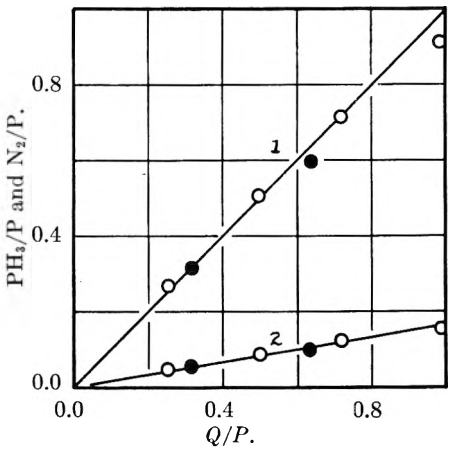

Fig. 1.—Electrolysis of alkali metal dihydrophosphides in liquid ammonia; O, $NaPH_2$; ●, KPH_2. Curve 1, PH_3/P, moles phosphine evolved per gram-atom phosphorus in the alkali metal salt. Q/P, faradays of electricity passed to gram-atoms phosphorus in the alkali metal salt. Curve 2, moles nitrogen evolved to gram-atoms phosphorus in the alkali metal salt. Solid lines computed according to equation (1); points, experimental.

the fact that the anions are converted quantitatively to the corresponding hydrides during electrolysis. How such a transformation can be brought about appears obscure until it is recalled that normally, in the oxidation of ammonia, we should expect protons to be liberated along with nitrogen at the anode. In view of the highly protophilic nature of the PH_2^- and GeH_3^- ions, it seems reasonable to suppose that they should combine with those protons immediately in a secondary reaction forming the respective hydrides. In effect, then, if we are willing to assume that with these systems the primary anode reaction is the oxidation of solvent, we have here a relatively simple means of accounting for the evolution of phosphine or germane. And, in addition, it may be pointed out that this formulation of the problem has proved particularly fruitful in interpreting the results obtained on electrolyzing solutions of tetrasodium diphosphide which will be discussed in the following section.

Admittedly we have no direct experimental evidence for the above mechanism and several alternative schemes leading to the same stoichiometrical end result might be offered to account for the anode products. However, any mechanism calling for the direct discharge of PH_2^- ions seems inferior for our present purposes. As a matter of fact, had this reaction occurred to any appreciable extent, one might have expected some conversion to biphosphine, H_4P_2. But such a process would have resulted in lower yields of both nitrogen and phosphine than are called for by equation (1) and there is no evidence pointing in this direction. It also seems unlikely that amide ions might be present in sufficiently high concentrations to undergo appreciable direct discharge. The very fact that stable solutions of the alkali metals may be obtained would indicate that the self-ionization of ammonia is practically nil.[7]

(7) The ion product for ammonia is reported to be 1.9×10^{-33} at $-50°$: V. A. Pleskov and Monoszon *Acta Physicochim., U.S.S.R.*, **1**, 725 (1935).

A more satisfying mechanism for the formation of molecular nitrogen and liberation of protons would seem to be one patterned after that suggested by Eyring, *et al.*,[8] to account for the overvoltages of hydrogen and oxygen in aqueous systems. As an essential feature of this theory it is proposed that these gases result from a break-down of the solvent itself and are not necessarily formed by the discharge of hydrogen or hydroxyl ions. It seems likely that some such mechanism is operative during the electrolysis of the alkali metal phosphides under our experimental conditions.

Electrolysis of Tetrasodium Diphosphide

Data showing the course of phosphine evolution on electrolyzing solutions of tetrasodium diphosphide are presented graphically in Fig. 2. As in Fig. 1, the ratios, PH_3/P and Q/P, represent the moles of phosphine evolved and the faradays of electricity passed, respectively, both divided by the gram-atoms of phosphorus used in preparing the diphosphide salt.

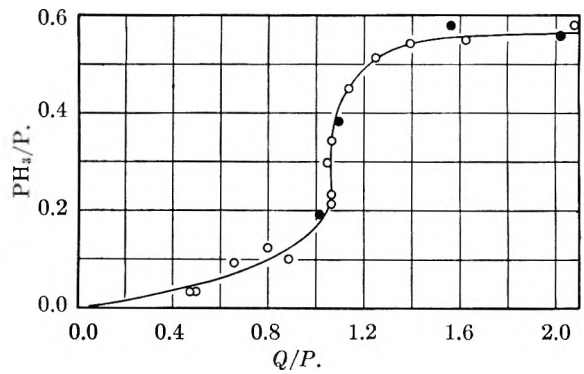

Fig. 2.—Electrolysis of tetrasodium diphosphide in liquid ammonia: PH_3/P, moles of phosphine evolved per gram-atom of phosphorus in the diphosphide; Q/P, the ratio of faradays of electricity passed to gram-atoms of phosphorus in the diphosphide: O, data based on phosphine evolved; ●, data based on residual analyses.

Obviously the situation here is more complicated than with the dihydrophosphides and there is no simple relation between the yield of phosphine and the extent of electrolysis. But a clue as to what may be occurring is given by the constancy of the production of nitrogen. As noted above, the average ratio of moles of nitrogen produced to equivalents of electricity passed was 0.165. This certainly suggests that we should consider the oxidation of solvent among the primary anode reactions since the equation representing this reaction, namely

$$8NH_3 = N_2 + 6NH_4^+ + 6e^- \qquad (3)$$

predicts a nitrogen to electricity ratio of 1:6 or 0.167. Then, as in the case of the dihydrophosphides, secondary reactions of protons with solute might account for the evolution of phosphine.

On reference to Fig. 2 it may be noted that very little phosphine was evolved until approximately 50% electrolysis, *i.e.*, up to a value of unity on the abscissa axis. At this point the curve has a vertical segment which can only mean that the addition of

(8) H. Eyring, S. Glasstone and K. J. Laidler, *Trans. Electrochem. Soc.*, **76**, 145 (1939).

a few ammonium ions (by electrolysis of solvent) in this region causes the evolution of an exceedingly large number of phosphine molecules. In fact, substantially all the phosphine is evolved at this point. Thereafter, the production of phosphine falls off measurably with additional electrolysis and the curve approaches the horizontal.

The above results may be more readily interpreted by reference to Fig. 3. Here there is plotted what might be termed the "solute composition" *versus* the extent of electrolysis. The ordinate values, H/P', represent the equivalents of hydrogen introduced by electrolysis minus those evolved as phosphine divided by the gram-atoms of phosphorus remaining in the solution; the axis of abscissas is the same as that employed in preparing Fig. 2.

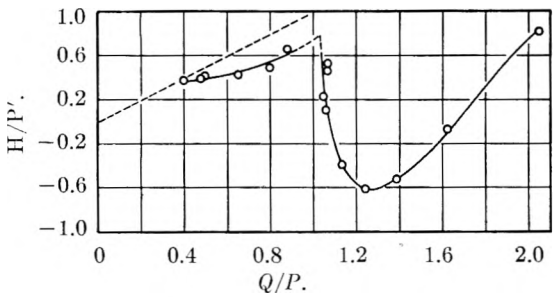

Fig. 3.—Electrolysis of tetrasodium diphosphide in liquid ammonia; curve for "solute" composition. H/P', gram-atoms hydrogen introduced by electrolysis minus that evolved as phosphine over the gram-atoms of phosphorus remaining in solution. Q/P, faradays electricity passed to gram-atoms phosphorus in the alkali metal salt. Dotted line represents composition curve if no phosphorus were evolved as phosphine.

Three distinct regions, marked by breaks in the curve, may be noted in Fig. 3. The first region ranges from zero on the abscissa axis, Q/P, to approximately 0.5; the second includes the region between approximately 0.5 and 1.0; the third extends to 2.0, where electrolysis may be assumed to be complete, based on the number of faradays needed to electrolyze out the sodium ions.

Little or no phosphine evolution occurred for Q/P values between 0 and approximately 0.5, *i.e.*, before electrolysis was about 25% complete. This we interpret as being due to the absorption of protons by the diphosphide ion, forming the species P_2H^{-3} according to the equation

$$P_2^{-4} + NH_4^+ = P_2H^{-3} + NH_3 \qquad (4)$$

If phosphine were not evolved, the composition curve would follow the dotted line. However, after a Q/P value of approximately 0.5 some phosphine is produced, the curve bends somewhat toward the abscissa axis and the experimental points fall under the dotted line. Between a Q/P value of 0.5 and 1.0 it seems reasonable to propose that the principal reaction is one between protons liberated at the anode and protophilic P_2H^{-3} ions which leads to the species, $P_2H_2^{-2}$, according to the equation

$$P_2H^{-3} + NH_4^+ = P_2H_2^{-2} + NH_3 \qquad (5)$$

The existence of a dihydrodiphosphide ion also seems reasonable on the basis of certain chemical studies reported previously[3b] and the species appears to be stable in liquid ammonia solution. To summarize the chemical evidence: (1) When two equivalents of ammonium bromide are added to solutions of tetrasodium diphosphide there is a perceptible change in color and very little phosphine is evolved. (2) If less than an equivalent of sodium metal is added to the above solution the blue color of free metal persists after many hours standing and no gas is evolved. This attests to the absorption of protons by the protophilic diphosphide ions and to the non-reducibility of the resulting product. Thus, evidence presented in (1) and (2) suggests that reaction between ammonium and diphosphide ions has proceeded to the stage indicated by equation (5) above.

In light of the evidence presented above we are led to conclude that the ion, $P_2H_2^{-2}$, exists and is stable in liquid ammonia, and that the evolution of phosphine in region 2 must result from a side reaction in which solvent may be involved. Undoubtedly, in this region there is competition for protons between the species P_2H^{-3} and $P_2H_2^{-2}$ and it does not seem unlikely that the latter may in part be converted to a more highly protonated species, which may either decompose directly or react with solvent evolving phosphine, perhaps by some such mechanism as is discussed below.

In region 3 there is direct evidence that solvent enters into reaction with one or more of the hydrogenated diphosphide species. As noted above, in the neighborhood of unity on the abscissa axis, the composition curve drops extremely rapidly from an ordinate value of approximately 0.6 to a value of −0.6. Negative values for the ordinate signify that more hydrogen has been evolved as phosphine than was introduced as protons by electrolysis. This can only mean that, in addition to anodic oxidation of solvent, there has been chemical attack of solvent. Furthermore, since this rapid drop in the curve occurs over such a small range of Q/P values, this extensive production of phosphine in some way must have been initiated by the anodic processes, probably through the introduction of protons. Though we refrain from offering a concrete mechanism for this process, we should like to propose a tentative explanation—and we feel its validity may be tested by further experiment—as pointed out below.

Referring back to Fig. 2, it is to be noted that after the rapid break in the curve, the PH_3/P values increase gradually and then level off at approximately 0.58 as electrolysis is continued, indicating that after approximately 50% electrolysis little or no additional phosphine is liberated and that most of the protons produced at the anode thereafter remain in solution as such or otherwise enter into reaction. At 100% electrolysis, then, roughly 58% of the phosphorus has been volatilized as phosphine. Since this value is not far removed from that obtained by the direct decomposition of biphosphine in liquid ammonia,[9] it seems likely that biphosphine may be involved as an end-product in the protonation process. At any rate, if we may assume this to be true, we have a tenta-

(9) Values ranging between 60 and 63% have been obtained; unpublished observations, E. H. Street, Jr., this Laboratory.

tive explanation for the form of the curve in the neighborhood of the point of 50% electrolysis, as explained below.

It would appear in the first place that the proton-catalyzed reaction is necessarily of the chain type, *i.e.*, a species produced by the absorption of protons initiates a reaction with solvent and is regenerated; and the chain-breaking step in which phosphine is produced is the decomposition of some other species, say biphosphine, which is one of the products of the chain reaction. Since it appears unlikely that either the $P_2H_2^{-2}$ ion or biphosphine undergoes reaction with the solvent[10] we are forced to attribute the catalytic activity to an intermediate species which logically may be formed by further protonation of the $P_2H_2^{-2}$ ion, namely, $P_2H_3^-$. In order for reaction to occur with solvent the $P_2H_3^-$ ion appears to be considerably more protophilic than its precursors. We suggest that reaction with solvent occurs according to the equation

$$P_2H_3^- + NH_3 = P_2H_4 + NH_2^- \qquad (6)$$

Then, to establish the chain, biphosphine reacts with the dihydrophosphide ion, which is present in considerable quantity at the break-point in the curve, according to the equation

$$P_2H_4 + P_2H_2^{-2} = 2P_2H_3^- \qquad (7)$$

Hence, by the addition of very few protons we may have an extensive reaction with solvent. The chain-breaking step then involves the somewhat slower decomposition of biphosphine leading to the evolution of phosphine. It would seem possible that the above mechanism might be verified by an attempt to determine whether amide ions are produced in the region of 50% electrolysis. But in any event, this research seems to demonstrate quite well that the diphosphide ion adds protons stepwise and is converted into partially hydrogenated species at the anode, and it suggests that the electrolytic method might be generally useful in investigating the behavior of protophilic anions.

In conclusion it is of interest to note that the mechanism postulated above, involving as it does the species $P_2H_3^-$, serves to augment certain of our previous deductions regarding the properties of the diphosphide ion which were based on chemical evidence.[3b] For example, as noted in the introduction, when solutions of the diphosphide are treated with an equivalent amount or more of ammonium bromide, phosphine is evolved much as in the electrolytic method. Undoubtedly in this case the reaction yields biphosphine by a stepwise process, but, probably, solvent is not involved since here the $P_2H_3^-$ ion would have protons available in a much more active form, namely, as ammonium ions. Furthermore, it provides a fairly satisfactory explanation for the course of the reaction whereby diphosphide ions may be reduced to dihydrophosphide ions. To accomplish this a solution containing tetrasodium diphosphide and free sodium is treated with four equivalents of ammonium bromide[3b]; reaction then occurs according to the equation

$$P_2^{-4} + 2e^- + 4NH_4^+ = 2PH_2^- + 4NH_3 \qquad (8)$$

Since a solution of the diphosphide salt containing two equivalents of metal was shown to be stable toward reduction, it was suggested that protonation probably proceeded stepwise through the stage $P_2H_2^{-2}$ to biphosphine before the P–P bond was subject to attack by the solvated electron. In light of the present research, it would seem that, under conditions leading to reaction according to equation (8), the species, $P_2H_3^-$, because of its extremely protophilic character, might have only a transitory existence; consequently, conversion from $P_2H_2^{-2}$ to P_2H_4 occurs immediately as ammonium bromide is added and the latter then undergoes attack by the solvated electron.[11]

(10) The solid residue from the decomposition of biphosphine in liquid ammonia contains nitrogen. This may be substantially removed as ammonia by pumping and heating; consequently, solvent does not appear to be involved chemically; unpublished observation, this Laboratory.

(11) Even though unstable in liquid ammonia, biphosphine may be quantitatively converted by sodium to the dihydrophosphide salt under suitable conditions; unpublished observations, E. H. Street, Jr., this Laboratory.

POLAROGRAPHY IN LIQUID AMMONIA. V.[1] THE POLAROGRAPHY OF LEAD, CADMIUM, ZINC, NICKEL, COBALT, CHROMIUM AND ALUMINUM IONS

By A. D. McElroy and H. A. Laitinen

University of Illinois, Urbana, Illinois

Received November 28, 1952

The reduction of the Pb(II), Cd(II), Ni(II), Zn(II), Co(III), Co(II) and Cr(III) ions has been studied at the dropping mercury electrode in anhydrous liquid ammonia. Of these ions, a reversible reduction was found for Pb(II), Cd(II), and for the first step in the reduction of Cr(III). The electrode reaction of Ni(II) was clearly irreversible, while that of Zn(II) deviated less from reversible behavior. The Co(III), Co(II) system was irreversible at the dropping mercury electrode. The second steps in the reduction of Co(III) and Cr(III) were not well defined. The Al(III) ion was not reduced at the dropping mercury electrode at potentials more positive than that required for electron dissolution. Attempts to produce stable Al(I) or Al(II) ions by chemical reduction of Al(III) and by anodic oxidation of metallic aluminum, and to detect these ions by means of the dropping mercury electrode, were unsuccessful.

Previous studies at the dropping mercury electrode in anhydrous liquid ammonia have included investigations of the mercury pool anode,[2] thallium(I), copper(II), the ammonium ion and molecular oxygen,[1] the alkali metal ions,[3] the electron electrode[4] and the alkaline earth ions.[5] In this work polarographic techniques have been used in an investigation of the electrochemical behavior of several other ions.

Experimental

The apparatus and experimental techniques, with the exception of a few minor modifications, have been previously described in detail.[2] The reference electrode consisted of the mercury pool; the potential and characteristics of this electrode have been previously determined.[2] The half-wave potentials were checked by the pilot ion method, using either the Tl(I) or the Cd(II) ion as the reference. The current–voltage curves were recorded with a Sargent model XXI polarograph. The measured potentials were checked with a student type potentiometer.

Materials.—The ammonia, which was obtained from a cylinder of the commercial product, was freed of oxygen and water by condensation over potassium. Anhydrous aluminum iodide was prepared by a method outlined by Fitzgerald.[6] The product, freed of iodine by fractional sublimation, was pure white in color. Hexamminecadmium(II) nitrate and tetramminezinc(II) nitrate were precipitated from aqueous ammonia-saturated solutions by the addition of ethyl alcohol; the precipitates were washed with alcohol and ether. Hexamminenickel(II) iodide[7] and hexamminecobalt(III) nitrate[8] were prepared by methods given in "Inorganic Syntheses." Hexamminechromium(III) iodide was synthesized by a method described by Jorgensen.[9] The product was purified by three recrystallizations from a 1:1 HI solution. Cobalt(II) chloride and cobalt(II) iodide were prepared by oven-drying the hydrated salts at 115° and 135°, respectively.

The supporting electrolytes consisted of potassium iodide, potassium nitrate, ammonium iodide and tetrabutylammonium iodide. The first three salts, of reagent grade, were oven-dried at 100°. Tetrabutylammonium iodide was purified by recrystallization from anhydrous ethyl acetate.

Results and Discussion

Reduction of Lead(II) Ion.—In the presence of a trace of methyl cellulose and with a supporting electrolyte of 0.1 *M* KI or 0.1 *M* NH_4I the Pb(II) ion gave a wave with no maximum. The value of the reciprocal slope of a plot of log $(i_d - i)/i$ *vs.* E, 0.027 as compared with the theoretical value of 0.024 for a two electron reduction at −36°, indicates that the electrode reaction is reversible.

Pleskov and Monosson[10] have calculated that the standard potential of the Pb–Pb(II) electrode is 0.043 v. *versus* the lead–0.1 *N* lead nitrate electrode at −50°. With this information and data concerning the potential of a saturated lead amalgam,[11,12] the theoretical half-wave potential for Pb(II) is calculated, neglecting temperature differences, to be 0.04 v. *versus* the lead–0.1 *N* lead nitrate electrode.

While the polarographic wave for the Pb(II) ion is very regular in appearance, it was observed that in general polarograms recorded on freshly prepared solutions were somewhat erratic. This behavior was accentuated when samples of lead iodide were added to solutions containing ammonium ion at millimolar concentrations, or when a small quantity of ammonium ion was added to neutral or slightly acidic solutions of lead iodide. Under these conditions the solutions had to be allowed to stand for about 30 minutes to obtain a well developed polarogram. The wave, in freshly prepared solutions, appeared to be roughly divided into two parts, the first occurring about 0.2 volt before the second, which coincided with the upper portion of the normal wave. The first wave was very ragged in appearance; its height on the first polarogram taken after preparation of the solution, was about 0.8 of the combined heights of both waves. It disappeared completely in about 30 minutes; the limiting current remained unchanged during this period of time.

These facts can be most readily explained in terms of a slow reaction involving the Pb(II) ion. Franklin[13] reports that this ion is extensively ammonolyzed in a neutral solution. The ammonobasic salts NH_2–Pb–NH–Pb–NO_3 and Pb=N–Pb–I·2NH_3 can be isolated from such a solution. The dissolved salts are converted to insoluble

(1) For paper IV of this series, see H. A. Laitinen and C. E. Shoemaker, *J. Am. Chem. Soc.*, **72**, 4975 (1950).

(2) H. A. Laitinen and C. E. Shoemaker, *ibid.*, **72**, 663 (1950).

(3) H. A. Laitinen and C. J. Nyman, *ibid.*, **70**, 2241 (1948).

(4) H. A. Laitinen and C. J. Nyman, *ibid.*, **70**, 3002 (1948).

(5) C. J. Nyman, *ibid.*, **71**, 3914 (1949).

(6) F. F. Fitzgerald, *ibid.*, **29**, 1693 (1907).

(7) L. F. Audrieth, *et al.*, "Inorganic Syntheses," Vol. III, McGraw-Hill Book Co., Inc., New York, N. Y., 1950, p. 194.

(8) W. C. Fernelius, *et al.*, "Inorganic Syntheses," Vol. II, McGraw-Hill Book Company, Inc., New York, N. Y., 1946, p. 218.

(9) S. M. Jorgensen, *J. prakt. Chem.*, [2] **30**, 22 (1884).

(10) W. A. Pleskov and A. M. Monosson, *Acta Physicochim. U.R.S.S.*, **1**, 871 (1935).

(11) R. H. Gerke, *J. Am. Chem. Soc.*, **44**, 1684 (1922).

(12) C. S. Hoyt and G. Stegeman, This Journal, **38**, 753 (1934).

(13) E. C. Franklin, "The Nitrogen System of Compounds," Reinhold Publishing Corp., New York, N. Y., 1935, pp. 75, 76.

ammonobasic salts by the addition of potassium amide. It is reasonable to assume that the attainment of ammonolytic equilibrium is rather slow, since the ions involved are rather complex. To explain the partial reduction of Pb(II) at early potentials, one may postulate the existence for a short time of ions, probably relatively simple, incompletely ammonolyzed ions, which are more readily reduced than the ions which exist at equilibrium conditions.

Polarograms of the lead(II) ion, with tetrabutylammonium iodide as the supporting electrolyte, did not furnish evidence of a reduction to the normal plumbide or to one of the polyanions, such as Pb_7^{4-} and Pb_9^{4-}, which have been reported in the literature.[14,15]

TABLE I

Ion	Concn. $\times 10^3$	I[a]	$-E_{1/2}$,[b] volt	Slope, E *vs.* log $i_d - i/i$
Pb(II)	1.33[c]	4.80	0.01	0.027
	0.44[d]	4.83	.01	.026
	1.45[d]	4.76	.01	.028
Cd(II)[e]	0.62	4.76	.45	.028
	1.23	4.70	.45	.028
Zn(II)[e]	0.33	4.95	.89	.037
	1.22	5.07	.89	.035
Ni(II)[e]	0.68	4.62	.79	.042
	1.15	4.75	.79	.046

[a] $I = i_d/Cm^{2/3}t^{1/6}$. [b] *Versus* lead–0.1 *N* lead nitrate electrode. [c] 0.1 *M* KI as supporting electrolyte. [d] 0.1 *M* NH_4I as supporting electrolyte. [e] 0.1 *M* KNO_3.

Reduction of Cadmium(II) Ion.—The reduction of Cd(II) at the dropping mercury electrode proceeded in one reversible two-electron step, the plot of log $(i_d - i)/i$ *vs.* E being a straight line with a reciprocal slope of 0.028. The wave possessed a slight maximum which was effectively suppressed by a trace of methyl cellulose. The diffusion current was directly proportional to concentration.

Pleskov and Monosson[10] constructed the cell

$$\bar{\text{Cd}}\,|\text{Cd(NO}_3)_2\ (0.1\ N)\,|\text{KNO}_3\ (\text{satd.})|\,\text{Pb(NO}_3)_2\ (0.1\ N)\,|\dot{\text{Pb}}$$

and found its e.m.f. to be 0.522 v. at −50°. Using the Nernst equation, the standard potential of the cadmium–cadmium(II) electrode was calculated to be −0.48 v. *versus* the lead–0.1 *N* lead nitrate electrode. Neglecting temperature differences, the value of the theoretical half-wave potential of Cd(II), calculated from the standard potential and the potential of a saturated cadmium amalgam,[15,17] is −0.41 v.

Reduction of Nickel(II) Ion.—The polarographic wave for the reduction of the Ni(II) ion, with supporting electrolytes of 0.1 *M* potassium nitrate or 0.1 *M* potassium iodide, was entirely symmetrical in form, even in the absence of a maximum suppressor. Of the dipositive ions investigated, however, its reduction appeared to be the most irreversible, the reciprocal slope of the plot of log $(i_d - i)/i$ *vs.* E being 0.042 to 0.050. In this respect the ammonated Ni(II) ion is similar to the aquated Ni(II) ion. The half-wave potential of the current-voltage curve was −0.79 v. There is no value in the literature for the standard potential, in liquid ammonia, of the nickel–nickel(II) electrode, hence it is not possible to calculate a theoretical half-wave potential. The observed half-wave potential may be appreciably more negative than the true reversible half-wave potential.

Reduction of Zinc(II) Ion.—The polarographic wave for Zn(II), with a supporting electrolyte of 0.1 *M* potassium nitrate or 0.1 *M* potassium iodide, was characterized by a maximum which was nearly completely suppressed by a trace of methyl cellulose. The plot of log $(i_d - i)/i$ *vs.* E was a straight line with a reciprocal slope of 0.035 to 0.039; this indicates a significant departure from reversibility, although the effect may be due in part to incomplete suppression of stirring at the dropping mercury electrode.

Pleskov and Monosson[10] measured the e.m.f. of the cell

$$\bar{\text{Zn}}\,|\text{Zn(NO}_3)_2\ (0.1\ N)\,|\text{KNO}_3\ (\text{satd.})\,|\text{Pb(NO}_3)_2\ (0.1\ N)\,|\dot{\text{Pb}}$$

and found it to be 0.848 v. at −50°. The value of the standard potential of the zinc–zinc (II) electrode was calculated by means of the Nernst equation to be −0.81 v. at −50°. Using this value and the potential of a saturated zinc amalgam[18,19] the theoretical half-wave potential of Zn(II) is calculated to be −0.80 v. The disagreement between this value and the observed half-wave potential, −0.89 v., may be attributed largely to the lack of complete reversibility in the reduction of Zn(II) at the dropping mercury electrode.

The Reduction of Cobalt(III) and Cobalt(II) Ions.—Cobalt(III) was reduced, as expected, in two steps, the diffusion current of the second wave being twice that of the first. The first wave was well developed in the presence of either potassium nitrate or tetrabutylammonium iodide as the supporting electrolyte. Its half-wave potential was +0.05 v.; neglecting differences of diffusion coefficients and activity coefficients of the cobaltic and cobaltous ions, this potential should be close to the standard potential of the cobaltic–cobaltous ion electrode if the reduction may be considered reversible. The reciprocal slope of the plot of log $(i_d - i)/i$ *vs.* E was 0.058, as compared to the theoretical value of 0.047; on this basis the electrode reaction would appear to be nearly reversible. The assumption of reversibility is in this case without justification, however, as the Co(II) ion was not oxidized at potentials more negative than that at which mercury starts to dissolve anodically.

According to Bjerrum,[20] Co(II) is extensively ammonated only in the presence of a large excess of ammonia, in aqueous systems. The hexamminecobalt(III) ion is not reversibly reduced in aqueous solutions.[21] If the reduction involved only the transfer of an electron without loss of ammonia of coördination it might be expected to be reversible.

(14) C. A. Kraus, *Chem. Revs.*, **8**, 251 (1931).

(15) E. Zintl, J. Goubeau and W. Dullenkopf, *Z. physik. Chem., Abt. A*, **154**, 1 (1931).

(16) G. A. Hulett, *Trans. Am. Electrochem. Soc.*, **7**, 333 (1905).

(17) C. E. Teeter, *J. Am. Chem. Soc.*, **53**, 3917, 3927 (1931).

(18) W. J. Clayton and W. C. Vosburgh, *ibid.*, **58**, 2093 (1936).

(19) J. N. Pearce and J. F. Eversole, THIS JOURNAL, **32**, 209 (1928).

(20) J. Bjerrum, "Metal Ammine Formation in Aqueous Systems," P. Haase and Sons, Copenhagen, 1941, p. 189.

(21) H. A. Laitinen, J. C. Bailar, H. F. Holtzclaw and J. V. Quagliano, *J. Am. Chem. Soc.*, **70**, 2999 (1948).

Reasoning on this basis one might have predicted that the cobaltic–cobaltous electrode would be reversible in liquid ammonia. A strict parallel cannot be drawn between the water and ammonia systems, however, as in liquid ammonia both ions are undoubtedly subject to ammonolysis as well as ammonation, and therefore probably do not exist as simple ammonated ions[22] as does the hexamminecobalt(III) ion in water. The irreversibility of the cobaltic–cobaltous system in liquid ammonia may, in accordance with the above statement, be due to a low attainment of an ammonolytic equilibrium.

The second step in the reduction of Co(III) exhibits a pronounced maximum which was not suppressed by methyl cellulose. The half-wave potential, about −1.1 v., could not be established accurately. The diffusion current plateau was well defined, however.

Reduction of Cobalt(II) Ion.—As stated previously, this ion did not oxidize at the dropping mercury electrode. The reduction of Co(II) to the amalgam occurred at a half-wave potential of −1.1 v. The polarographic wave had a maximum, and appeared to be very similar to the wave for the second step in the reduction of Co(III).

Table II

Ion	Concn. × 10³	I A[a]	I B[b]	$-E_{1/2}$, volt A[a]	$-E_{1/2}$, volt B[b]	Slope, E vs. $\log (i_d - i)/i$ A[a]	Slope, E vs. $\log (i_d - i)/i$ B[b]
Cr(III)	0.33[f]	2.46		0.74		0.048	
	1.03[c]	2.51		.73		.051	
	0.43[d]	2.25	4.32	.73	1.41	.057	0.08
	1.01[d]	2.37	5.07	.74	1.46	.059	0.09
Co(III)	0.49[e]	2.24		− .05		.058	
	1.56[e]	2.14		− .04		.059	
	0.46[d]	2.15	4.25	− .04	(1.1)	.058	
	1.06[d]	2.24	4.20	− .04	(1.1)	.060	

[a] First wave. [b] Second wave. [c] 0.1 *M* NH_4I. [d] Saturated solution of tetrabutylammonium iodide. [e] 0.1 *M* KNO_3.

Reduction of Chromium(III) Ion.—Here also a two-step reduction was found. The first wave was preceded by a prewave, with either tetrabutylammonium iodide or ammonium iodide as the supporting electrolyte. The height of this prewave, 0.25 μa., did not vary with changing concentration of Cr(III). Otherwise the wave form seemed to be quite normal. The half-wave potential, −0.79 v., was the same in both media. The reduction was reversible in acid solutions, but departed somewhat from reversibility in neutral solutions, the reciprocal slopes of plots of log $(i_d - i)/i$ *vs.* E being 0.049 and 0.058, respectively. The diffusion limited current for this wave was proportional to the concentration of Cr(III) if the prewave was considered as part of the first step.

The second wave, obtained only with tetrabutylammonium iodide as the supporting electrolyte, was marred by a slight irregularity on the diffusion current plateau about 0.2 v. after diffusion limited current had been attained. At concentrations of Cr(III) greater than 0.5 millimolar, the irregularity became a pronounced hump, the currents on either side of the hump being equal. The wave height of the second step was only approximately (2.0 ± 0.1) twice that of the first step.

Experiments with Aluminum(III) Ion.—Jirik and Davidson[23] have recently postulated a transitory existence of the Al(I) ion to account for results obtained with the anodic oxidation of aluminum in anhydrous acetic acid. Bennett, Kleinberg and Davidson[24] advanced a similar explanation for results of experiments on the anodic oxidation of aluminum in liquid ammonia. Watt, Hall and Choppin[25] titrated liquid ammonia solutions of aluminum iodide with potassium, potentiometrically, and concluded that the Al(III) ion was reduced stepwise to Al(II) and Al(I).

Experiments performed in this Laboratory have not furnished evidence of the existence of stable lower oxidation states of aluminum in liquid ammonia. A single polarographic wave, with a maximum, was found for solutions saturated with tetrabutylammonium iodide and containing anhydrous aluminum chloride or aluminum iodide. The half-wave potential was −1.4 v., approximately equal to the half-wave potential, −1.37 v., found for the reduction of the ammonium ion. In three experiments in which the concentrations of aluminum iodide were 0.19, 0.60 and 1.00 millimolar, the values of the diffusion current constant, I, were 12.1, 9.9 and 8.9, respectively. Assuming that the ionic conductance at infinite dilution of the Al(III) ion is around 150 ohm^{-1} $cm.^{-1}$, a value of about 6.0 is calculated for I, if the electrode reaction consists of a three-electron reduction of the Al(III) ion. The observed diffusion currents thus are higher than required for a three-electron reduction. Since the half-wave potential is nearly equal to the half-wave potential for ammonium ion, the possibility exists that a fraction of the total current can be attributed to ammonium ion reduction, the ammonium ion being produced by ammonolysis of the amphoteric Al(III) ion. The high diffusion current may, at least in part, be attributed to the low concentration, 0.0057 *M*, of the supporting electrolyte. The results of the following experiment indicates that no reaction other than a three electron reduction of the Al(III) ion to aluminum amalgam occurs at a mercury cathode. Forty-five milliamperes of current were passed for 2.5 hours through a cell containing 50 ml. of 0.06 *M* aluminum iodide, with the electrodes consisting of an aluminum anode and a mercury pool cathode. The mercury pool eventually became semi-fluid in nature, and the amount of dissolved aluminum was found by analysis to be that required for the reaction $Al(III) + 3e^- + Hg = Al(Hg)_x$. It can be concluded from these experiments that no intermediate oxidation states of aluminum are formed at a mercury cathode.

Two other types of experiments were performed in which the object was to detect, by means of the dropping mercury electrode, any lower oxidation states of aluminum which might be formed by anodic oxidation of aluminum or by reduction of

(22) F. W. Bergstrom, *J. Am. Chem. Soc.*, **46**, 2632, 2634 (1924).

(23) F. Jirik and A. W. Davidson, *ibid.*, **72**, 1700 (1950).

(24) W. E. Bennett, J. Kleinberg and A. W. Davidson, *ibid.*, **74**, 732 (1952).

(25) G. W. Watt, J. L. Hall and G. R. Choppin, *ibid.*, **73**, 5920 (1951).

Al(III) with potassium. The lower oxidation states should be easily oxidized at the dropping mercury electrode.

An aluminum anode was suspended in a liquid ammonia solution 0.166 molar in ammonium nitrate and 0.078 molar in ammonium bromide. The anode compartment was separated from the cathode compartment by a sintered glass disc to avoid any contact of the anolyte with the cathode. A current of about 0.07 ampere was passed for one hour. A dropping mercury electrode was inserted in the anode compartment and three polarograms were recorded at intervals throughout the electrolysis. There was no evidence that any oxidizable material existed in the solution, although the mean valence of the oxidized aluminum was 2.0.

In the final experiment, 0.33 mmole of potassium and 0.20 mmole of aluminum iodide were placed in 40 ml. of liquid ammonia. A dropping mercury electrode was inserted after the blue color had completely disappeared. Here again the polarogram did not indicate the existence in solution of oxidizable ions. In this experiment the observation was made that a gas was evolved when the solid potassium was added to the liquid ammonia solution of aluminum iodide. In another similar experiment this gas was collected and found to correspond in quantity with that required for the reaction

$$K + NH_3 = {}^1/_2H_2 + NH_2^- + K^+$$

The variations in potential observed by Watt, Hall and Choppin[25] during the titration of aluminum iodide solutions with potassium do not, in view of this observation, appear to be attributable to the formation of Al(II) and Al(I) ions.

Acknowledgment.—The authors are indebted to the Office of Naval Research for financial support.

POTENTIOMETRIC TITRATION OF HALIDES OF ALUMINUM, GALLIUM, INDIUM AND THALLIUM WITH POTASSIUM IN LIQUID AMMONIA[1,2]

BY GEORGE W. WATT, JAMES L. HALL AND GREGORY R. CHOPPIN

Department of Chemistry, The University of Texas, Austin, Texas

Received November 28, 1952

The potentiometric titration of the iodides of gallium(III) and indium(III) with solutions of potassium in liquid ammonia provides evidence only for the three-electron changes resulting in the formation of the corresponding elemental metals. Similar titrations involving thallium(III) chloride are complicated by the fact that the elemental thallium first produced competes in the reduction of the +3 chloride. These studies provide evidence for the formation of Tl^{+1}; elemental thallium is the end-product of the reduction reaction. Further studies on the potentiometric titration of aluminum(III) iodide with liquid ammonia solutions of potassium and potassium amide and different possible reaction mechanisms are considered. The reaction with potassium amide produces aluminum(III) amide which is thereafter converted to potassium ammonoaluminate.

This paper is concerned with results obtained in studies involving a novel approach to the detection and characterization of unusual oxidation states of the elements. The method in question consists of the potentiometric titration of liquid ammonia solutions of appropriate salts of higher oxidation states of the elements with standard solutions of alkali or alkaline earth metals in liquid ammonia. The titrations are conducted below the normal boiling point of ammonia (*e.g.*, −38 to −40°) in an anhydrous and oxygen-free system using equipment and procedures substantially identical with those described by Watt and Otto.[3]

Experimental

Materials.—With the exceptions noted below, all materials employed in this work consisted of reagent grade chemicals.

Aluminum(III) iodide was prepared by direct union of the elements by a method especially designed to yield a product free of elemental iodine. This procedure will be described elsewhere.[4]

Anal. Calcd. for AlI_3: Al, 6.6; I, 93.4. Found: Al, 6.5; I, 93.2.

Gallium(III) iodide was prepared by essentially the method described by Johnson and Parsons.[5]

Anal. Calcd. for GaI_3: I, 84.5. Found: I, 84.5.

With only minor modifications, the method of Johnson and Parsons was also used in the preparation of indium(III) iodide.

Anal. Calcd. for InI_3: I, 77.0. Found: I, 77.0.

In the absence of a satisfactory procedure for the preparation of either the iodide or bromide of thallium(III), the corresponding chloride was obtained from the City Chemical Corporation and used without further purification despite its lesser solubility in liquid ammonia.

Methods.—Since the equipment and procedures involved in carrying out the potentiometric titrations have been described in considerable detail elsewhere[3] they need not be discussed here except to point out that the initial volume of the liquid ammonia solutions titrated was in all cases approximately 50 ml. Reactions carried out on a larger scale and having as their objective the isolation and identification of intermediates and/or final products employed equipment and techniques of the type described by Watt and Keenan.[6]

Titration of Thallium(III) Chloride.—A solution and suspension of 0.91 meq. of thallium(III) chloride and 2.61 meq. of sodium chloride (in solution, as a supporting electrolyte) was titrated with a 0.0586 *M* solution of potassium in liquid ammonia. The data for a typical case are given in Fig. 1. When the first portion of potassium solution was added a

(1) This work was supported in part by the Office of Naval Research, Contract N6onr-26610.

(2) Presented at the Symposium on Liquid Ammonia Chemistry, September, 1952, Meeting of the American Chemical Society, Atlantic City, N. J.

(3) G. W. Watt and J. B. Otto, Jr., *J. Electrochem. Soc.*, **98**, 1 (1951).

(4) G. W. Watt and J. L. Hall, "Inorganic Syntheses," Vol. IV, in press.

(5) W. C. Johnson and J. B. Parsons, THIS JOURNAL, **34**, 1210 (1930).

(6) G. W. Watt and C. W. Keenan, *J. Am. Chem. Soc.*, **71**, 3833 (1949).

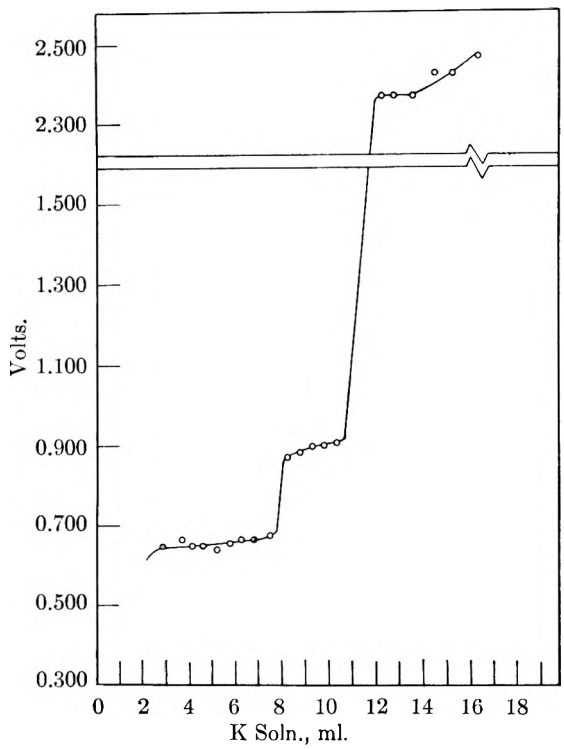

Fig. 1.—Potentiometric titration: thallium(III) chloride with potassium.

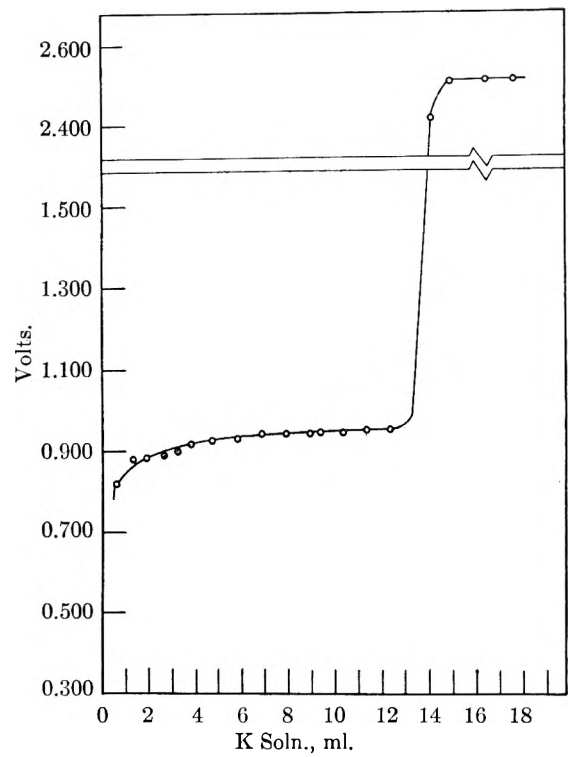

Fig. 2.—Potentiometric titration: indium(III) iodide with potassium.

black precipitate formed but rather quickly disappeared. As the titration proceeded, however, the rate of disappearance of this product decreased; some of it agglomerated and settled to the bottom of the reactor where it thereafter reacted slowly if at all. Finally, upon addition of potassium solution in excess of that required for complete reduction to elemental thallium, the solution assumed the characteristic blue color of solutions of alkali metals in ammonia and the accompanying increase in potential was that characteristic of such solutions.[3] The blue color, however, was not permanent, but it decreased in intensity only slowly. The ammonia-insoluble product of the reduction reactions was identified as elemental thallium by means of an X-ray diffraction pattern obtained using CuKα radiation, a nickel filter, a tube voltage of 30 kv., a filament current of 15 ma. and an exposure time of 4 hr. Found (relative intensities in parentheses): d = 2.62 (strong), 1.72 (medium) and 1.57 (medium). The corresponding values from the literature[7] are: d = 2.62 (1.00), 1.73 (0.3) and 1.57 (0.5).

Titration of Indium(III) Iodide.—A solution containing 0.70 meq. of indium(III) iodide was titrated with a liquid ammonia solution 0.0498 M with respect to potassium (see Fig. 2). Upon the first addition of potassium solution there appeared a black precipitate of elemental indium which continued to form as the titration proceeded.

Titration of Gallium(III) Iodide.—The titration of a solution of 0.49 meq. of gallium(III) iodide with 0.0403 M potassium solution to form elemental gallium (Fig. 3) proceeded in a manner substantially identical with that described for indium.

Titration of Aluminum(III) Iodide.[8]—In a typical case, 0.83 meq. of aluminum(III) iodide in solution in liquid ammonia was titrated with 0.0541 M potassium solution (see Fig. 4). As the progress of the titration approached the first minimum shown in the curve (Fig. 4) a very finely divided gray-white solid began to separate from the solution and this persisted throughout the remainder of the titration. After the addition of that increment of potassium solution which provided the first excess of alkali metal, the blue potassium solution and the gray-white solid coexisted apparently without change over periods greater than five hours.

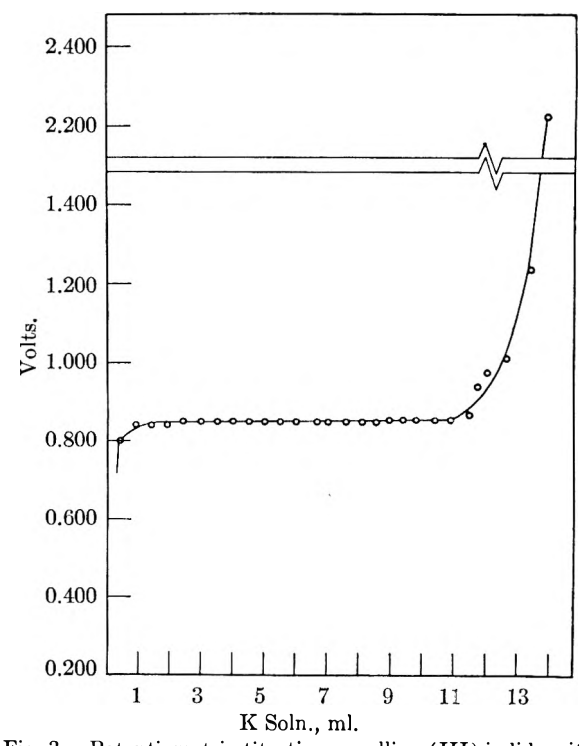

Fig. 3.—Potentiometric titration: gallium(III) iodide with potassium.

In order to choose between different possible mechanisms that might be compatible with experimental results of the type shown in Fig. 4, it would be helpful to know whether any hydrogen is evolved during the course of the reduction reactions. It is impractical to attempt to secure this information from the potentiometric titration runs since the solutions that are titrated are stirred by means of a stream of anhydrous oxygen-free nitrogen that is presaturated with

(7) A.S.T.M. Index of X-Ray Diffraction Patterns.

(8) *Cf.* G. W. Watt, J. L. Hall and G. R. Choppin, *J. Am. Chem. Soc.*, **73**, 5920 (1951).

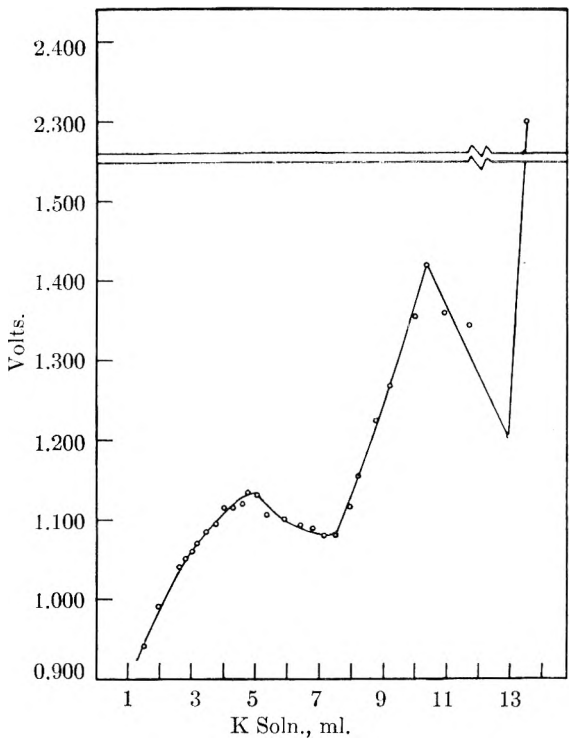

Fig. 4.—Potentiometric titration: aluminum(III) iodide with potassium.

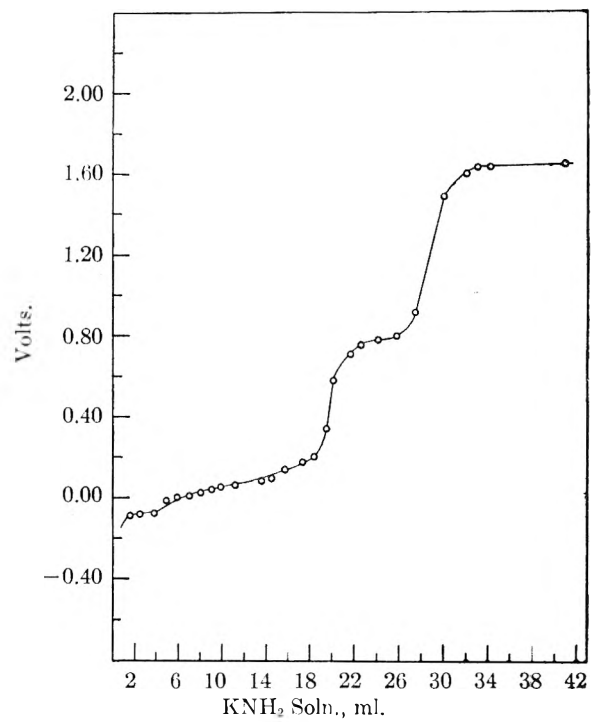

Fig. 5.—Potentiometric titration: aluminum(III) iodide with potassium amide.

ammonia.[3] Hence if hydrogen were formed, its volume would be negligible in relation to the volume of nitrogen collected and the measurement of the quantity of hydrogen would be quite inaccurate. Accordingly, this difficulty was overcome by reducing aluminum(III) iodide with potassium solution on a considerably larger scale using equipment of the type described previously[6] which provides for stirring with a stream of ammonia only and for the collection and analysis of water-insoluble gases. In four separate experiments, 4.5, 4.0, 7.2 and 2.5 meq. of aluminum(III) iodide (each sample in an initial volume of approximately 40 ml. of liquid ammonia) were titrated with, respectively, 0.19, 0.22, 0.64 and 0.34 *M* potassium solutions. The major variable in these four experiments was the rate of addition of the potassium solutions which was varied (respectively) from *ca.* 7 to 0.5 hr. Although the four results were not entirely internally consistent, the volumes of hydrogen collected during the course of the reduction reactions varied from 0 to > 100% of that calculated on the assumption that all of the potassium added reacted to form an equivalent quantity of hydrogen. Further, the volume of hydrogen formed appears to depend upon the rate at which the potassium solution is added.

Titration of Aluminum(III) Iodide with Potassium Amide.—In other experiments potentially of importance in the interpretation of the reduction reactions described above, 1.06 meq. of aluminum(III) iodide in *ca.* 50 ml. of liquid ammonia solution was titrated with 0.0478 *M* potassium amide solution. The resulting data are shown in Fig. 5.

Discussion

In view of the well established stability of the Tl^{+1} it was anticipated that the potentiometric titration of thallium(III) chloride with potassium might at least give evidence of the successive formation of Tl^{+1} and Tl^0. For the case shown in Fig. 1, corresponding changes in potential should occur upon addition of 10.3 and 15.5 ml. of potassium solution. However, the reaction that occurs as the result of the addition of the first 2.2 ml. of potassium solution (see Fig. 1) evidently involves the partial reduction of Tl^{+3} to black ammonia-insoluble Tl^0 which in turn reacts fairly rapidly to reduce some of the remaining Tl^{+3} to Tl^{+1} and/or Tl^{+2}. The reaction between Tl^0 and Tl^{+3} seems more probable than a possible interaction of Tl^0 and the solvent[9] since the rate at which the Tl^0 reacts appears to decrease progressively as the supply of Tl^{+3} decreases. Following the addition of 2.2 ml. of potassium solution, the black solid (identified as elemental thallium at the end of the run) was present as a solid phase in increasing quantity as the titration progressed and it appeared to react only relatively slowly for a time and finally not at all. Owing to the interference by this concurrent reaction involving Tl^0, it is not to be expected that the two subsequent changes in potential could be correlated strictly with the anticipated stoichiometry corresponding to possible intermediates in the reduction process. Thus in the case of the data of Fig. 1, it is apparently fortuitous that the increase in potential amounting to 0.2 v. that occurs upon addition of 8.0 ml. of potassium solutions agrees well with the value of 7.8 ml. calculated on the assumption that the Tl^0 first produced then reduces Tl^{+3} to Tl^{+2} and Tl^{+1}. Actually, this increase in potential probably corresponds to the completion of reduction to Tl^{+1} but is displaced to the left owing to reduction attributable to Tl^0. In effect, the intermediation of reduction reactions involving the freshly precipitated Tl^0 renders the data for the remainder of the titration almost impossible of rigorous interpretation. Furthermore, it has been found that data of the type shown in Fig. 1 are not strictly reproducible; the same changes in potential are observed from run to run but the relative positions

(9) A. D. McElroy, J. Kleinberg and A. W. Davidson, *J. Am. Chem. Soc.*, **74**, 738 (1952); *cf.* C. A. Seely, *via* Mellor, "Comprehensive Treatise on Inorganic and Theoretical Chemistry," Vol. V, Longmans, Green and Co., New York, N. Y., 1937, p. 421.

at which these changes occur are somewhat subject to variation.

The data shown in Figs. 2 and 3 indicate that the reduction of the iodides of indium(III) and gallium(III) involves only the three-electron changes corresponding to reduction to the respective elemental metals. Evidently the +2 and +1 oxidation states of these elements are not stable in liquid ammonia under the conditions involved in these experiments. These results are somewhat surprising in view of existing evidence for these lower oxidation states in liquid ammonia, other solvent media, and in the solid state.[10]

The results obtained in the potentiometric titration of aluminum(III) iodide with potassium have previously been interpreted[8] as evidence for the existence of the +2 and +1 oxidation states of aluminum. With reference to Fig. 4, for example, the calculated volumes of potassium solution required for reduction of Al^{+3} to Al^{+2} and Al^{+1} are 5.1 and 10.2 ml., respectively. An inspection of Fig. 4 shows that the experimental results are in excellent agreement with these values and the reproducibility of these results has been amply demonstrated.

It has been suggested, however, that these results might also be explained in terms of a series of acid–base equilibria,[11] *e.g.*

$$Al^{+3} + NH_3 \rightleftharpoons AlNH_2^{+2} + NH_4^+$$
$$AlNH_2^{+2} + NH_3 \rightleftharpoons Al(NH_2)_2^{+1} + NH_4^+$$
$$Al(NH_2)_2^{+1} + NH_3 \rightleftharpoons Al(NH_2)_3 + NH_4^+$$

wherein the observed changes in potential could correspond successively to the three aluminum-containing species shown above. Thus it is proposed in effect that the aluminum(III) iodide is ammonolyzed and that the reaction that occurs upon addition of potassium is that with NH_4^+ to liberate hydrogen. Our experiments designed to determine whether hydrogen is evolved have led to results that are not satisfactorily conclusive. It appears that hydrogen is indeed evolved in substantially the stoichiometric quantity if the reaction is carried out rapidly but that the quantity of hydrogen liberated decreases as the time of addition of potassium solution is increased to as much as 7 hr. Since the potentiometric titration must be carried out very slowly (*e.g.*, periods of time of the order of 48 hr.) in order to ensure the re-establishment of equilibrium after each addition of potassium, there remains the question as to whether any hydrogen is produced in runs of the type that led to the data of Fig. 4. Additional experiments concerned with the questions of hydrogen formation and the identity of other ammonia-insoluble intermediate and final reduction products are in progress.

Two additional lines of evidence bearing upon the mechanism of the reduction of aluminum(III) iodide with potassium also merit consideration. If the data of Fig. 4 are to be interpreted in terms of ammonolysis, it might be expected that the same intermediate and final species should be formed by the reaction between aluminum(III) iodide and potassium amide in liquid ammonia. That such is clearly not the case is shown by the data of Fig. 5. The changes in potential that occur upon addition of 22.1 and 29.5 ml. of potassium solution conform almost exactly to the reactions

$$Al^{+3} + 3KNH_2 \longrightarrow Al(NH_2)_3 + 3K^+$$
$$Al(NH_2)_3 + KNH_2 \longrightarrow KAl(NH_2)_4$$

The white ammonia-insoluble aluminum(III) amide that is formed first then reacts with additional potassium amide to form a soluble salt of an amphoteric base. Finally, it should be pointed out that if aluminum(III) amide were the final product of the reduction of aluminum(III) iodide with potassium, any excess of the metal added would undoubtedly react with the insoluble amide to form one or more salts of this amphoteric base. It was observed, however, that solutions of potassium do not react with the end-product of the reduction reaction over periods up to several hours.

(10) For review and primary references see: J. Kleinberg, "Unfamiliar Oxidation States and Their Stabilization," University of Kansas Press, Lawrence, Kan., 1950; *J. Chem. Education*, **29**, 324 (1952).

(11) H. A. Laitinen, private communication.

UNFAMILIAR OXIDATION STATES IN LIQUID AMMONIA

BY ARTHUR W. DAVIDSON AND JACOB KLEINBERG

Department of Chemistry, University of Kansas, Lawrence, Kansas

Received November 28, 1952

This paper reports the attainment of unfamiliar oxidation states of certain elements in liquid ammonia by means of two widely diverse methods: (1) electrolytic oxidation of metallic anodes; (2) reduction by alkali metals (a) of gaseous oxygen, (b) of cyanide complexes of transition metals.

(1) In the anodic oxidation of aluminum, coulometric measurements indicate a mean initial oxidation state lower than 3 whenever the electrolyte contains nitrate ion. Evidence is presented to support the hypothesis of primary oxidation of the metal to a cation of low charge (presumably +1), which reduces nitrate ion to free nitrogen in a secondary reaction concurrent with the electrolysis. In the cases of gallium and thallium, stable mixtures of unipositive and tripositive ions are obtained by anodic oxidation. In the case of indium, the ion of charge lower than 3 formed by primary oxidation immediately disproportionates into metallic indium and In(III) ion. (2) (a) It has long been known that liquid ammonia solutions of potassium, rubidium and cesium, upon rapid oxidation with free oxygen, give good yields of the superoxides. It may now be added that sodium, under suitable conditions, yields a product of empirical formula $Na_{1.67}$, and that in the case of lithium there is evidence for the existence of a superoxide stable at −78°, which, however, has not been isolated. (b) The existence of Ni(I) as $Ni(CN)_3^{--}$ and of Ni(0) as $Ni(CN)_4^{-4}$, both obtained by the reduction of tetracyanonickelate(II) ion, has been previously reported, as has the formation of Pd(0) as $Pd(CN)_4^{-4}$ from tetracyanopalladate(II) ion. In our laboratory, the reduction of hexacyanochromate(III) ion has been found to yield a product containing Cr(I), while under similar conditions hexacyanomanganate(III) ion yields a product of empirical formula $K_{11}Mn_2(CN)_{12}\cdot 2NH_3$, containing both Mn(I) and Mn(0).

The fact that liquid ammonia is an especially useful and convenient medium for the carrying out of reactions with very strong reducing agents was pointed out many years ago by Kraus,[1] and has been re-emphasized in more recent reviews by Fernelius and Watt.[2,3] As a corollary, it follows that elements may be expected to exist in liquid ammonia in low valence states which, in aqueous solution, would be subject to rapid oxidation by the solvent. Further, the relatively low degree of self-ionization of ammonia permits the preparation in this medium of certain substances, such as superoxides, which are subject to immediate and extensive hydrolysis in water.

The purpose of this paper is to bring together the results of a number of relatively recent studies of the existence of elements in unfamiliar oxidation states, either as ions in liquid ammonia solution or in compounds formed by reactions which take place in liquid ammonia as a medium. The many instances of compounds between alkali metals and other metals, especially those of Groups IV and V of the periodic system, in which the latter metals exist either as simple anions or as homopolyatomic anions have been extensively reviewed by others[1-4] and will not be discussed here.

In our laboratory, two general types of reaction have been studied: (1) the electrolytic oxidation of metallic anodes; (2) reduction by means of solutions of alkali metals.

Electrolytic Oxidation of Metals of the Aluminum Family

Aluminum.—The anodic oxidation of aluminum[5] was carried out by passing a direct current between an aluminum anode and a platinum cathode, through a solution either of a single salt or of a mixture of two salts in liquid ammonia. An inert atmosphere of nitrogen was maintained throughout the electrolysis, which was usually carried out at −33°. The quantity of electricity which passed through the circuit was determined by means of a silver coulometer in series with the electrolytic cell, while the amount of aluminum anodically oxidized was determined from the weight of the anode at the beginning and at the end of each electrolysis.

A quantity designated as the apparent initial valence number, V_i, of the aluminum ion produced by electrolysis was calculated by means of the equation

$$V_i = \frac{\text{wt. of Ag deposited in coulometer} \times 26.98}{107.9 \times \text{wt. of Al lost from anode}}$$

In the case of anodic oxidation to the familiar tripositive aluminum ion, this quantity would, of course, have the value 3.

In a number of electrolyses carried out as just described in ammonia solutions of single salts other than nitrates, the values found for V_i were close to 3 (within 0.1 unit). In a few other instances, values *higher* than 3 were observed; this result may be regarded as indicative of partial passivity, in that the anodic reaction must have included oxidation of some substance other than metallic aluminum. In every instance, however, in which a nitrate was used as electrolyte, whatever the cation, the value of V_i was found to be less than 3—usually in the neighborhood of 2.7. This value, furthermore, showed little dependence upon concentration of electrolyte, current density or duration of the electrolysis. Since there was no evidence of direct (non-electrolytic) reaction between aluminum and any of the solutions, these results were interpreted as indicating that the anode was electrolytically oxidized, in part, to an aluminum ion of charge lower than +3.

Since the results just described pointed toward the presence of nitrate ion as the determining factor in bringing about the anodic dissolution of aluminum in this lower oxidation state, experiments were made to determine whether or not this effect of nitrate would persist in electrolytes containing both nitrate and other anions. It was found that in nitrate–chloride and nitrate–bromide mixtures it was possible to attain apparent initial valence

(1) C. A. Kraus, *Chem. Revs.*, **8**, 251 (1931).
(2) W. C. Fernelius and G. W. Watt, *ibid.*, **20**, 195 (1937).
(3) G. W. Watt, *ibid.*, **46**, 289 (1950).
(4) F. W. Bergstrom, *J. Am. Chem. Soc.*, **47**, 1503 (1925).
(5) W. E. Bennett, A. W. Davidson and J. Kleinberg, *ibid.*, **74**, 732 (1952).

numbers much lower than those found for solutions of nitrates alone. The value of V_i, in fact, was found to vary regularly with the *ratio* of the concentrations of nitrate and halide, reaching a minimum close to 1.5 for mixtures containing about 2 moles of nitrate to 1 of bromide, regardless of the total concentration of electrolyte. Again, the original mixtures were found to have no action upon test rods of aluminum; further, an aluminum rod used as *cathode* in some of the electrolyses underwent no detectable loss of weight, nor was any significant change in initial valence number observed when an intermittent instead of a continuous direct current was used for electrolysis. These facts appear to preclude the possibility of non-electrolytic corrosion as a disturbing factor.

Most of the electrolyses of bromide–nitrate mixtures were carried out in a cell in which the anode and cathode were separated by a sintered Pyrex disk, in order that the separate examination of anodic and cathodic processes might be facilitated. No compound of lower valent aluminum could be detected in the grayish anodic deposit, nor in solution in the anolyte, after electrolysis; both of these phases were quite devoid of reducing power. It was noted, however, that an appreciable diminution in the concentration of nitrate took place during the electrolysis, and that measurable quantities of nitrogen were evolved at both anode and cathode. Furthermore, the quantity of hydrogen evolved at the cathode was always somewhat less than that calculated from coulometric data, on the assumption of hydrogen liberation as the sole cathode reaction.

In order to account for the phenomena which have been described, the following electrode reactions were postulated.

$$\text{Cathode: } 2NH_4^+ + 2e^- = 2NH_3 + H_2$$
$$2NO_3^- + 12NH_4^+ + 10e^- = N_2 + 12NH_3 + 6H_2O$$

$$\text{Anode: } \left.\begin{matrix} Al = Al^{+++} + 3e^- \\ Al = Al^{+} + e^- \end{matrix}\right\}\text{primary}$$

$$5Al^+ + 2NO_3^- + 12NH_4^+ = 5Al^{+++} + N_2 + 12NH_3 + 6H_2O \text{ secondary}$$

If these hypotheses are correct, the total number of gram-equivalents of nitrate ion reduced during the electrolysis, or of free nitrogen evolved, should be given by the equation

No. of gram-equivalents = 3 × no. of g.-atoms of Al dissolved − no. of g.-equiv. of H_2 evolved

while the number of *moles* of nitrate lost, or of nitrogen evolved, should be 1/5 and 1/10, respectively, of this figure. Several experiments were carried out in which the amount of nitrate lost during electrolysis was determined by analysis, while the total volume of gas evolved was measured, and its hydrogen content determined by combustion. Results of these experiments are shown in Table I; the fairly good agreement between columns (E) and (F) is in accord with the postulated electrode reactions.

In the anodic oxidation of gallium, indium and thallium in liquid ammonia solutions[6] under conditions similar to those used with aluminum, the initial mean valence number of the cations produced was almost always appreciably lower than 3, but otherwise the results obtained varied markedly from one element to another, as well as from those observed for aluminum.

TABLE I

REDUCTION OF NITRATE DURING ELECTROLYSIS

(A) Quantity of elect., faraday	(B) Al dissolved, g.-atom	(C) V_i, from (A) and (B)	(D) H_2 evolved, g.-equiv.	(E) NO_3^- reduced or N_2 evolved, mole: calcd. from (B) and (D)		(F) observed
0.003783	0.001928	1.96	0.002513	0.000654	NO_3^-	0.000641
.004460	.002080	2.14	.002560	.000736	NO_3^-	.000751
.003593	.002002	1.79	.001955	.000810	NO_3^-	.000773
.004917	.003235	1.52	.004240	.000547	N_2	.000478
.002573	.001354	1.90	.002450	.000161	N_2	.000165

Gallium.—Electrolyses were carried out in a divided cell with a gallium anode and a platinum cathode in solutions of ammonium bromide, which had been found to show no appreciable non-electrolytic reaction with gallium. No measurable quantity of gas was evolved from the anode during electrolysis. The values of V_i, calculated by means of an equation exactly analogous to that used for aluminum, *i.e.*

$$V_i = \frac{\text{wt. of Ag deposited in coulometer} \times 69.72}{107.9 \times \text{wt. of Ga lost from anode}}$$

were found to be in the neighborhood of 2.25. With ammonium nitrate–ammonium bromide mixtures as electrolyte the value of V_i, as in the case of aluminum, was found to be a function of the fraction of nitrate in the mixed solute, with a minimum of 2.0 at about 17 mole % nitrate. This minimum value need not be regarded as evidence for the formation under these conditions of dipositive gallium, since it may more plausibly be interpreted as corresponding to an equimolar mixture of unipositive and tripositive gallium ions.[7]

In contrast to the observations reported for aluminum, the anodic deposit and the anolyte resulting from anodic oxidation of gallium were found to exhibit measurable reducing properties; in this case, therefore, the ion of lower charge is relatively stable in the presence of liquid ammonia. The primary anode reactions were postulated to be

$$Ga = Ga^{+++} + 3e^-$$
$$Ga = Ga^{+} + e^-$$

The grayish-white residue remaining on evaporation of ammonia from the anolyte after electrolysis, and the insoluble solid which had been formed in the anode compartment, were tested separately for reducing power in the following way. Each was dissolved in standard aqueous iodine solution which had been acidified with acetic acid. After 15 minutes, the excess iodine was titrated with standard sodium thiosulfate solution. The gallium, now completely oxidized to the tripositive state, was determined by precipitation with 8-hydroxyquinoline. The reducing power, *R.P.*, in each case, expressed in gram-equivalents, was equal to the number of gram-equivalents of iodine reduced; and the mean valence number of the gallium at the

(6) A. D. McElroy, J. Kleinberg and A. W. Davidson, *J. Am. Chem. Soc.*, **74**, 736 (1952).

(7) A. W. Davidson and F. Jirik, *ibid.*, **72**, 1700 (1950).

end of the reaction, V_f, as determined from the reducing power, was calculated by means of the equation

$$V_f = 3 - \frac{R.P. \times 69.72}{\text{wt. of Ga found in solution}}$$

A few typical results of these experiments are shown in Table II.

TABLE II

ANODIC OXIDATION OF GALLIUM IN LIQUID AMMONIA SOLUTIONS OF AMMONIUM BROMIDE

V_i coulometric	V_f Anolyte	V_f Anode deposit	V_f Over-all	% of theoretical reducing power recovered
2.26	2.24	2.44	2.32	90
2.23	2.12	2.56	2.29	91
2.27	2.27	2.60	2.33	91

Indium.—Metallic indium is not attacked by liquid ammonia solutions of ammonium bromide. In electrolyses carried out on this electrolyte in a divided cell with an indium anode and an aluminum cathode, the results were found to vary in a highly erratic manner. Values of V_i ranged all the way from 2.01 to 4.72; the values higher than 3 can be accounted for only on the basis of the occurrence of some anode reaction other than the oxidation of indium. Noteworthy observations on these electrolyses included the evolution of hydrogen in the anode compartment as well as at the cathode, the occasional liberation of nitrogen at the anode, and the precipitation of finely divided indium in the anolyte.

These observations may be accounted for in terms of the following hypotheses. (1) Indium is anodically oxidized to a mixture of indium(I) and indium(III) ions. (2) The anodic hydrogen results from the reduction of the electrolyte by indium(I) ion. (3) The anodic nitrogen results from a competing primary reaction involving the oxidation of ammonia. (4) Indium(I) ion, unlike the corresponding ions of aluminum and gallium, is subject to disproportionation into indium(III) ion and free metal.

Thus the anode reactions may be listed as

$$\left.\begin{aligned} In &= In^+ + e^- \\ In &= In^{+++} + 3e^- \\ 8NH_3 &= N_2 + 6NH_4^+ + 6e^- \end{aligned}\right\}\text{primary}$$

$$\left.\begin{aligned} In^+ + 2NH_4^+ &= 2NH_3 + H_2 + In^{+++} \\ 3In^+ &= 2In + In^{+++} \end{aligned}\right\}\text{secondary}$$

After several of the electrolyses, the ammonia was allowed to evaporate, the residue was extracted with water, and the finely divided indium was weighed. The water solution was then titrated with standard potassium dichromate solution, and the reducing power, in gram-equivalents, was calculated from the equation

$$R.P. = \frac{\text{wt. of } Cr_2O_7^{--} \text{ reduced}}{36.01} + \frac{3 \times \text{wt. of pptd. In}}{114.8}$$

The mean valence number of the indium at the end of the electrolysis, V_f, as determined from the reducing power of the residue, was calculated from

$$V_f = 3 - \frac{R.P. \times 114.8}{\text{wt. of indium lost from anode}}$$

Before the mean valence number so calculated might properly be compared, however, with the coulometric value, it was necessary that the former be modified to V_f' to take into account the oxidation of In(I) ion in solution by ammonium ion

$$\left(V_f' = V_f - \frac{2 \times \text{no. of moles of anodic } H_2}{\text{no. of g.-atoms of In lost from anode}}\right)$$

and that the latter be corrected to V_i' to allow for the competing anode reaction

$$\left(V_i' = V_i - \frac{6 \times \text{no. of moles of } N_2 \text{ liberated}}{\text{no. of g.-atoms of In lost from anode}}\right)$$

As shown in Table III, the agreement between the corrected values is, in most cases, fairly good, lending support to the validity of the postulated electrode reactions.

TABLE III

ANODIC OXIDATION OF INDIUM IN LIQUID AMMONIA SOLUTIONS OF AMMONIUM BROMIDE

V_i	V_f	V_i'	V_f'
2.60	2.75	2.60	2.62
3.20	2.86	2.28	2.61
2.53	2.70	2.53	2.60
2.75	2.80	2.27	2.32
2.72	2.89	1.98	2.10
2.92	2.94	1.89	2.15
2.82	2.92	2.30	2.58
2.01	2.22	2.01	2.16
4.48	2.98	2.91	2.85

Thallium.—Unlike the other metals of this family, thallium reacts fairly rapidly with liquid ammonia, especially in the presence of certain dissolved salts. Although this non-electrolytic dissolution was taken into consideration in the calculation of the mean valence number on electrolytic oxidation by the method previously described, yet the results obtained must be regarded as no more than approximate.

Although anodic oxidation of thallium in nitrate solutions was found to yield thallium(I) ion exclusively, yet in chloride, bromide or amide solutions a mixture of thallium(I) and thallium(III) ions was formed. Both of these ions remained unchanged throughout the electrolysis, and could be identified by qualitative tests in the final product.

Reduction of Gaseous Oxygen by Alkali Metals

It has long been known[3] that when potassium, rubidium or cesium in solution in liquid ammonia is treated with a rapid stream of oxygen, at temperatures ranging from −70 to −33°, the superoxide of the metal is formed. In a recent investigation of the oxidation of sodium under similar conditions,[8] it was found that if a solution of sodium in liquid ammonia was slowly added to another portion of ammonia through which oxygen was being passed rapidly, a product of constant composition was obtained, regardless of the temperature of the solution. In the absence of moisture, this yellow product was fairly stable at room temperature. Analysis of eleven samples by measurement of the oxygen liberated on treatment with an

(8) W. H. Schechter, J. K. Thompson and J. Kleinberg, *J. Am. Chem. Soc.*, **71**, 1816 (1949).

aqueous suspension of manganese dioxide, and determination of the sodium by titration with standard acid, yielded from 1.65 to 1.70 atoms of oxygen per atom of sodium, the average being close to 1.67. This composition corresponds to a mixture of four moles of sodium superoxide, NaO_2, to one of sodium peroxide, Na_2O_2.

The product prepared as just described was highly paramagnetic, having a specific susceptibility at 20° of 21.6×10^{-6} c.g.s. unit, as compared with an estimated value of 33.0×10^{-6} unit for pure sodium superoxide.[9] Although the accuracy of the measurement of susceptibility was not very high, yet when the observed value was compared with a linear plot of specific susceptibility against weight percentage in synthetic Na_2O_2–NaO_2 mixtures,[9,10] the percentage of sodium superoxide found in this way, 67.5%, was in fair agreement with the figure of 73.8% calculated from the analytical data.

In a study of the oxidation of lithium in liquid ammonia,[11] it was found that when the metal was dropped into liquid ammonia at −78° through which a stream of oxygen was being passed, a bright yellow solution was formed. When this solution was allowed to warm up to −33°, the yellow color disappeared and a white suspension of lithium monoxide and lithium peroxide appeared. However, a study of the absorption spectrum of the yellow solution showed a marked maximum in absorption at a wave length of 380 mμ. Since solutions of sodium and potassium superoxides exhibit absorption maxima at the same wave length, it may be concluded that lithium forms a superoxide which is stable in liquid ammonia solution at −78°.

Reduction of Transition Metals by Alkali Metals

It has been previously reported[12] that when excess potassium tetracyanonickelate(II), $K_2Ni(CN)_4$, is treated with sodium or potassium in liquid ammonia, a bright red precipitate of potassium tricyanonickelate(I), $K_2Ni(CN)_3$, is formed. This compound is soluble in water, giving a red solution which slowly loses its color, with the evolution of hydrogen. When potassium tetracyanonickelate(II) is treated with an excess of potassium in liquid ammonia, the product is a yellow precipitate of potassium tetracyanonickelate(0), $K_4Ni(CN)_4$. When freed from ammonia, this is a copper-colored solid, which reacts with water to give hydrogen and a red solution of potassium tricyanonickelate(I).

Similarly, the reduction of potassium tetracyanopalladate(II), $K_2Pd(CN)_4$, by potassium in liquid ammonia[13] yields a light yellow crystalline precipitate of potassium tetracyanopalladate(0), $K_4Pd(CN)_4$. In water, this substance momentarily gives a clear solution; then hydrogen and hydrogen cyanide are evolved and metallic palladium is precipitated.

In our laboratory, in a recent study[14] of the reduction of potassium hexacyanochromate(III) by potassium in liquid ammonia, a dark brown product was obtained which was extremely susceptible to oxidation by air or moisture. In order to determine its reducing power, an excess of solid silver nitrate was added to a suspension of the chromium compound in liquid ammonia; a black precipitate of silver was immediately formed. After the excess silver nitrate had been washed out with liquid ammonia, the precipitated silver was washed with water and with dilute hydrochloric acid, and then dissolved in hot dilute nitric acid. Silver was determined in the resulting solution by precipitation as the chloride. The mean of five values of the reducing power so determined (in gram-atoms of silver per gram-atom of chromium) was found to be 2.09. This result appears to indicate the presence in the compound of Cr(I).

A more intensive investigation was made of the reduction by potassium in liquid ammonia of potassium hexacyanomanganate(III).[15] A yellow product, difficulty soluble in liquid ammonia and possessing strong reducing properties, was obtained. The characterization of this product was carried out by four different methods, all of which gave concordant results.

(a) A study was made of the ratio by weight in which potassium and the starting compound reacted with each other. It was found that the blue color due to excess potassium persisted in the solution for more than a few minutes only when more than 2.5 atoms of potassium were added per mole of compound. This fact suggested that the stoichiometry of the reaction might be represented by the equation

$$2K_3Mn(CN)_6 + 5K = K_5Mn(CN)_6 + K_6Mn(CN)_6$$

and that the product might contain unipositive and zerovalent manganese, atom for atom.

(b) After a scheme of analysis applicable to manganese complexes had been devised and shown to be valid on known synthetic mixtures containing potassium, manganese and cyanide, the reduction product, which contained some ammonia which was slowly lost on standing, was subjected to complete analysis. The ratio $K:Mn:CN:NH_3$ as calculated from the analytical data (mean of several determinations of each constituent on freshly prepared samples) was 5.42:1:5.93:1.11. These results indicate a compound of the empirical formula $K_{11}Mn_2(CN)_{12}\cdot 2NH_3$, as may be seen also from the following figures.

Anal. Calcd. for $K_{11}Mn_2(CN)_{12}\cdot 2NH_3$: K, 48.53; Mn, 12.40; CN, 35.23; NH_3, 3.84. Found: K, 48.29; Mn, 12.51; CN, 35.11; NH_3, 4.29.

(c) The reducing power of the product was determined by treating a liquid ammonia suspension with an excess of an ammonia solution of silver nitrate, and proceeding just as in the case of the chromium compound. The mean of four values of the reducing power (in gram-atoms of silver per

(9) S. E. Stephanou, W. H. Schechter, W. J. Argersinger, Jr., and J. Kleinberg, *J. Am. Chem. Soc.*, **71**, 1819 (1949).

(10) The sodium superoxide used in the preparation of these mixtures had been prepared by reaction between sodium peroxide and oxygen at elevated temperatures and pressures.

(11) J. K. Thompson and J. Kleinberg, *J. Am. Chem. Soc.*, **73**, 1243 (1951).

(12) J. W. Eastes and W. M. Burgess, *ibid.*, **64**, 1187 (1942).

(13) J. J. Burbage and W. C. Fernelius, *ibid.*, **65**, 1484 (1943).

(14) E. Colton, unpublished work.

(15) V. J. Christensen, Ph.D. Thesis, University of Kansas, 1952

gram-atom of manganese) was found to be 1.53. Since the manganese was oxidized by silver ion to the dipositive state, the results of these experiments pointed toward an initial mean valence state of one-half, a figure which is in complete accord with the observed reaction ratio and with the analytical data.

(d) The magnetic susceptibility of the reduction product was measured. As might have been expected of a substance containing manganese in the zerovalent state, it was found to be distinctly paramagnetic. When the molar weight was calculated on the basis of the formula $K_{11}Mn_2(CN)_{12}\cdot 2NH_3$, the mean of five values found for the effective magnetic moment was 1.25 Bohr magnetons, as compared to a calculated value for one unpaired electron of 1.73 Bohr magnetons. The discrepancy, however, is less serious than it might at first appear, since a very slight degree of oxidation of the product would appreciably lower the value of the effective magnetic moment. Thus a mixture of 40 mole % of the zerovalent and 60 mole % of the unipositive manganese compound would have a theoretical moment of the same magnitude as that found experimentally.

In view of the substantial concordance of all four lines of evidence, there can be little doubt that the reduction product contains manganese in both the unipositive and the zerovalent state, in at least approximately the atomic ratio of 1:1. Its composition may perhaps best be represented by the formula $K_5Mn(CN)_6\cdot K_6Mn(CN)_6\cdot 2NH_3$.

Acknowledgment.—The authors are indebted to the Research Corporation for a Frederick Gardner Cottrell grant which made possible some of the work described in this paper.

THE SOLUBILITY OF NAPHTHALENE IN SUPERCRITICAL ETHYLENE. II

BY G. A. M. DIEPEN AND F. E. C. SCHEFFER

Contribution from the Laboratory for Inorganic and Physical Chemistry at The Technical University, Delft, Holland

Received September 23, 1952

A previously described apparatus for the precise measurement of the saturation concentration of slightly volatile solids in fluids above their critical temperature has been used to determine the saturation concentration of naphthalene in ethylene at 12, 25, 35, 45, 50 and 60° at various pressures. It was found that these measured concentrations are, to high degree, dependent on the pressure and the temperature and that they vary from a tenth of a per cent. to 80% by weight.

In an earlier paper[1] we reported the solubilities of naphthalene in supercritical ethylene at temperatures of 12, 25 and 35° and for pressures to about 110 atmospheres. Since the above publication, we have measured the second critical end-point in the ethylene–napthalene system and it appears to be at 52° and 174 atmospheres.[2] Thus between the temperatures of the first (11°) and the second critical end-point (52°) concentration measurements can be made without the formation of a second fluid phase. In other words, between 11 and 52° it is impossible at all pressures, for another

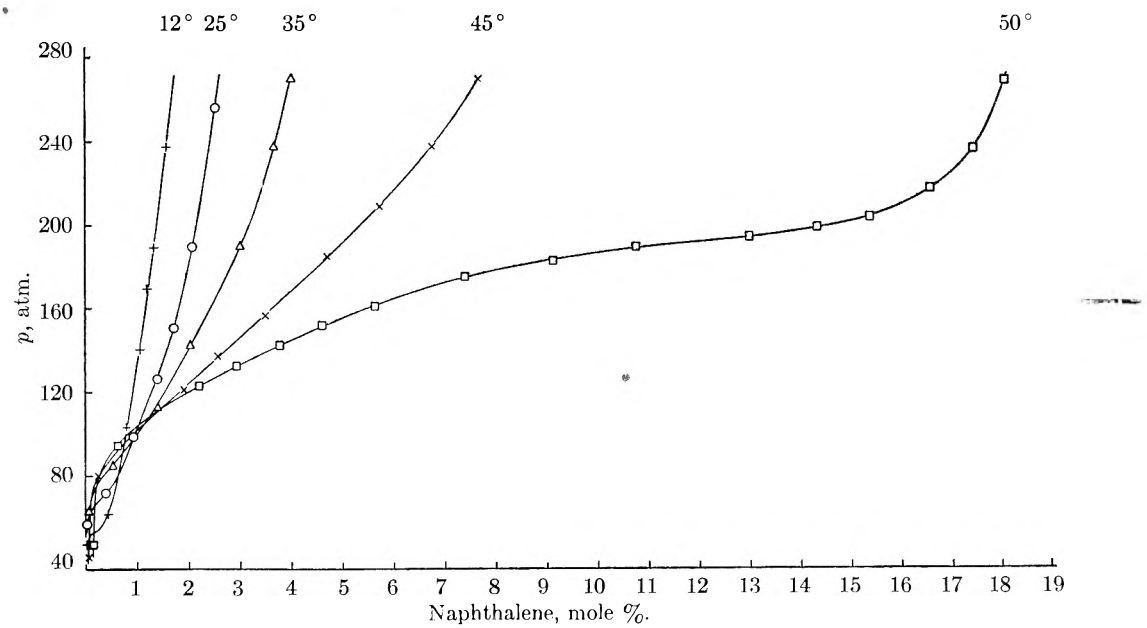

Fig. 1.—Pressure composition sections of the system ethylene–naphthalene at 12, 25, 35, 45 and 50°.

(1) G. A. M. Diepen and F. E. C. Scheffer, *J. Am. Chem. Soc.*, **70**, 4085 (1948).

(2) C. A. van Gunst, F. E. C. Scheffer and G. A. M. Diepen, THIS JOURNAL, **57**, 578 (1953).

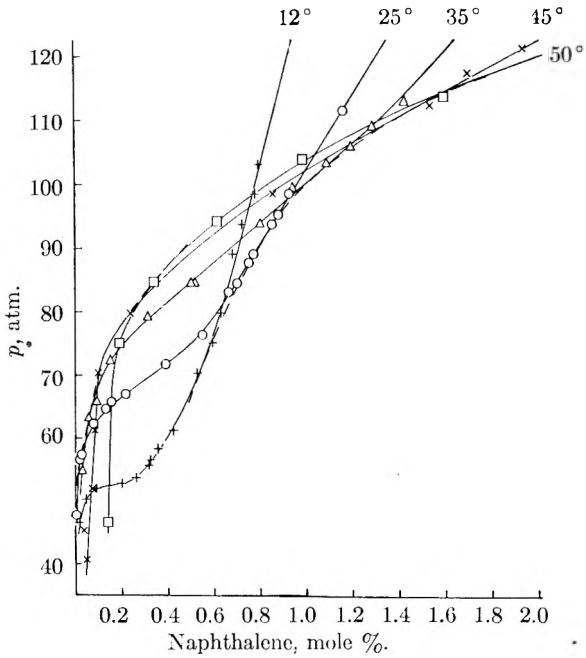

Fig. 2.—Part of the pressure-composition sections of Fig. 1.

fluid phase to be formed. Moreover, it is possible to find the same circumstances at temperatures higher than the temperature of the second critical end-point, when at least the pressure is higher than the pressure of the critical line which runs from the second critical end-point to the critical point of naphthalene. Since some of the points on this critical line were measured, an extrapolation can be made, showing that the pressure has to be somewhat above 200 atmospheres if we wish to observe up to 80° (the melting point of naphthalene at normal pressure). Using the same apparatus[1] the measurement of the isotherms at 12, 25 and 35° were continued at higher pressures. In addition the isotherms at 45 and 50° and finally one point at 60° and 270 atmospheres were measured.

Results and Discussion

The data obtained at the various temperatures are shown in the table whereas these data at 12, 25, 35, 45 and 50° together with the data from the first paper[1] are shown in Fig. 1. Whereas in the previous measurements only the isotherms of 12° had a slight slope $(dp/dx)_T$ in the neighborhood of the first critical end-point, the present data indicate that the isotherm of 50° has a slight slope in the neighborhood of 190 atmospheres and 12 mole % naphthalene where $(dp/dx)_T$ is small. If we raise the temperature to 52° (the temperature of the second critical end-point), the p–x curve must have a horizontal point of inflection situated at 174 atmospheres. Consequently the concentration of naphthalene in the supercritical fluid phase has to be there in approximately 12 mole %.

Figure 2 shows the part of Fig. 1 up to 120 atmospheres and 2 mole %. From Fig. 2 it is evident that the p–x sections at various temperatures supply a bundle of curves possessing two envelopes (drawn with dotted lines) bounding the curves at their left and right sides. As pointed out earlier[1] these two envelopes of the p–x lines are the loci of the points where $(dp/dT)_x = 0$ and $(dT/dx)_P = \infty$. In Fig. 3 and Fig. 4 the t–x and p–t sections, derived from the p–x figures found, are drawn for different pressures and different compositions. The points where $(dT/dx)_P = \infty$ and $(dp/dT)x = 0$ are connected with dotted lines. Therefore on these dotted lines the points are to be found for both envelopes of the p–x figure.

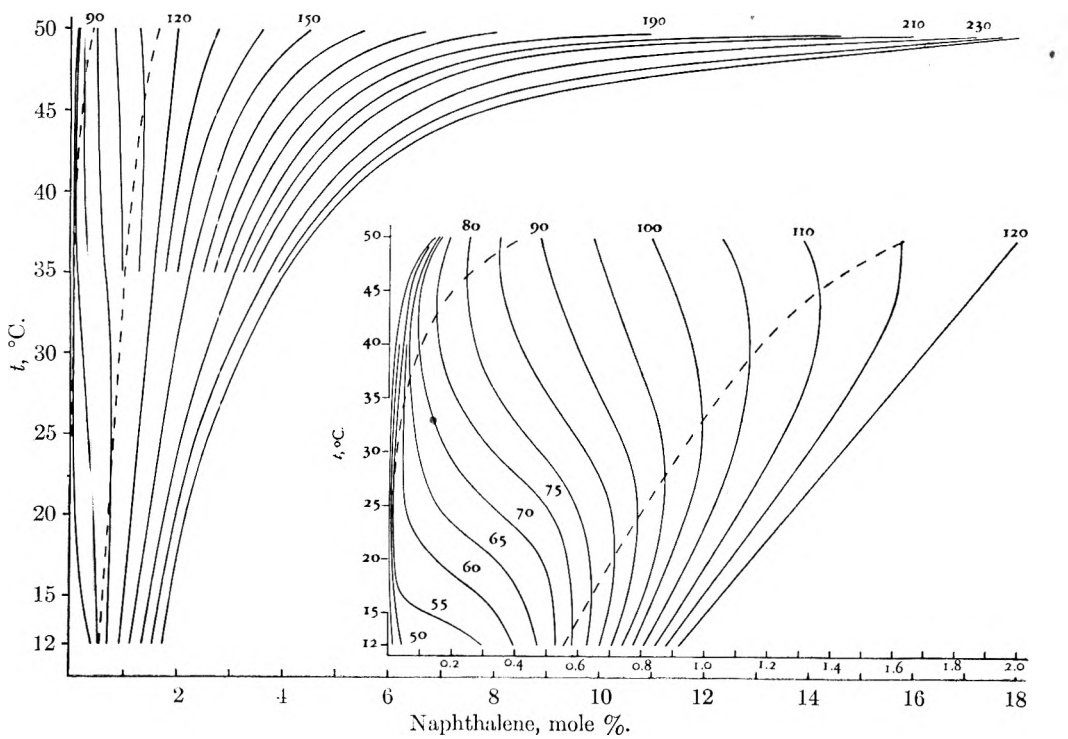

Fig. 3.—Temperature-composition sections of the system ethylene-naphthalene for various pressures.

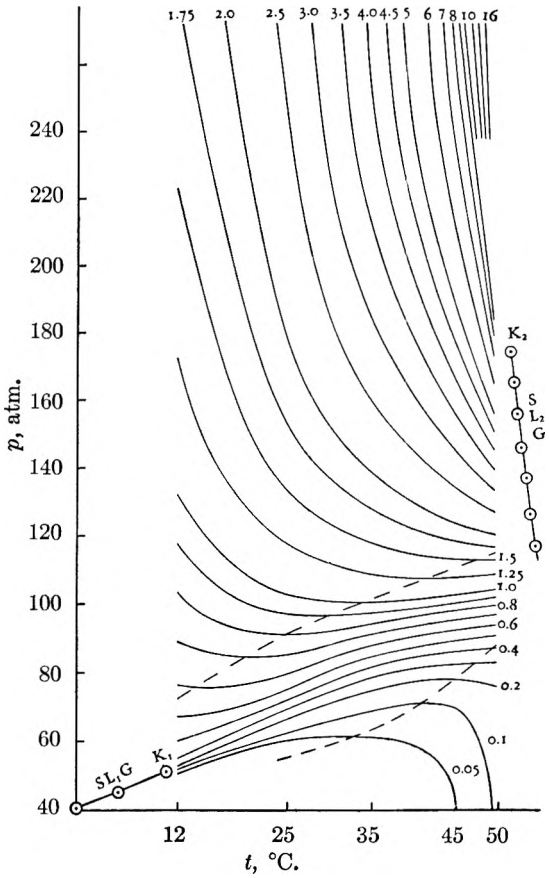

Fig. 4.—Pressure–temperature sections of the system ethylene–naphthalene for various concentrations.

Furthermore it is evident from these results that by raising the pressure as well as the temperature the solubility of naphthalene in supercritical ethylene increases enormously and that, for instance, at 50° and 270 atmospheres it amounts to 50 wt. % (18 mole %). Actually these are very concentrated solutions of slightly volatile solids in a supercritical fluid phase.

In the table we gave one observation at 60° and 270 atm. This is therefore an observation above the critical line running from the second critical end-point to the critical point of naphthalene. It was our intention to obtain several more data at this pressure at temperatures rising to the melting point of naphthalene. This appeared not to be possible, because these very concentrated solutions caused obstructions in the apparatus. With the aid of this observation at 60° and other observed or extrapolated values a t–x section for the whole range of concentrations at 270 atm. was compiled (Fig. 5). The solubility line has to end in the melting point of naphthalene at 270 atmospheres and this is calculated to be 90.0°.[3] The initial slope of the solubility line has to be in agreement with the molecular depression of the freezing point of naphthalene. This was calculated to be 73° for a melting point of 90.0° and a heat of fusion of 36.0 cal. g.[4] The shape of the solubility line

(3) "International Critical Tables," Vol. IV, p. 10.
(4) J. H. Perry, *Chem. Eng. Handbook*, 213 (1950).

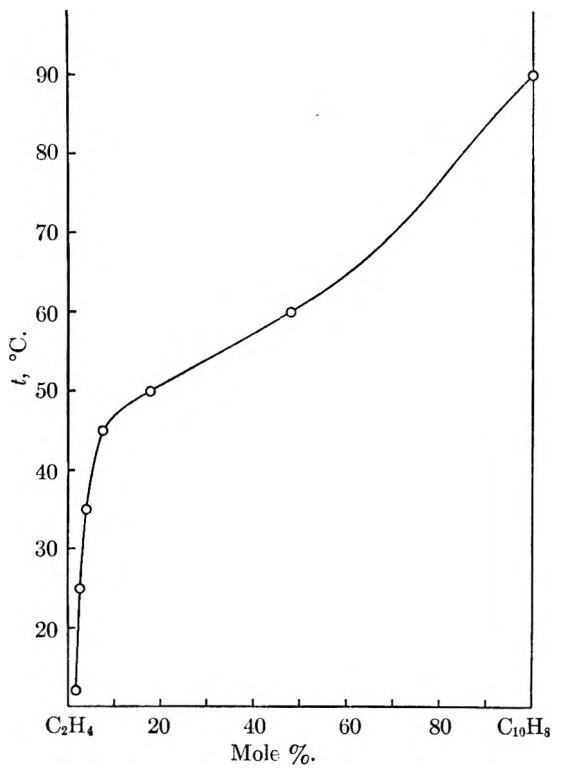

Fig. 5.—Temperature–composition section of the system ethylene–naphthalene at 270 atm.

indicates still the influence of the second critical end-point (two points of inflection).

TABLE I

PRESSURE–COMPOSITION DATA FOR ETHYLENE–NAPHTHALENE SYSTEM

p, atm.	x, mole %	p, atm.	x, mole %	p, atm.	x, mole %
12°		45°		50°	
237.4	1.57	270.3	7.66	270.3	17.98
189.8	1.33	237.4	6.76	237.4	17.37
169.6	1.19	208.8	5.75	218.3	16.54
140.2	1.06	185.1	4.71	204.2	15.34
		156.4	3.51	199.4	14.32
25°		142.2	2.86	194.7	12.98
		137.2	2.57	189.8	10.75
255.9	2.53	121.2	1.915	183.2	9.13
189.8	2.09	117.4	1.682	175.5	7.39
150.6	1.72	112.3	1.522	161.0	5.63
126.3	1.41	98.5	0.854	151.8	4.61
111.4	1.15	79.8	.239	142.2	3.78
		70.4	.098	132.4	2.94
35°		61.2	.083	123.0	2.20
		52.0	.070	113.6	1.575
270.3	4.01	45.4	.034	103.9	0.980
237.4	3.66	40.6	.048	94.2	.614
189.8	3.01			84.7	.339
145.7	2.17	60°		75.1	.188
142.2	2.04			65.2	.156
126.3	1.70	270.3	48.2	46.6	.139

Acknowledgment.—The experimental work described in this publication was performed by L. A. van Almkerk and J. F. P. Albert with the financial aid of the "Delftse Hogeschoolfonds." We wish to express our thanks for this valuable assistance.

ON CRITICAL PHENOMENA OF SATURATED SOLUTIONS IN BINARY SYSTEMS. II

BY C. A. VAN GUNST, F. E. C. SCHEFFER AND G. A. M. DIEPEN

Laboratory for Inorganic and Physical Chemistry at the Technical University, Delft, Holland

Received September 23, 1952

(1) Data are given for a number of binary systems, consisting of a volatile component (ethylene) and a slightly volatile substance (anthracene, hexamethylbenzene, hexaethylbenzene, stilbene, *m*-dinitrobenzene, hexachloroethane or naphthalene). They all belong to the type of system with an interrupted liquid–vapor critical locus. Measurement of the second critical end-point of the system ethylene–naphthalene is also reported. (2) For measurement of the solubility of mixtures of two solids in a fluid above the critical temperature, the system ethylene–naphthalene–hexachloroethane was chosen.

The present paper presents a continuation of studies of critical phenomena in systems of two components of widely differing volatility. In a previous paper[1] it has been pointed out that systems of this type possessing an interrupted liquid–vapor critical locus can be divided into the two groups shown in Figs. 1 and 2, both showing two critical end-points, K_1 and K_2, involving equilibrium with the solid phase, B (the less volatile component). In the first case, only one liquid phase occurs. The second case is characterized by metastable liquid–liquid immiscibility in the presence of vapor. The two cases are not positively distinguishable experimentally unless measurements can be made in the metastable region. However, strong inferences can be drawn from the trends of the two stable segments of the liquid–vapor critical locus and from the character of the curve or curves describing the equilibrium between solid, liquid and vapor. In the paper cited a number of systems have been discussed which almost certainly belong to the second group. The system ethylene–naphthalene is considered extensively in some later publications.[2]

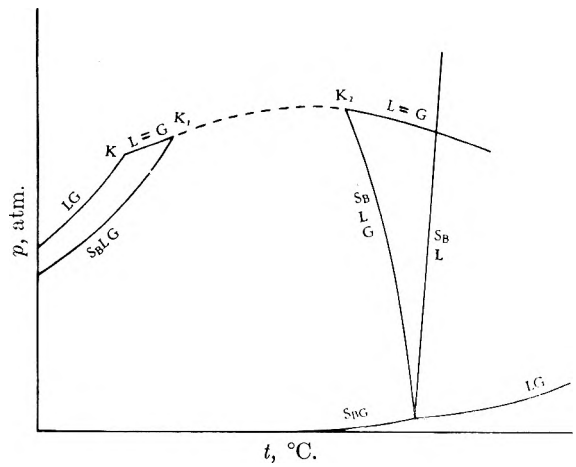

Fig. 1.—Pressure–temperature projection of a system with two critical end-points: ——, stable equilibria; - - - - -, metastable equilibria.

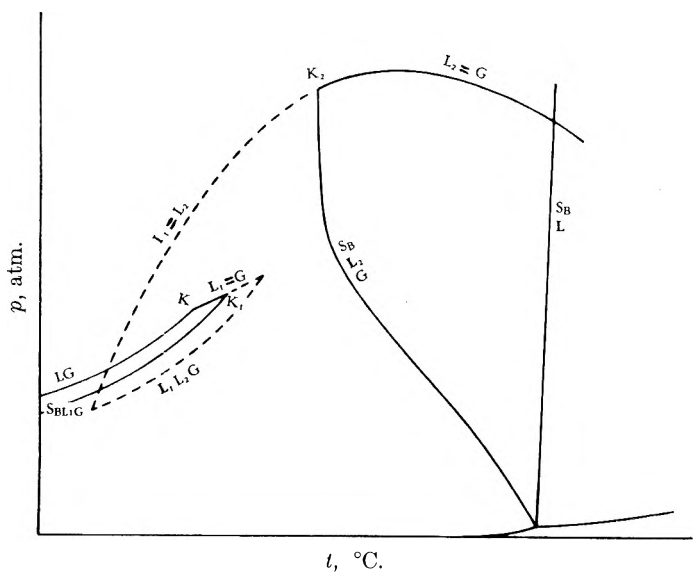

Fig. 2.—Pressure–temperature projection of a system with two critical end-points and metastable liquid–liquid immiscibility: ——, stable equilibria; - - - -, metastable equilibria.

The purpose of the present investigation is to find a slightly volatile component which will form with the system ethylene–naphthalene a ternary system, upon which measurements of the solubility of a mixture of two solids in a supercritical fluid can be performed. This substance should possess the following properties: (1) With ethylene a binary system must be formed in which the critical curve cuts the three-phase line S_B–L–G. (2) The ternary system with ethylene and naphthalene must possess a supercritical region, analogous to the system ethylene–naphthalene. This can be best fulfilled, if the eutectic temperature of the binary system with naphthalene is rather high.[3] (3) The solubility in supercritical ethylene must be of such an order that determinations can be performed accurately. An indication of this solubility near the critical point is found in the temperature difference between the first critical end-point of the system with ethylene and the critical point of ethylene.[4] The quantitative determination in mixtures with naphthalene, containing some impurities, such as drops of mercury and particles of grease should be simple. In order to test the agreement with these desiderata, the pressure–temperature projections of a number of binary systems

(1) G. A. M. Diepen and F. E. C. Scheffer, *J. Am. Chem. Soc.*, **70**, 4081 (1948).

(2) G. A. M. Diepen and F. E. C. Scheffer, *ibid.*, **70**, 4085 (1948); THIS JOURNAL, **57**, 575 (1953).

(3) C. A. van Gunst, F. E. C. Scheffer, and G. A. M. Diepen, *ibid.*, **57**, 581 (1953).

(4) M. Centnerzwer, *Z. physik. Chem.*, 427**46**, (1903); **60**, 441, (1907); **61**, 356 (1908); **69**, 81 (1909); E. Schroer, *ibid.*, **129**, 79 (1927).

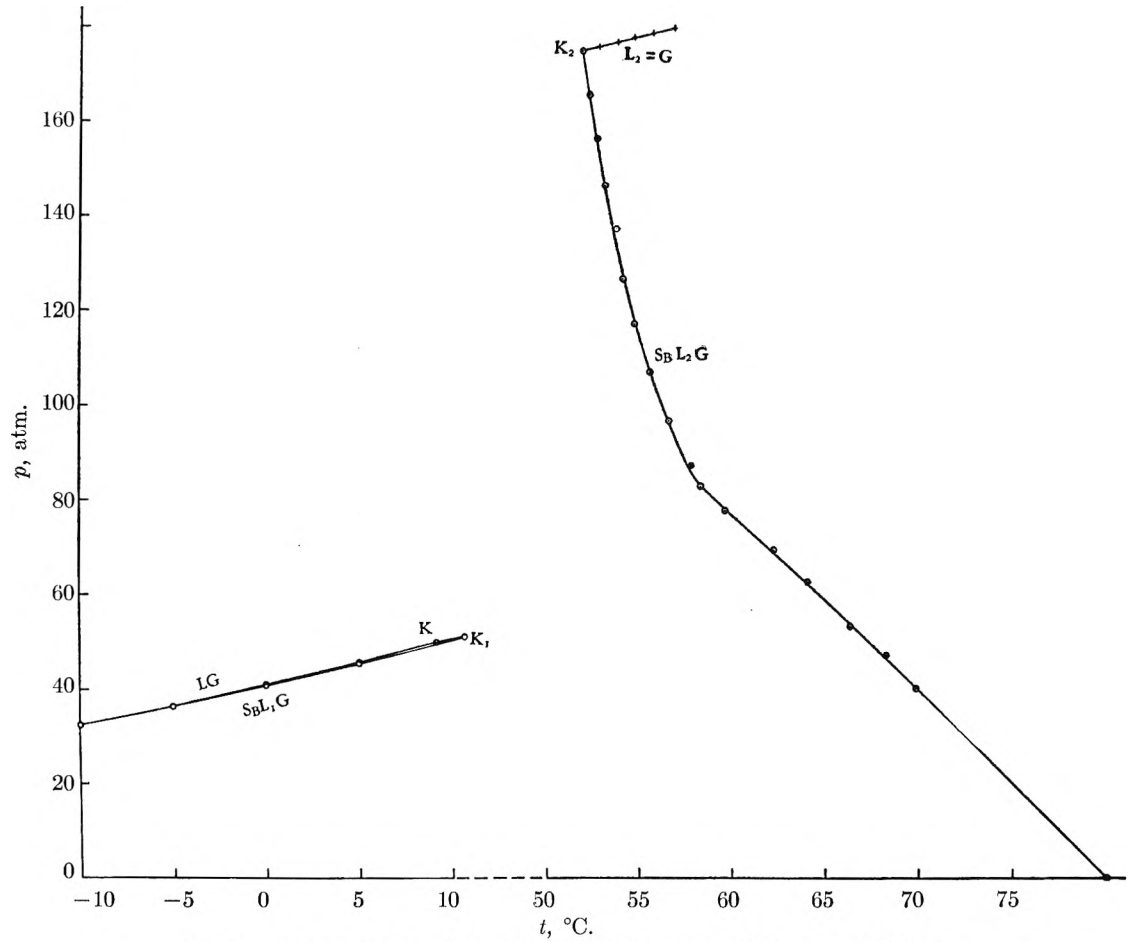

Fig. 3.—Pressure–temperature projection of the system ethylene–naphthalene.

were measured, with ethylene as the volatile component, and anthracene, hexamethylbenzene, hexaethylbenzene, stilbene, *m*-dinitrobenzene or hexachloroethane, as the slightly volatile component. A remeasurement of the system ethylene–naphthalene was performed to find the second critical endpoint.

Experimental Method.—All pressure–temperature measurements were carried out in glass Cailletet tubes with electromagnetic stirring according to Kuenen. Temperatures were determined with calibrated Anschütz thermometers while pressures were read from regularly controlled Schaeffer and Budenberg precision pressure gages.

A different supply of ethylene was used from that in the previous research. The material used here was prepared from a commercial product.[5] After washing it thoroughly first with ammoniacal Cu_2Cl_2 solution and then with dilute sulfuric acid, it was dried by passing it over P_2O_5. Next the non-condensable gases were removed (controlled with Tesla-apparatus) and finally the ethylene was further purified by eliminating ten times the most volatile and the least volatile fraction during condensation.

As an indication of the purity of the sample, several points were measured on the vapor pressure curve using different volume ratios of vapor and liquid; no detectable pressure differences were noted at constant temperature. Measurements of the critical constants were found to be in good agreement with those of Maass and co-workers[6] using the classical definition of critical point (t = 9.22°; p = 49.74 atm.).

The values for the p–t line of ethylene differ slightly from those cited in an earlier publication.[1]

Experimental Results.—The measurements are summarized in the Tables I–VII. The curve S_B–L_2–G of the system ethylene–hexachloroethane could not be measured, because the second component reacted with mercury at such high temperatures. Under 60° this reaction was unnoticeable. Only the measurements of the system ethylene–naphthalene are shown graphically in Fig. 3.

Discussion of Results.—In all systems described, the three-phase line S_B–L–G has two critical endpoints K_1 and K_2. The pressure–temperature projections of the systems ethylene–anthracene, ethylene–hexaethylbenzene, ethylene–hexamethylbenzene, ethylene–*m*-dinitrobenzene, ethylene–hexachloroethane and ethylene–stilbene are analogous to the one for ethylene–naphthalene (Fig. 3). Although metastable immiscibility could not be detected in any of these cases, it is probable, from the curvature of the three-phase lines S_B–L–G, that they all belong to the systems with metastable immiscibility. Particularly in the case of ethylene–

(5) Ohio Chemical and Manufacturing Co. 99.5% pure.

(6) J. Dacey, R. McIntosh and O. Maass, *Can. J. Research*, **17B**, 206 (1939); S. M. Naldrett and O. Maass, *ibid.*, **18B**, 118 (1940).

TABLE I

SYSTEM ETHYLENE–ANTHRACENE

M.p. anthracene 215°

t°, C.	p, atm.
L_1–G for ethylene	
−10.0	32.40
−5.0	36.35
0.0	40.85
5.0	45.55
9.2 = t_K	49.90 = p_K
S_B–L_2–G	
195.6	72.30
196.7	64.35
197.3	58.50
197.6	53.65
198.0	46.55
198.6	41.90
201.6	36.40
204.0	28.70
215	1.00
S_B–L_1–G	
−10.0	32.40
−5.0	36.35
0.0	40.80
+5.0	45.50
+9.4 = t_{K1}	50.05 = p_{K1}

TABLE II

SYSTEM ETHYLENE–HEXAETHYLBENZENE

M.p. hexaethylbenzene 128°

t°, C.	p, atm.
S_B–L_1–G	
−10.0	32.35
−5.0	36.25
0.0	40.80
2.5	43.25
5.0	45.35
8.0	48.35
9.3	49.50
10.0	50.30
11.0	51.80
11.6 = t_{K1}	52.20 = p_{K1}
S_B–L_2–G	
105.3	64.35
105.6	62.45
105.8	61.40
106.6	58.35
106.8	55.20
108.8	47.55
111.0	43.35
112.2	38.35
114.6	33.20
116.4	28.55
118.2	23.75
120.1	19.20
121.2	16.10
128	1
L_1 = G	
9.2	49.90
10.1	50.85
10.2	50.95
10.4	51.15
11.1	51.75
11.6 = t_{K1}	52.20 = p_{K1}

TABLE III

SYSTEM ETHYLENE–HEXAMETHYLBENZENE

M.p. hexamethylbenzene 165°

t°, C.	p, atm.
S_B–L_1–G	
−10.0	32.40
−5.0	36.20
0.0	40.75
5.0	45.40
9.8 = t_{K1}	50.40 = p_{K1}
S_B–L_2–G	
142.6	83.10
144.2	76.00
146.6	66.20
149.0	57.00
151.8	47.45
154.2	37.95
156.7	28.45
159.6	19.20
161.1	14.85
165	1

TABLE IV

SYSTEM ETHYLENE–STILBENE

M.p. stilbene 122°

t°, C.	p, atm.
S_B–L_1–G	
−10.0	32.40
−5.0	36.30
0.0	40.70
5.0	45.50
9.5 = t_{K1}	50.20 = p_{K1}
S_B–L_2–G	
109.0	78.25
109.5	71.75
109.9	68.20
110.4	62.75
111.4	58.60
112.2	53.75
112.6	49.35
122.0	1

TABLE V

SYSTEM ETHYLENE–*m*-DINITROBENZENE

M.p. m-dinitrobenzene 89.9°

t°, C.	p, atm.
S_B–L_1–G	
−10.0	32.40
−5.0	36.35
0.0	40.85
5.0	45.55
9.3 = t_{K1}	50.00 = p_{K1}
S_B–L_2–G	
83.5	78.15
83.7	74.30
83.9	68.70
84.2	64.35
84.5	59.60
84.8	55.55
85.3	51.00
89.9	1

TABLE VI

SYSTEM ETHYLENE–HEXACHLOROETHANE

M.p. (under slightly elevated pressure) 187°

t°, C.	p, atm.
S_B–L_1–G	
−10.0	32.15
−5.0	36.05
0.0	40.30
5.0	44.80
10.0	49.80
12.4 = t_{K1}	52.70 = p_{K1}

TABLE VII

SYSTEM ETHYLENE–NAPHTHALENE

M.p. naphthalene 80.0°

t°, C.	p, atm.
S_B–L_1–G	
−10.0	32.40
−5.0	36.35
0.0	40.70
5.0	45.25
10.7 = t_{K1}	51.15 = p_{K1}
L_2 = G	
52.0 = t_{K2}	174.1 = p_{K2}
52.9	175.1
53.9	176.0
54.8	177.0
55.8	177.9
56.9	178.9
S_B–L_2–G	
52.0 = t_{K2}	174.1 = p_{K2}
52.4	165.0
52.8	155.7
53.2	145.8
53.8	136.7
54.2	126.1
54.8	116.7
55.6	106.7
56.6	96.4
57.8	87.1
58.3	82.5
59.6	77.5
62.2	69.2
64.0	62.4
66.3	53.1
68.2	47.1
69.8	40.0
80.0	1

naphthalene, where the two measured parts of the critical line do not seem to be parts of one curve without cusps, the metastable immiscibility is highly probable.

In the same system it was possible to determine the second critical end-point by direct observation and by graphical extrapolation from the three-phase line S_B–L_2–G and the critical curve (L_2 = G).

At the second critical end-point, contrary to the first critical end-point, a saturated solution which coexists with a gas phase becomes critical by a slight temperature lowering.

The system ethylene–hexachloroethane shows a maximum increment of the critical temperature, has a rather extended supercritical region, and gives a ternary system (with naphthalene) of the desired type which will be reported in another paper.[3] Furthermore hexachloroethane easily can be determined quantitatively. Therefore hexachloroethane seems promising for use as a third component, together with ethylene and naphthalene, for measurements of the solubility of mixtures of solids in a supercritical fluid.

ON CRITICAL PHENOMENA OF SATURATED SOLUTIONS IN TERNARY SYSTEMS

BY C. A. VAN GUNST, F. E. C. SCHEFFER AND G. A. M. DIEPEN

Contribution from the Laboratory for Inorganic and Physical Chemistry at the Technical University, Delft, Holland

Received September 23, 1952

Pressure–temperature measurements are given for the ternary system ethylene–naphthalene–hexachloroethane, including the critical phenomena of saturated solutions. Observations are discussed from the viewpoint of the theory of the phase equilibria in the critical region. The system shows a temperature range where solubility measurements can be made of two solids in a supercritical fluid.

Introduction

The purpose of this investigation was to study the phase-equilibria of a ternary system which could be adapted for exact measurements of the solubility of mixtures of two solids in a supercritical fluid.

To find such a system the necessary conditions must be traced. In some previous[1–4] papers binary systems, consisting of a volatile component A and a slightly volatile component B showing an interrupted liquid–vapor critical locus with two critical end-points are described. In such systems a temperature range is noticed between the first and second critical end-points where, at any pressure, only one fluid phase can coexist with solid B.

Now we want to find a ternary system of a volatile component A and two slightly volatile components B and C which has a temperature range in which solids B and C can coexist only with a supercritical phase. Such a ternary system can be built from two binary systems A–B and A–C in which the three-phase lines S_B–L–G and S_C–L–G, respectively, cut the critical liquid–vapor curve. If we now consider the ternary univariant equilibrium: solid B, solid C, liquid and gas with increasing temperature, there will be the possibility, at least if the solubility of B and C in liquid A is not too high, that this series of univariant equilibria ends in a first double critical end-point,[5] where the liquid and gas phase become identical. The four-phase line S_B–S_C–L–G will appear again at the second double critical end-point and run to the corresponding quadruple point of the binary system B–C. The p–t projection of such a system is depicted in Fig. 1. K_1K_1' and K_2K_2' are the first and second critical end-points, respectively, of the two binary systems. Two critical lines run from these points to the ternary critical end-points p and q of the four-phase line S_B–S_C–L–G. On these lines the ternary critical points are found for liquids saturated with one of the solids.

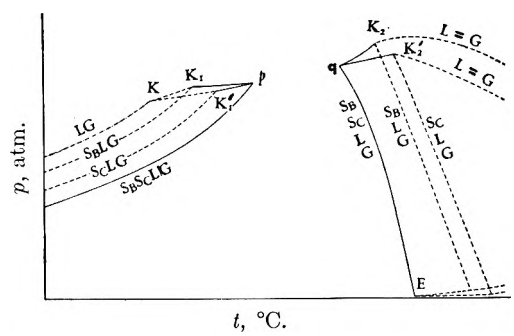

Fig. 1.—Pressure–temperature projection of a ternary system with a four-phase line S_B–S_C–L–G cut in two parts. Full drawn lines are univariant ternary curves, dotted lines are the univariant curves of the binary systems.

Between the temperatures of p and q there is a temperature range where together with solid B, C or both only one supercritical phase can coexist at all pressures.

From Fig. 1 it follows that the eutectic temperature of the binary system B–C has to be well above the temperature of the critical point of A. If this eutectic temperature is too low, there will be a possibility that the four-phase line S_B–S_C–L–G will not intersect the liquid–vapor critical locus.

(1) G. A. M. Diepen and F. E. C. Scheffer, *J. Am. Chem. Soc.*, **70**, 4081 (1948).

(2) C. A. van Gunst, F. E. C. Scheffer and G. A. M. Diepen, THIS JOURNAL, **57**, 578 (1953).

(3) G. A. M. Diepen and F. E. C. Scheffer, *J. Am. Chem. Soc.*, **70**, 4085 (1948).

(4) G. A. M. Diepen and F. E. C. Scheffer, THIS JOURNAL, **57**, 575 (1953).

(5) So denoted by A. Smits, Verslag Gewone Vergadering Wisen.-Natuurk. Afd.; *Nederland Akad. Wetenschap.* **21**, 149 (1912); **24**, 731 (1915).

Another type of ternary system for which the stable equilibria are very similar to the above mentioned can be found if A, B and C are selected so that the binary system A–B and A–C show a supercritical region, both possessing metastable immiscibility in the liquid phase, the eutectic temperature E of the binary system B–C will be well above the critical point of A, and the solubilities of B and C in liquid A will be rather low. Such a system is shown in Fig. 2.

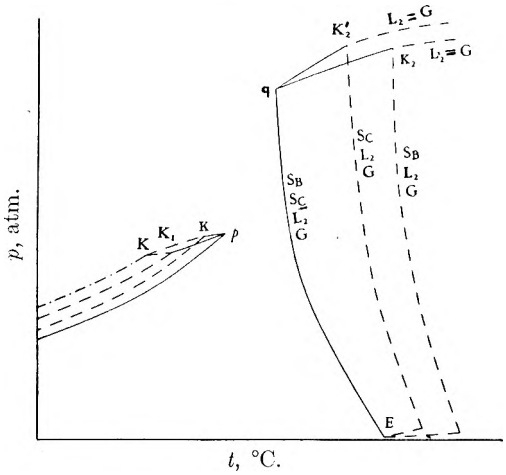

Fig. 2.—Pressure–temperature projection of a ternary system of two slightly volatile substances (B and C) and a volatile one (A) showing metastable immiscibility in the liquid phase. Full drawn lines are univariant ternary curves, dotted lines are the univariant curves of the binary systems.

Again a supercritical region is found between the temperatures of the first and second double critical end-points, where at all pressures, at least in the stable state, together with solid B, solid C or mixtures of both only one fluid phase can exist.

In the stable equilibria a direct proof of the (metastable) immiscibility is impossible. Indications can only be found from the form of the four-phase line S_B–S_C–L_2–G and from the less probable coherence of the critical curves of saturated solutions.

Until now it has been assumed that the binary system B–C had an eutectic temperature in the melting diagram. In the case that B and C possess a continuous series of solid solutions in the solid phase analogous views can be held. Experimental proofs for such cases have been reported for the system SO_2–$HgBr_2$–HgI_2 by Niggli[6] and for H_2–CO–N_2 by Verschoyle.[7] However for experimental purposes such systems are far less attractive.

It can be concluded that two types of ternary systems, *viz.*, those shown in Fig. 1 and Fig. 2, are suitable for measurement of the solubility of a mixture of solids in a supercritical fluid.

Experimental Results

For reasons stated earlier[2] measurements were carried out on the system ethylene–naphthalene–hexachloroethane using a Cailletet apparatus with a glass capillary above mercury. Pressures were measured by means of a calibrated Schaeffer and Budenberg high pressure gage. Temperatures were read from calibrated Anschütz thermometers.

(6) P. Niggli, *Z. anorg. allgem. Chem.*, **75**, 161 (1912); **77**, 321 (1912).
(7) T. T. A. Verschoyle, *Phil. Trans.*, **230A**, 189 (1932).

TABLE I

$C_{10}H_8$–C_2Cl_6–L_1–G

t, °C.	p, atm.
−10.0	31.90
−7.4	33.95
−5.0	35.55
−2.4	38.30
0.0	39.85
2.4	42.60
5.0	44.45
7.4	46.45
10.0	49.15
12.4	51.80
15.0	54.70
15.3 = t_p	55.10 = p_p

TABLE II

$C_{10}H_8$–C_2Cl_6–L_2–G

t, °C.	p, atm.	t, °C.	p, atm.
56.6	1	35.2	48.7
49.3	17.3	33.4	51.7
48.0	19.4	31.4	53.5
46.5	20.5	30.2	56.0
45.6	24.8	28.9	57.9
44.9	27.5	28.3	58.9
44.2	29.4	26.3	61.9
43.0	31.2	26.3	63.2
42.1	34.4	25.6	65.2
41.6	35.4	25.5	65.9
40.2	38.8	25.5	68.0
40.0	38.8	25.6	69.1
39.1	41.5	25.7	74.8
37.2	45.2	25.6	77.6
36.8	45.8	25.5	82.5
35.9	47.7	25.5 = t_q	86.6 = p_q

TABLE III

$C_{10}H_8 + L_1 = G$

t, °C.	p, atm.
10.7 = t_{K1}	51.5 = p_{K1}
13.6	54.10
15.3 = t_p	55.10 = p_p

TABLE IV

$C_2Cl_6 + L_1 = G$

t, °C.	p, atm.
12.4 = t_{K1}	52.70 = p_{K1}
15.3 = t_p	55.10 = p_p

TABLE V

$C_{10}H_8 + L_1 = G$

t, °C.	p, atm.
52.0 = t_{K2}	174.1 = p_{K2}
49.8	165.0
46.5	152.4
46.3	151.9
43.1	140.6
38.8	126.3
36.7	119.6
35.1	114.6
33.1	108.1
29.2	96.8
27.2	91.2
26.2	88.6
25.7	87.3
25.5 = t_q	86.6 = p_q
25.3	86.0 (metastable)

TABLE VI

$C_2Cl_6 + L_2 = G$

t, °C.	p, atm.
41.0	103.4
39.2	101.5
37.5	99.5
35.8	97.7
32.8	94.1
31.1	92.4
29.6	90.8
28.5	89.5
27.6	88.5
26.8	88.7
26.4	87.3
26.0	86.9
25.5 = t_q	86.6 = p_q
25.4	86.4 (metastable)

The results are shown graphically in Fig. 3.

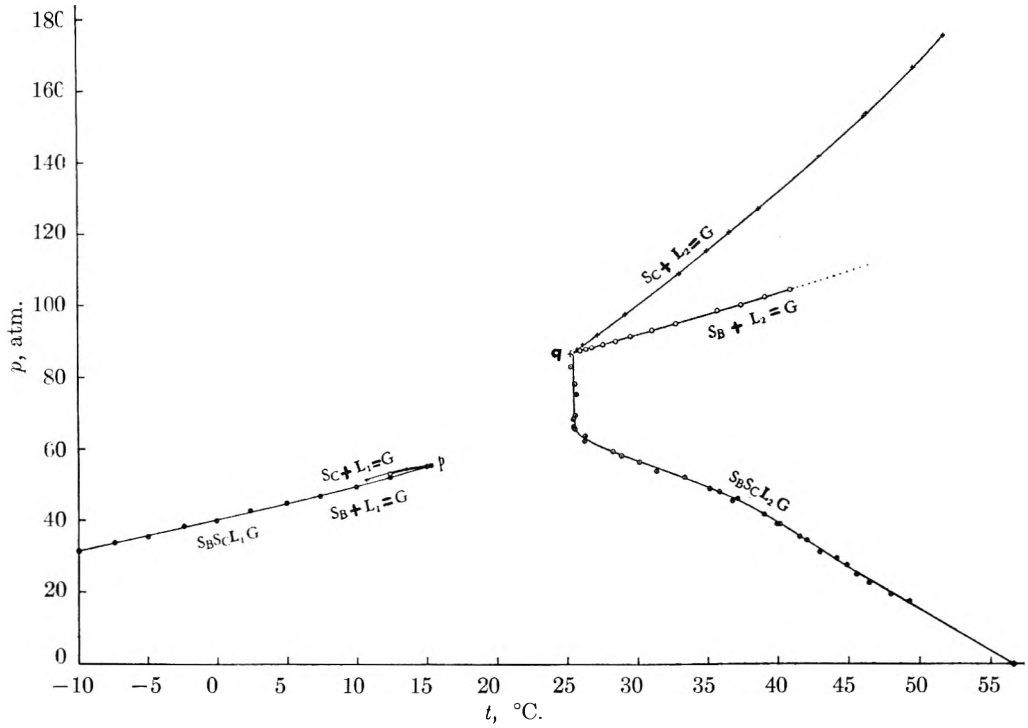

Fig. 3.—Pressure-temperature projection of some univariant equilibria in the ternary system ethylene–naphthalene–hexachloroethane (B = hexachloroethane; C = naphthalene).

The ethylene was prepared as described in an earlier paper.[2] The naphthalene was purified by repeated crystallization from alcohol (m.p. 80.0°), the hexachloroethane by the same procedure (m.p. under slightly increased pressure 187°). 56.6° for the eutectic temperature of naphthalene–hexachloroethane was found to be in agreement with Parijs.[8] The four-phase line S_B–S_C–L_1–G was measured analogous to vapor-pressure measurements. The four-phase line S_B–S_C–L_2–G was determined by the first melting for two considerably different compositions. The critical curves of solutions, saturated with one solid, including the first and second double critical end-points, were measured for a number of different compositions. For each composition in the Cailletet tube the quantity of B and C could be changed to some degree by bringing a portion under the mercury.

Table I gives the four-phase line naphthalene–hexachloroethane–L_1–G. Table II contains the measurements of the four-phase line naphthalene–hexachloroethane–L_2–G. Tables III and IV give points from the critical curves (L_1 = G) for solutions, saturated with naphthalene or hexachloroethane. In Tables V and VI the measurements are recorded for the critical curves (L_2 = G) of solutions saturated with naphthalene or hexachloroethane. The curve naphthalene–L_2 = G terminates in the second critical end-point of the system ethylene–naphthalene published in another paper.[2] The curve hexachloroethane–L_2 = G has not been measured up to the second critical end-point of the system hexachloroethane, because hexachloroethane reacts at such high temperatures with mercury. From these results the constants of the first and second ternary critical end-points can be taken as t_p = 15.3°, P_p = 55.1 atm. and t_q = 25.5°, p_q = 86.6 atm.

Discussion of Results

The four-phase line naphthalene–hexachloroethane–L_2–G must possess a five-phase point, as the result of a conversion of the triclinic α-form of hexachloroethane to the rhombic β-modification. This point can be calculated at 29 atm. as 44.4°, using the measurement of the transition-temperature from Wiebenga[9] and the pressure–temperature dependence by Bridgman.[10] An alteration of the slope of the four-phase line is not self-evident from the measurements. The temperature range where, together with solid naphthalene, hexachloroethane, or mixtures of both, only one fluid phase can coexist is between 15.3 and 25.5°.

Notwithstanding our efforts in realizing the metastable immiscibility in the liquid phase, we did not succeed. In this case, however, the choice between the types of Fig. 1, without, and Fig. 2, with metastable immiscibility, is not difficult. The metastable immiscibility is highly probable because of the form of the four-phase line naphthalene–hexachloroethane–L_2–G, the relatively great pressure difference of the first and second double critical end-points and the fact that the critical curves of saturated solutions do not seem to be parts of two curves without cusps. The results of the solubility measurements of naphthalene and hexachloroethane in ethylene in the temperature range between 15.3 and 25.5° will be reported in another paper.

(8) S. Parijs, *Z. anorg. allgem. Chem.*, **225**, 425 (1936).

(9) E. H. Wiebenga, *ibid.*, **225**, 38 (1935).

(10) Bridgman, *Proc. Am. Acad. Arts Sci.*, **51**, 55 (1916).

THE ADSORPTION OF FLEXIBLE MACROMOLECULES[1]

BY ROBERT SIMHA, H. L. FRISCH[2] AND F. R. EIRICH

New York University and Polytechnic Institute of Brooklyn, New York, N. Y.

Received November 5, 1952

The formation of a monolayer from dilute solution is considered. A statistical analysis indicates that only a fraction $\sim t^{1/2}$ of the total number t of chain segments is deposited on the average. The adsorbed segments are arranged in short sequences, separated by bridges extending into the solution. From the respective frequency distributions, the free energy changes arising from the mixing with sites on the surface and with solvent are obtained. For very large chains, the adsorption isotherm approaches the form expected for molecules which dissociate on the surface into single units. The heat of adsorption is proportional to the square root of the molecular weight for low degrees of occupancy of the surface. Thereafter a term proportional to the molecular weight is to be added. It represents the interaction of the adsorbed segments and hence depends on the cohesion energy of the polymer. For a given molecular weight, the number of anchor points and consequently the heat of adsorption are the larger, the smaller the radius of the free coil, that is, the more flexible the molecule. In this manner the results have a bearing on the adhesion problem also. Certain recent experiments are briefly discussed in respect to the effect of solvent, temperature and molecular weight.

I. Introduction

The statistical mechanics of adsorption of gases on solids has been developed in great detail.[3] Simultaneously there have occurred important developments in the theory of solutions. Because of fundamental similarities this was, of course, not accidental. In recent years the physical chemistry of high polymer solutions has received considerable attention, yet we are not aware of any recent treatment of the adsorption problem.[4]

In the following an equilibrium theory of adsorption is presented. Since we are concerned with flexible chains, two aspects are to be considered. First there is the statistics of deposition of chain units on the substrate. It is obvious that deposition of the whole chain is extremely unlikely and only a fraction of the total number of chain segments will be "trapped" on the surface. These form segments of varying length which are separated by portions extending into the solution. Secondly the thermodynamic properties of the monomolecular layer on the surface are to be determined. This yields the adsorption isotherm and the free energy of adsorption as a function of, among others, the molecular weight and flexibility of the polymer. The monolayer will be regarded as localized.

The manner in which a chain anchors itself to a substrate is important also for the problem of adhesion. Hence our results have a bearing on this question.

The following assumptions will be made. The original polymer is supposed to be in dilute solution. The adsorbing surface is thought of as consisting of a regular array of "active spots," closely packed on the surface. It is at these sites that interaction between the surface and some part of the polymer chain occurs, leading finally to a strong adhesion of the part of the polymer chain to a given site. The number of sites, N_s, is taken to be proportional to the surface area of the adsorbent.

The active spots of the polymer chain which are capable of directly participating in the interaction with the surface may each be part of a single monomer unit, or included once, on the average, in r monomer segments ($r \geqq 1$) making up the chain. The hypothetical polymer we will study will consist of t such "statistical segments" whose length is A, roughly the size of the statistical segment which characterizes the behavior of the amorphous polymer chain in solution. Furthermore, we assume throughout that the area of an active adsorption site is equal to the area of the statistical segment of the polymer. Once a segment of the polymer finally adheres to a given site, this site will be considered as saturated and henceforth no further adsorption will occur at that locus. The immediate area surrounding a given site can be thought of as being planar, since the adsorbent or particles of the adsorbent are many times larger in size than the polymer. The solvent is supposed not to participate in the adsorption.

II. Statistics of Deposition

The polymer chain, in dilute solution, exists as a more or less flexible random coil. Let it be characterized by a Gaussian distribution of end to end distances

$$W(x, y, z, t)\mathrm{d}x\,\mathrm{d}y\,\mathrm{d}z = \frac{C^3}{(ft)^{3/2}} \exp\left[-(x^2 + y^2 + z^2)/4ft\right]\mathrm{d}x\,\mathrm{d}y\,\mathrm{d}z \quad (1)$$

where x, y, z are the components of the vector $\vec{r}$, connecting one end of the polymer chain to the other end located at the origin of our coördinate system. x, y, z are expressed here in units of A. C^3 is part of the normalization constant and equal to $(2\pi^{1/2})^{-3}$. f is a pure number and accounts for the valence angle $\pi - \xi_1$ between successive bonds of the polymer as well as the flexibility of the chain determined primarily by the intermolecular potential barrier $V(\xi_2)$ restricting rotation. Using eq. (1) we will be able to calculate the configuration of a polymer molecule adsorbed by the adsorbent. We note that eq. (1) can be written as

$$W(x, y, z, t) = \frac{C}{(ft)^{1/2}} e^{-x^2/4ft} \cdot \frac{C}{(ft)^{1/2}} e^{-y^2/4ft} \cdot \frac{C}{(ft)^{1/2}} e^{-z^2/4ft} = W_x(x, t) \cdot W_y(y, t) \cdot W_z(z, t) \quad (1a)$$

That is, the components of the end to end distance are independent of each other. When a molecule is located in the immediate vicinity of the adsorbing surface, eq. (1) no longer holds. Letting $z - h = 0$ be the equation of the adsorbing surface, eq. (1) has to be modified, since no part of the polymer

(1) Presented at the 122nd Meeting of the American Chemical Society, Atlantic City, N. J., September 14–19, 1952.

(2) Department of Physics, Syracuse University, Syracuse, N. Y.

(3) A. R. Miller, "The Adsorption of Gases on Solids," Cambridge University Press, 1949.

(4) For an early discussion, see E. Broda and H. Mark, *Z. physik. Chem.*, **A180**, 302 (1937).

chain may penetrate the surface. In random-walk terminology the surface acts as a reflecting wall.[5] The distribution function of the end to end distance vector becomes consequently

$$W_h(x, y, z, t)\mathrm{d}x\,\mathrm{d}y\,\mathrm{d}z = W(x, y, z, t)\mathrm{d}x\,\mathrm{d}y\,\mathrm{d}z + W(x, y, 2h - z, t)\mathrm{d}x\,\mathrm{d}y\,\mathrm{d}z; \quad z \leqq h$$

or

$$W_h(x, y, z, t) = \frac{C^3}{(ft)^{3/2}} e^{-(x^2 + y^2)/4ft}[e^{-z^2/4ft} + e^{-(2h - z)^2/4ft}] \quad (2)$$

The x, y, z components are again independent, *cf.* eq. (2). In what follows, little error is made by setting $h = 0$. This is equivalent to assuming that every polymer molecule adhering to the surface is adsorbed at the first segment. Equation (2) becomes

$$W_0(x, y, z, t) = \frac{2C^3}{(ft)^{3/2}} e^{-(\rho^2 + z^2)/4ft}$$

where

$$\rho^2 = x^2 + y^2 \text{ and } z \leqq 0 \quad (2a)$$

The relation exhibited by eq. (2a) will allow us to calculate the probability that ν out of t segments of a polymer chain are adsorbed. First however we must find the probability $p(\tau)$ that, provided the first segment of a polymer molecule is adhering to the surface located at $z = 0$, the τth of the t segments of the polymer chain also adheres. Making implicit use of the random placing of segments of the chain and letting α be the constant probability that if a segment touches the surface it will adhere, we find for the desired probability ($\phi = \tan^{-1} y/x$),

$$\begin{aligned} p(\tau) &= \alpha \int_0^{\tau}\int_0^{2\pi} \sum_{\text{all } x', y'; z' \leqq 0} W^{(2)}(x, y, 0, \tau/x', y', z', t - \tau)\rho\mathrm{d}\rho\mathrm{d}\phi \\ &= \alpha \int_0^{\tau}\int_0^{2\pi} W_0(x, y, 0, \tau)\Sigma W_0(x', y', z', t - \tau)\rho\mathrm{d}\rho\mathrm{d}\phi \\ &= \alpha \int_0^{\tau}\int_0^{2\pi} W_0(x, y, 0, \tau)\rho\mathrm{d}\rho\mathrm{d}\phi = \frac{8\pi C^3\alpha}{f^{1/2}t^{1/2}}(1 - e^{-\tau/4f}) \end{aligned} \quad (3)$$

Since t is very large (effectively infinite) it is of interest to calculate the average value of $p(\tau)$ over all t segments

$$p = \langle p(\tau)\rangle_t = \frac{1}{t}\sum_{\tau=1}^{t} p(\tau) \doteq \frac{1}{t}\int_1^t p(\tau)\mathrm{d}\tau$$

Evaluating this integral we find

$$p = 2\alpha/(\pi ft)^{1/2} - O\left(\frac{1}{t}\right) \quad (4)$$

Treating $p(\tau)$ as a random variable one easily finds that the variance of $p(\tau)$, $\langle[p(\tau) - p]^2\rangle_t$ is $0(1/t)$ for large t, and therefore the error made in replacing $p(\tau)$ by p if p is very small.

We are now ready to evaluate the probability $u(\nu, t)$ that a given chain adheres to the surface at ν segments out of a total of t, these ν segments being randomly placed. A polymer chain will adhere to the surface with ν segments if either of two mutually exclusive conditions are fulfilled. (a) At the $(t - 1)^{st}$ segment, $\nu - 1$ segments adhere and the t^{th} segment is so placed that it adheres, or (b) at the $(t = 1)^{st}$ segment, ν segments adhere and the t^{th} segment is so placed that it does not adhere.

Hence $u(\nu, t)$ satisfies

$$u(\nu, t) = p(\tau)u(\nu - 1, \tau - 1) + [1 - p(\tau)]u(\nu, \tau - 1) \quad \text{for } \tau = 1, 2, \ldots t;\ \nu \geqq 1 \quad (5)$$

This difference equation has to be solved with the initial and boundary conditions

$$\begin{aligned} u(\nu, t) &= 0 \text{ for } \nu > t \\ u(1, t) &= 0 \text{ for } t = 0 \\ &= 1 \text{ for } t = 1 \end{aligned} \quad (6)$$

Introducing the moment generating function

$$\phi_\tau(S) = \sum_{\nu=0}^{\infty} S^\nu u(\nu, \tau)$$

we find from eqs. (5) and (6)

$$\phi_t(S) = \prod_{\tau=1}^{t}\{p(\tau) - [1 - p(\tau)]S\}$$

and consequently

$$u(\nu, t) = \prod_{\tau=1}^{t}[1 - p(\tau)][(-1)^\nu S_\nu(\alpha_1, \alpha_2, \ldots \alpha_t)] \quad (7)$$

where

$$\alpha_\tau = \frac{p(\tau)}{1 - p(\tau)}$$

and $S_\nu(\alpha_1, \ldots, \alpha\tau, \ldots \alpha_t)$ is the ν^{th} elementary symmetric function in the variables $\alpha_1, \ldots \alpha_t$, *i.e.*

$$S_\nu(\alpha_1, \ldots, \alpha_t) = (-1)^\nu \sum_{j_1, j_2, \ldots j_\nu} \alpha_{j_1}\alpha_{j_2}\ldots\alpha_{j_\nu}$$

From eq. (7) one finds

$$\langle\nu\rangle = \sum_{\nu=1}^{t} \nu u(\nu, t) = pt \quad (8)$$

where p is given by eq. (4).

For large values of t, all $p(\tau)$ may be replaced by p and eq. (7) for $u(\nu,t)$ simplifies to the Bernoulli distribution

$$u(\nu, t) = \frac{t!}{(t - \nu)!\nu!} p^\nu(1 - p)^{t-\nu} = \binom{t}{\nu} p^\nu(1 - p)^{t-\nu} \quad (7a)$$

whose first moment $\langle\nu\rangle$ is also pt and which satisfies identically

$$u(\nu, t) = pu(\nu - 1, t - 1) + (1 - p)u(\nu, t - 1)$$

If N_0 polymer molecules are transferred from the solution to the surface, the number N_ν of these which adhere with ν segments out of a total of t, is given by

$$N_\nu = N_0 u(\nu, t) = N_0\binom{t}{\nu} p^\nu(1 - p)^{t-\nu} \quad (7b)$$

We can think of these adsorbed polymer chains as each consisting of subchains of 1, 2, ... λ, ... adjacent adsorbed segments connected by "bridges" of non-adhering segments which will stick out of the adsorbent surface. The "λ-mers" will arrange themselves on the surface, mixing with the unoccupied adsorption sites and forming essentially a two dimensional solution of "λ-mers" and unoccupied sites. Corresponding to this process we observe a free energy as well as an entropy of mixing.

(5) See, for instance, S. Chandrasekhar, *Revs. Modern Phys.*, **15**, 1 (1943).

The probability of finding a "λ-mer" among the adsorbed sites is given for large t by $p^{\lambda-1}(1-p) \backsimeq p^{\lambda-1}$, since $1-p \backsimeq 1$. Assuming that each of the N_ν chains is adsorbed at $<\nu>$ points which is a valid approximation, the average number of λ-mers from the N_0 chains is

$$M_\lambda = N_0<\nu>(1-p)p^{\lambda-1}(1-p) = N_0p^\lambda(1-p)^2t \quad (8)$$

If we take into account the finite magnitude of t, we must write, as do Montroll and Simha,[6] for M_λ

$$M_\lambda = N_0p^{\lambda-1}(1-p)[2+(pt-\lambda)(1-p)]$$

Considering the actual values of p, t and λ, eq. (8) is adequate.

Between the adsorbed sequences of chain segments, there are portions, anchored to the substrate at the sequence boundaries but otherwise extending into the solution. The size distribution of these bridges is given by

$$M_\epsilon = N_0p^2(1-p)^\epsilon; \quad \sum_\epsilon \epsilon M_\epsilon = (t-<\nu>)N_0 \quad (8a)$$

and the number average chain length of a bridge is

$$<\epsilon> = t/<\nu> - 1 = (1-p)/p$$

III. Thermodynamic Properties of the Monolayer

Next we consider the free energy of the system which consists of sites partially occupied by λ-sequences and the solution containing bridges and dissolved polymer chains. The mole fractions n_0 and n_λ of empty sites and sites occupied by λ-sequences are

$$n_0 = 1 - \Sigma M_\lambda/N_s = 1 - N_0pt(1-p)/N_s;$$
$$n_\lambda = M_\lambda/N_s = N_0p^\lambda(1-p)^2t/N_s \quad (9)$$

and the corresponding volume fractions

$$\varphi_0 = 1 - \Sigma M_\lambda\lambda/N_s = 1 - N_0pt/N_s;$$
$$\varphi_\lambda = \lambda M_\lambda/N_s = N_0\lambda p^\lambda t(1-p)^2/N_s \quad (10)$$

where N_s represents the number of sites available for adsorption.

Let there be altogether N polymer molecules, N_0 of which are (partially) adsorbed. The partition function, Z_f, of the whole system is then

$$Z_f = Z_{mix}^{(\lambda)}Z_{mix}^{(\epsilon)} \exp(N_0<\nu>x/kT)\left[\prod_{i=1}^{t} j_i(T)\right]^N [j_s(T)]^{<\nu>N_0}(j_{tr})^{N-N_0}Z_{mix}(N-N_0,\epsilon) \quad (11)$$

$Z_{mix}^{(\lambda)}$ describes the mixing of λ-sequences of all lengths and the empty sites, $Z_{mix}^{(\epsilon)}$ the mixing of the ϵ-bridges and the solution consisting of N_L solvent and $N-N_0$ polymer molecules. x is the energy required to remove an adsorbed segment from the surface and $N_0<\nu>$ is the total number of adsorbed segments. $j_i(T)$ is the partition function for the internal degrees of freedom of segment i, taking as the state of zero energy the lowest energy state in the monolayer, referred to the polymer dissolved in an infinitely dilute solution. It is assumed here that the adsorption process does not affect these internal degrees of freedom, although there will be a difference in the internal rotations. The general form of the equations to be derived is not altered by this postulate. j_{tr} accounts for the translational degrees of freedom in the solution and j_s for the vibrations around adsorption sites.

(6) E. W. Montroll and R. Simha, *J. Chem. Phys.*, **8**, 721 (1940).

No corresponding terms for the solvent have been written since the solvent is assumed not to participate in the adsorption process. Also the configurational partition function of the solid polymer has been omitted in eq. (11) and subsequent equations. The factor $Z_{mix}(N-N_0,\epsilon)$ arises from the mixing of $N-N_0$ chains with a solution containing M_ϵ bridges, $\epsilon = 1, 2 \ldots$, and N_L solvent molecules. Prior to the adsorption, the partition function is

$$Z = Z_{mix}(N)\left[\prod_{i=1}^{t} j_i(T)\right]^N (j_{tr})^N \quad (12)$$

where $Z_{mix}(N)$ refers to the mixing of N polymer and N_L solvent molecules. From eqs. (11) and (12) the free energy change ΔF_{ads} resulting from the deposition of N_0 out of N chains, each at $<\nu>$ sites, is

$$\Delta F_{ads} = -kT \ln (Z_f/Z) \quad (13)$$

Explicit expressions for the mixing terms are most simply obtained from the Flory–Huggins theory of polymer solutions. Since we wish to treat the whole concentration range on the surface, the difficulties of this theory at moderate concentrations will persist here. Furthermore, special orientation effects, arising at the boundaries between λ- and ϵ-sequences will be disregarded. In this way we find[7,8]

$$-kT \ln Z_{mix}^{(\lambda)} = \Delta F_{mix}^{(\lambda)} = kT N_s[n_0 \ln \varphi_0 + \sum_\lambda 1/\lambda\varphi_\lambda \ln \varphi_\lambda + K_1\sum_{\lambda,l}\varphi_\lambda\varphi_l] \quad (14)$$

The interaction between the adsorbed segments is expressed by means of a van Laar–Hildebrand–Scatchard term. K_1 is a measure of the interaction energy, but contains also an entropy contribution. A more refined treatment of the interaction would follow the lines indicated by Miller.[3] On carrying out some of the summations and introducing θ, the fraction of the surface covered

$$\theta = \sum_\lambda \lambda n_\lambda = N_0<\nu>/N_s \quad (15)$$

there results

$$\Delta F_{mix}^{(\lambda)}/kTN_s = (1-\theta)\ln(1-\theta) + K_1\theta^2 + \theta(1-p)^2 \ln [\theta(1-p)^2] + \theta(1-p)^2\sum_{\lambda=2} p^{\lambda-1} \ln [\lambda p^{\lambda-1}(1-p)^2\theta] \quad (16)$$

This can be approximated by

$$\Delta F_{mix}^{(\lambda)}/kTN_s = (1-\theta)\ln(1-\theta) + \theta \ln \theta + p\theta \ln [p(1-\theta)/\theta] + K_1\theta^2 + O(p^2) \quad (16a)$$

The computation of all further mixing terms is simplified by the condition stated in Section I, that the solution from which deposition occurs is already infinitely dilute to start with. This eliminates interference between bridges and dissolved molecules. Thus we compute the free energy change on mixing N_L solvent molecules with the bridges

(7) P. J. Flory, *ibid.*, **12**, 425 (1944).

(8) R. L. Scott and M. Magat, *ibid.*, **13**, 172 (1945).

$$-kT \ln Z_{mix}^{(\epsilon)} = \Delta F_{mix}^{(\epsilon)} = kTN_L \ln (N_L/N_L + \Sigma\epsilon M_\epsilon) + K_2 N_0 \Sigma\epsilon M_\epsilon/(N_L + \Sigma\epsilon M_\epsilon)$$

or from eq. (3a)

$$\Delta F_{mix}^{(\epsilon)} = kTN_1 \{\ln (N_L/[N_L + (t - <\nu>)N_0] + K_2(t - <\nu>)N_0/[N_L + (t - <\nu>)N_0]\} \quad (17)$$

The absence of a term depending on the number of bridges is due to the immobilization of the bridge termini. K_2 is, in the usual fashion, a measure of the polymer–solvent interaction and contains also an entropy contribution.

For the solution of $N - N_0$ chains, we write, disregarding the presence of bridges in accord with our assumptions

$$-kT \ln Z_{mix}(N - N_0, \epsilon) = \Delta F_{mix}(N - N_0, \epsilon) = kTN_L\{\ln N_L/[N_L + t(N - N_0)] + (N - N_0)/N_L \ln t(N - N_0)/[N_L + t(N - N_0)] + K_2 t(N - N_0)/[N_L + t(N - N_0)]\} \quad (18)$$

This is small in comparison with the solution term $\Delta F_{mix}(N)$

$$-kT \ln Z_{mix}(N) = \Delta F_{mix}(N) = kTN_L[\ln N_L/(N_L + tN) + N/N_L \ln tN/(N_L + tN) + K_2 tN/(N_L + tN)] \quad (19)$$

Hence we adopt for the following the approximations $\Delta F_{mix}(N - N_0, \epsilon) \approx 0$, and $N \approx N_0$ in eq. (19).

Omitting the factor $Z_{mix}(N - N_0, \epsilon)$ in eq. (11) and dropping the distinction between the partition functions of the whole system, including the partially depleted solution, and of the monolayer, we deduce from eqs. (16a) and (17)

$$-kT \ln Z_t = F_t = \Delta F_{mix}^{(\lambda)} + \Delta F_{mix}^{(\epsilon)} - N_0<\nu>x - kTN_0\Sigma \ln j_i(T) - kT<\nu>N_0 \ln j_s(T) = kTN_s\{(1 - \theta) \ln (1 - \theta) + \theta \ln \theta + p\theta \ln [p(1 - \theta)/\theta] + K_1\theta^2 + 0(p^2)\} + kTN_L[\ln N_L/N_L + (t - <\nu>)N_0 + K_2(t - <\nu>)N_0/N_L + (t - <\nu>)N_0] - N_0<\nu>x - kTN_0 \sum_i \ln j_i(T) - kT<\nu>N_0 \ln j_s(T) \quad (20)$$

The partial molal free energy of the adsorbed polymer is found by considering that $\partial/\partial N_0 = <\nu>/N_s \partial/\partial\theta$. Hence

$$\mu_f/kT = 1/kT\,\partial F_t/\partial N_0 = <\nu>\{\ln \theta/(1 - \theta) + p \ln [p(1 - \theta)/\theta] - p/(1 - \theta) + 2K_1\theta - N_L<\epsilon>/N_L + (t - <\nu>)N_0 + K_2<\epsilon>[N_L/N_L + (t - <\nu>)N_0]^2 - x/kT\} - \Sigma \ln j_i(T) - <\nu> \ln j_s(T) \quad (21)$$

Since $N_L >> (t - <\nu>)N_0$, the contribution of the bridges reduces to

$$-<\nu><\epsilon>(1 - K_2) = -(t - <\nu>)(1 - K_2)$$

From eq. (21) the adsorption isotherm is derived in the customary way by considering the equilibrium between adsorbed and dissolved polymer. The absolute activity of the latter is in dilute solution

$$\exp (\mu_p^\circ/kT) \cdot t(N - N_0)/N_L e^{-(1-K_2)t}$$

where μ_p° represents the chemical potential of the pure amorphous polymer. This can be written in terms of all the degrees of freedom of the chain and the configurational partition function of the solid Ω. On converting to the concentration c in weight by volume and considering the changes in the degrees of freedom on adsorption, the adsorption isotherm assumes the form

$$\{\theta e^{2K_1\theta}/(1 - \theta)[p(1 - \theta)/\theta e^{-1/(1-\theta)}]^p\}^{<\nu>} = K(T, t, x, K_2)c \quad (22)$$

with

$$K = \frac{M(\text{solv})}{M(\text{segm})d(\text{solv})} \exp \left\{ \frac{<\nu>}{kT} [x - kT(1 - K_2)] \right\} \frac{h^3}{(2\pi mkT)^{3/2}} (j_s)^{<\nu>} \bar{V}^{-1}$$

The ratio of the two molecular weights M is to be set equal to unity, d is the density of the solvent and $\bar{V}$ may be regarded as the "free volume" per molecule of solid. It will be noted that the first three factors on the left hand side of eq. (22) would represent a Langmuir-type isotherm corrected for lateral interactions, provided the exponent $<\nu>$ were unity. In the limit $p \to 0$, when all λ-sequences consist of single segments, the equation reduces to

$$[\theta e^{2K_1\theta}/(1 - \theta)]^{<\nu>} = Kc \quad (22a)$$

Except for the definition of K, this is formally identical with the result for the adsorption of $<\nu>$-mers which dissociate completely into monomer on the surface. Since $<\nu>$ is a relatively large number, θ depends only slightly on the polymer concentration c after an initial steep increase and remains below the values predicted by the Langmuir isotherm over a large range of c. This pattern is mitigated by a finite value of p.

Equations (11), (12), (13), (16a), (17) and (19) yield for the integral free energy change ΔF_{ads} on adsorption of N_0 chains at $N_0<\nu>$ sites for $N_L >> tN_0$

$$\Delta F_{ads}/kTN_s = (1 - \theta) \ln (1 - \theta) + \theta \ln \theta + p\theta \ln [p(1 - \theta)/\theta] + \theta/<\nu> \ln j_{tr} - \theta \ln j_s - \theta(x/kT + K_2) + K_1\theta^2 \quad (23)$$

The integral heat of adsorption is thus approximately equal to

$$\Delta H_{ads}/kT = -N_0<\nu>(x/kT + K_2') + (K_1'N_0^2/N_s)(<\nu>)^2 \quad (24)$$

neglecting the temperature dependence of the j's and of p. The primes indicate that only the energy contributions in K_1 and K_2 are to be included. For low degrees of surface coverage the first term is predominant. Under these conditions the heat of adsorption is proportional to the square root of the molecular weight, since $<\nu> = pt \sim t^{1/2}$. As the coverage increases, the second term, due to the lateral interactions and proportional to M, can become appreciable. The approximations made in calculating the heat of adsorption may be gaged by a comparison with more elaborate expressions developed in the theory of adsorption of gases.[3] These affect the second term in eq. (24) and hence will not be important for small θ and p. When this is the case, the difficulties connected with the use of eq. (14) are also not very important, since preponderantly single anchored segments are separated by long sequences of units sticking out of the adsorbent plane. In attempting estimates of K_1, it should be recalled that it measures merely an excess over the segment interaction in the bulk polymer.

IV. Discussion

Although the present theory deals exclusively with monomolecular adsorption and does not consider the deposition of further layers and rate

processes, the results obtained have a bearing on the problem of adhesion insofar as the strength of the bond between adherent and adhesive, due to molecular forces, is a determining factor. For, one important quantity, *ceteris paribus*, should be the average number of anchor points of the chain on the substrate. In a flexible, randomly coiled macromolecule, $<\nu> \sim f^{-1/2}t^{1/2}$ and the number of anchor points increases with the $^1/_2$ power of the molecular weight. $<\nu>$ depends furthermore on the flexibility of the chain which appears in the factor f. As shown by several authors[9]

$$6f = \bar{r}^2/A_0^2 t = \frac{1 + \cos \xi_1}{1 - \cos \xi_1} \times \frac{1 + <\cos \xi_2>}{1 - <\cos \xi_2>} \quad (25)$$

Here $\bar{r}^2$ is the mean square separation of chain ends of the free chain, $\pi - \xi_1$ the fixed valence angle, A_0 the length of a C–C bond, ξ_2 the angle of rotation of a segment relative to a given stable position and

$$<\cos \xi_2> = \int_0^\pi \cos \xi_2 \exp [-V(\xi_2)/kT] d\xi_2 / \int_0^\pi \exp [-V(\xi_2)/kT] d\xi_2$$

$V(\xi_2)$ is the potential restricting this rotation. A highly flexible chain is characterized by a small value of $<\cos \xi_2$ and hence of f, and the molecule is attached to the substrate with a relatively high number of units. Qualitatively it appears to be a matter of experience that chain flexibility is a favorable factor in adhesion. By the same reasoning, deposition from a poor solvent, in which f is effectively small, should be advantageous for adsorption. Although fundamentally this effect is not independent of, it occurs in addition to the increase of thermodynamic activity in a poor solvent (large K_2). This also favors adsorption by making the constant K larger. In the framework of the present theory which operates with a dilute solution and chains attaching themselves independently to the surface, no precipitation effects need to be considered.

At this point a comment about the use of the Gaussian distribution (1) is necessary, in view of the effect of excluded segment volume on the chain statistics and average chain dimensions. It seems quite clear that the distribution does not remain Gaussian when the volume effect is introduced, regardless of existing differences in point of view. This can change our relations (3) and (4) either by a constant factor only which can be absorbed in the definition of f, or alternatively have the more profound consequence of changing the exponent of the molecular weight in the expression for p. Even so, the characteristic features, in particular the existence of short sequences on the surface and long bridges, will persist. Considering the uncertainties regarding the distribution function, it would not be useful at this stage to attempt a modification of the results given in Section II. For very short chains, on the other hand, the situation changes. Because of the effective lack of flexibility, the relative number of anchor points will be reduced. Extremely short molecules, however, act as one rigid unit and are either completely deposited or attached normally to the surface.[10]

One more word about the derivation of eq. (3) and (4). It neglects any correlation between previously attached segments and the trapping of succeeding ones. In this sense our result for $<\nu> \sim t^{1/2}$ represents a minimum value, the strongest possible dependence being proportionality with t. Such a situation arises only if the surface exerts long range forces on the polymer, say, in the presence of electric charges. A partial correlation along the chain contour, however, is a short range effect in long chains and should merely introduce a factor larger than unity, but independent of molecular weight, in p and $<\nu>$. All this implies sufficiently long bridges and thus small p.

The theory has been restricted to extremely dilute solutions. In concentrated systems, not only the mixing terms in eq. (11) and (12) but also the statistical results in Section II are affected, since the probability of deposition of a given chain depends on the number which are already adsorbed. This applies particularly to the deposition in the case of adhesives. Under these conditions orientation effects appear. Furthermore, we are no longer dealing with an equilibrium and various rheological factors become important. Also, when θ is large, the bridges may be forced into preferred configurations, even in dilute solution.

Recently adsorption experiments with polymer fractions of methyl methacrylate, styrene and vinyl chloride have been reported by Jenckel and Rumbach.[11] Good solvents were used and the concentrations did not exceed 1 g.l.$^{-1}$. The adsorbents were Al-dust, sand, glass wool and activated charcoal. For the first three the surface could be obtained from microscopic determinations, whereas in the last case dye adsorption was used. However, because of the large internal surface, charcoal presents a special problem and is best left out for our purposes. The following facts and conclusions emerge from this work: 1. There is an inital steep increase in θ, followed by an apparent saturation at concentrations as low as 0.1 g. l.$^{-1}$. The authors fit Langmuir isotherms to their data. However, this type of behavior should be reproducible by our equations. The results are not available in a form which makes such an analysis readily possible. 2. From the weight of adsorbed material, one can calculate that layers of adsorbate ten or more monomer units thick must be piled up on the surface, if deposition of entire chains is to occur. Since there is no reason for such multilayers in dilute solutions, considering the short range of molecular forces, the authors conclude that adsorption occurs in sequences separated by some kind of bridges. The chain length of the latter can be estimated to be of the order of magnitude resulting from our equations, that is, of ten. 3. The amounts adsorbed are larger for the poorer solvent. 4. There is a positive temperature coefficient of adsorption, particularly in those instances in which the isotherm rises sharply.

(9) For instance, W. J. Taylor, *J. Chem. Phys.*, **16**, 257 (1948), or A. R. Ubbelohde and I. Woodward, *Trans. Faraday Soc.*, **48**, 113 (1952).

(10) The adsorption of rods has been treated recently by E. L. Mackor and J. H. van der Waals, Jr., *J. Colloid Sci.*, **7**, 533 (1952).

(11) E. Jenckel and B. Rumbach, *Z. Elektrochem.*, **55**, 612 (1951).

What can one conclude from our theory about this last point? From eq. (22) and the definition of K we derive the following principal contributions to the quantity $d\theta/dT$: (a) The dissociation from the surface of an isolated segment and loosening of lateral interactions, determined by x and K_1, respectively. (b) The improvement of the solvent with an increase in temperature. (c) A contribution of the translational and vibrational degrees of freedom and of the solvent density. All of these factors, with the exception of a possible repulsion between segments in (a) and the density and vibrational changes, in (c), make for a negative temperature coefficient. There is one more term namely, (d), the change in the flexibility parameter f and hence in $<\nu>$. In a good solvent we have $df/dT < 0$. For $p \to 0$, one finds for this term the expression

$$-(\pi/8\alpha^2)(<\nu>^2/t)df/dT\{1/kT[x - kT(1 - K_2)] - \ln [\theta e^{2K_1\theta}/(1 - \theta)]\}$$

to balance the foregoing contributions, in particular the desorption term. For a fixed t, the factor in front of the brace increases with the square of $<\nu>$, the same quantity which determines also the magnitude of the initial slope of the isotherm. This factor may be written as

$$-{}^1/_2 d \ln f/dT = -{}^1/_2 d \ln \bar{r}^2/dT$$

and therefore obtained from appropriate solution measurements. Although df/dT is small, there could well be an overbalance and positive $d\theta/dT$, considering values of x of the order of 5–10 kT or even more. The total change in θ observed is rather small, of the order of 15–30% in the flat portion of the isotherm between $T = 298$ and 323°K.

Eq. (22) yields positive values of $d\theta/dt$. On the other hand, Claesson and Claesson[12] observed $d\theta/dt < 0$ for various polymers. Their concentration range exceeded that in ref. 11. At higher concentrations such an effect may be due to the presence of the bridges.

Obviously thermodynamic measurements and determinations of the isotherm as function of molecular weight and temperature, and using both good and poor solvents, will be important on general grounds and in the light of the present theory. We hope to undertake such experiments.

(12) T. Claesson and S. Claesson, *Arkiv Kemi Mineral. Geol.*, **19A**, No. 5 (1945).

VARIATION OF THE VISCOSITY OF ETHYL CHLORIDE VAPOR WITH TEMPERATURE

BY M. EL NADI

Faculty of Science, Cairo University, Cairo, Egypt

Received November 7, 1952

The viscosity of ethyl chloride vapor is measured by the capillary tube method at temperatures well below the critical point. The applicability of the transpiration formula was tested at each of these temperatures and found to hold quite well. Then the validity of Sutherland's model was examined for ethyl chloride vapor.

Introduction

In studying the variation of the viscosity (η) of vapors with temperature (T), it was found that for some vapors, the observations at high temperatures fitted well with Sutherland's equation

$$\eta = k \frac{T^{3/2}}{C + T} \qquad (1)$$

while at lower temperatures deviations from this formula occur. K and C are constants; C is known as Sutherland's constant, and was shown to be proportional to the potential energy of attraction between molecules. To explain this deviation from Sutherland's formula at lower temperatures, Rankine[1] suggested either: (1) the non-applicability of the transpiration formula for the flow of vapors through the capillary tube at lower temperatures, or (2) the possibility of chemical association of the vapor at these temperatures.

The object of this paper is to investigate the effect of temperature on the viscosity of the ethyl chloride vapor at temperatures starting from just above its boiling point (285.3°K.), examining in each case the applicability of the transpiration formula and finally testing the validity of Sutherland's model for the ethyl chloride vapor.

(1) A. O. Rankine, *Proc. Roy. Soc. (London)*, **88A**, 575 (1913).

Experimental

The apparatus used in the present work is based on Edwards'[2] constant volume method, which provides a most convenient method for testing the transpiration formula at any temperature.

In the constant volume method, the vapor is enclosed in a large bulb and then allowed to escape through a capillary tube to the atmosphere for a given interval of time t. Then the coefficient of viscosity is given by the transpiration formula

$$\frac{1}{tP_0} \log_{10} \frac{(2P_0 + P_2)P_1}{(2P_0 + P_1)P_2} = k \frac{1 + 4\xi/a}{\eta} \qquad (2)$$

where $K = (15\ \pi a^4 g.\rho_0/4.606\ lV)$ is a constant depending on the dimensions of the bulb and the capillary tube. Here P_0 = atmospheric pressure during the experiment (measured in cm. of mercury), P_1 = initial excess pressure in bulb over the external atmospheric pressure; P_2 = final excess pressure in bulb over the external atmospheric pressure; t = time of flow (measured in minutes); ξ = coefficient of slip, and ρ_0 = density of mercury at 0°.

The volume (V) of the bulb was 755.4 cc. at 22.2°, the length (l) of the capillary tube, 154.3 cm. and the mean value (a) of its radius, 0.0203 cm. The capillary tube was bent twice so as to form three parallel parts. Both the bulb and the capillary tube were surrounded by a water (and then oil) bath to maintain the various constant temperatures at which observations were taken.

In equation (2) it is assumed that the flow of the gas through the capillary tube is streamlined. It is therefore essential that the pressure of the gas in the bulb must not

(2) R. S. Edwards, *ibid.*, **117A**, 248 (1928).

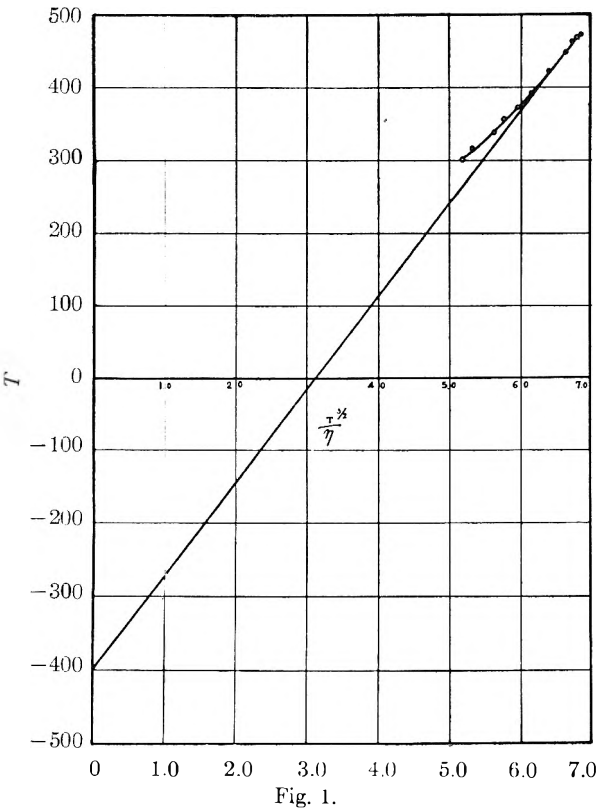

Fig. 1.

be high enough to give rise to turbulent flow through the capillary tube. Taking for the value of the critical Reynold's number, 2000, the following values for the critical pressure were calculated: $P_0 + 160$ and $P_0 + 37$ cm. of mercury for the cases of dry air and ethyl chloride vapor, respectively.

The coefficients of slip ξ between glass and methyl chloride vapor were calculated at each temperature by the formula

$$\xi = 0.81 \frac{8\sqrt{2}}{3\sqrt{\pi}} \frac{\eta}{P} \sqrt{\frac{RT}{M}}$$

where M is the molecular weight, and P the mean value of the pressure of the vapor through the tube. The value of the correction factor $\left(1 + \frac{4\xi}{a}\right)$ at the lowest temperature 28.7° was 1.0003 and at the highest temperature 197.5° 1.0012 which is of the same order of magnitude as the accuracy of the measurements, and so can be neglected.

Results

Since any slight error in the measurement of the radius of the capillary tube causes a much larger error in the value of K (see equation 2), it is convenient to adopt a comparative method. For this purpose a series of observations was taken on pure dry air at room temperature, 22.15°; in each set of values of P_0, P_1, P_2 and t were measured, and the value of the factor $\frac{K}{\eta}\left(1 + \frac{4\xi}{a}\right)$ was then calculated. The average value of this factor was found to be 0.001095.

Using Millikan's value for the slip coefficient for air, and its temperature factor, we get $\xi = 7.49 \times 10^{-6}$ c.g.s. units.

Similarly using Bearden's value[3] for the coefficient of viscosity of air together with his temperature coefficient, we get $\eta_{22.15°C.} = 1829.8 \times 10^{-7}$ c.g.s. units. From these three values we get for the constant K, the value of 2.0009×10^{-7} c.g.s. units.

Having determined the constant of the system, K, we carried out several sets of observations, each for a given temperature for the ethyl chloride vapor. The pressure conditions were varied in each case, so as to test the applicability of the transpiration formula (2). In the following table we have recorded the values of $\frac{K\left(1 + \frac{4\xi}{a}\right)}{\eta}$ at each temperature.

T, ° C.	28.7	43.9	64.8	82.2	98.0	120.8	151.0	175.0	190.7	197.5
$\frac{K\left(1 + \frac{4\xi}{a}\right)}{\eta}$	1.9799	1.8824	1.7969	1.7106	1.6728	1.5832	1.4774	1.4068	1.3581	1.3464
	1.9529	1.8756	1.8012	1.7412	1.6990	1.5666	1.4632	1.4036	1.3550	1.3265
	1.9788	1.8854	1.8061	1.7119	1.6643	1.5762	1.4823	1.4011	1.3594	1.3498
	1.9601	1.8849	1.7895	1.7229	1.6724	1.5918	1.4732	1.3990		
	1.9645	1.8765	1.8202	1.7111	1.6704	1.5690	1.4768	1.4016		
	1.9834	1.8815	1.8108	1.7143	1.6778	1.5697	1.4918	1.3902		
	1.9557	1.8884	1.8012	1.7187	1.6762	1.5896		1.4030		
	1.9943		1.7949	1.7262	1.6727	1.5839		1.4057		
	1.9673		1.8073	1.7190						
			1.7914	1.7075						
			1.7958							
Av.	1.9697	1.8821	1.8014	1.7187	1.6720	1.5787	1.4774	1.4014	1.3575	1.3409
$\eta \times 10^{-7}$ c.g.s. unit	1016.5	1053.8	1111.6	1165.1	1197.7	1268.8	1355.6	1429.4	1475.7	1493.9
$T^{3/2}/\eta \times 10^{7}$, c.g.s.	5.1578	5.3054	5.5879	5.7481	5.9690	6.1628	6.4425	6.6361	6.7687	6.8335

The constancy of the values of the factor $\frac{K\left(1 + \frac{4\xi}{a}\right)}{\eta}$ at each temperature for various values of the pressures P_0, P_1, P_2 and the time t, proves the applicability of the transpiration formula at the temperatures considered. This result might be considered as confirmed by the work of Braune, Basch and Wentzel who studied the viscosity of bromine vapor using the oscillating disc method, and found the same behavior as that found by Rankine using the capillary tube. This shows that the transpiration formula for the flow of gases

(3) J. A. Bearden, *Phys. Rev.*, **56**, 103 (1939).

and vapors through capillary tubes could in general be safely applied at temperatures near or even below the critical temperature where deviations from the gas laws occur. Thus it seems probable that the deviations from Sutherland's law, which occur for some vapors at lower temperatures, could be attributed to a probable change in the molecular field in this range of temperatures.

If, now, $(T^{3/2}/\eta)$ is plotted against T as ordinate, Sutherland's equation (1) gives a straight line, with the negative intercept on the T axis, as Sutherland's constant C. We see in Fig. 1 the experimental curve is first concave upwards and then becomes straight at higher temperatures. The straight part gives for C the value 398. Similar curves were obtained for bromine vapor by Rankine,[1] Braune and others[4]; for ethylene by Zimmer[5] and for sulfur dioxide by Trautz and Weitzel.[6]

As far as we know, the only measurement for the viscosity of ethyl chloride vapor was that by Vogel at 0°, using the oscillating disc method. His value is 937×10^{-7} c.g.s. units. It is easy to see that our extrapolated value is in complete agreement with that of Vogel.

Rankine[7] observed that for most gases $(T_c/C) = 1.14$, where T_c is the critical temperature For ethyl chloride vapor $T_c = 460.3$°K.; therefore, $(T_c/C) = (460.3/398) = 1.16$, in agreement with Rankine's rule.

In conclusion the writer wishes to express his appreciation to Prof. M. Fahmy for his helpful discussions during the progress of the work.

(4) H. Braune, R. Basch and W. Wentzel, *Z. physik. Chem.*, **137**, 447 (1928).

(5) O. Zimmer, *Vrndlg. Phys. Ges.*, **14**, 471 (1912).

(6) Trautz and W. Weitzel, *Ann. Phys.*, [4] **78**, 305 (1925).

(7) A. O. Rankine, *Proc. Roy. Soc. (London)*, **84A**, 190 (1911); **86A**, 106 (1912).

MOLECULAR INTERACTION BETWEEN *n*-PROPYL ALCOHOL AND IRON OR IRON OXIDES

BY EDWARD H. LOESER, WILLIAM D. HARKINS[1] AND SUMNER B. TWISS

Contribution from the Chrysler Corporation of Detroit, Michigan, and the Department of Chemistry, University of Chicago

Received November 28, 1952

The adsorption isotherms at 25° of *n*-propyl alcohol on reduced iron, untreated iron, Fe_2O_3 and Fe_3O_4 have been determined. The phase changes which occur in the adsorption isotherms at very low pressures are primarily first order, although one second-order change is observed. The phase changes are more prominent in the alcohol film than in heptane, and the presence of oxides on the iron surface has a marked effect on the phase changes of adsorbed alcohol. The values of π_e, decrease of free surface energy of a solid due to the adsorbed vapor, and W_A, work of adhesion between adsorbed liquid and solid, are given. These values, calculated from the adsorption data for *n*-propyl alcohol on the solids, increase in the order: reduced iron, Fe_3O_4, untreated iron and Fe_2O_3. The greater the oxygen in the solid surface, the higher the energy change of adsorption. Abnormal B.E.T. and Hüttig plots, which lead to negative values of "c," are obtained in several cases. Comparison of the area values for the four solids obtained by the Langmuir, B.E.T., Hüttig and H.J. methods indicates that use of *n*-propyl alcohol data for area measurements gives results of only fair self-consistency and accuracy. Unpublished data for *n*-propyl alcohol on anatase are included for purpose of area correlation.

Introduction

Practically no difference was found in the adsorption isotherms at 25° of a non-polar vapor, *n*-heptane, on a clean metal and on the same metal coated with oxide.[2] Although the values for the decrease of free surface energy of the solid (π) caused by the adsorbed heptane film increase in the order copper, silver, lead and iron, the π-value is essentially independent of the presence or absence of an oxide film on the surfaces of these metals. There is evidence[3] that the effective cross sectional area of the heptane molecule in the completed monolayer on the surface of non-porous solids is nearly independent of the nature and spacing of the solid lattice. The shape of the adsorption isotherms and the π-value for a polar vapor, water, appear to be related to the percentage of ash in graphite.[4] The purpose of this paper is to present the results of the adsorption studies of *n*-propyl alcohol, a molecular species having polar characteristics, on iron and iron oxides. Investigations of the physical adsorption of two other polar adsorbates, *n*-amyl chloride on reduced iron and iron oxide, Fe_2O_3, and oxygen-free water on reduced iron failed since these vapors reacted chemically with the powders at 25°.

Experimental

The volumetric apparatus and procedures used in the determination of the adsorption isotherms were described in an earlier paper.[5] Stock valves were used instead of stopcocks. The temperature of the bath surrounding the bulb which contained the adsorbent was maintained within ±0.05°. The mercury manometer M was made of 25 mm. tubing which should be large enough to minimize capillary depression errors and to allow the meniscus to move freely. Care was taken that the arms of the manometer were parallel and that the manometer assembly was clamped securely in a vertical position. The heights of the mercury in the arms of the manometer were determined with a traveling microscope of a sensitivity of 0.001 mm. The microscope was mounted on a transit mount; its arc of rotation was limited by means of stops. Thus, measurements were made at the same location on the flat section of each meniscus. A fluorescent lamp illuminated the menisci.

The following procedure was used for low pressure determinations. Approximately 24 hours were allowed to establish equilibrium between the solid and the vapor. Pressure readings were made after gently tapping the manometer. The absorbent was then isolated from the manometer by closing a Stock valve. After both arms of the manometer had been pumped out, the zero point cor-

(1) Deceased

(2) W. D. Harkins and E. H. Loeser, *J. Chem. Phys.*, **18**, 556 (1950).

(3) E. H. Loeser and W. D. Harkins, *J. Am. Chem. Soc.*, **72**, 3427 (1950).

(4) W. D. Harkins, G. Jura and E. H. Loeser, *ibid.*, **68**, 554 (1946)

(5) G. Jura and W. D. Harkins, *ibid.*, **66**, 1356 (1944).

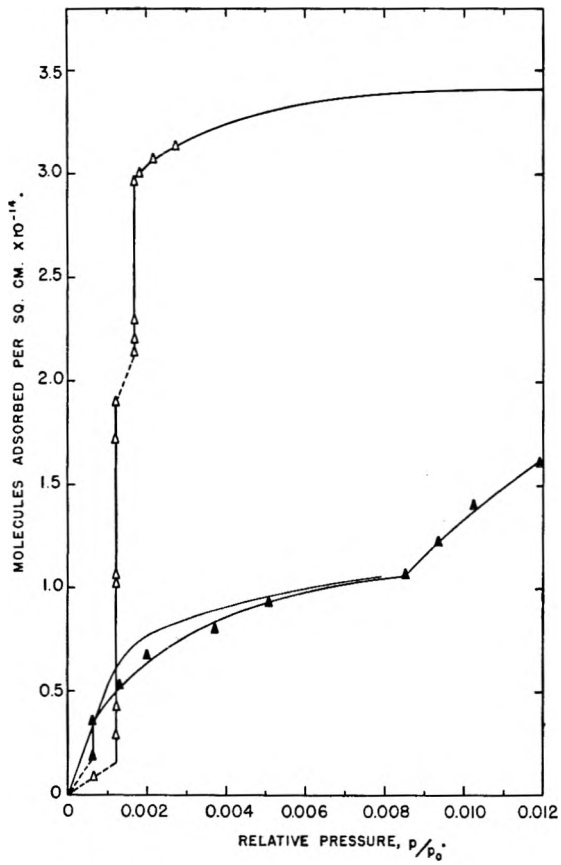

Fig. 1.—Low pressure isotherms at 25°: -△-, *n*-propyl alcohol on untreated iron: -▲-, *n*-propyl alcohol on reduced iron; —, *n*-heptane on untreated or reduced iron.

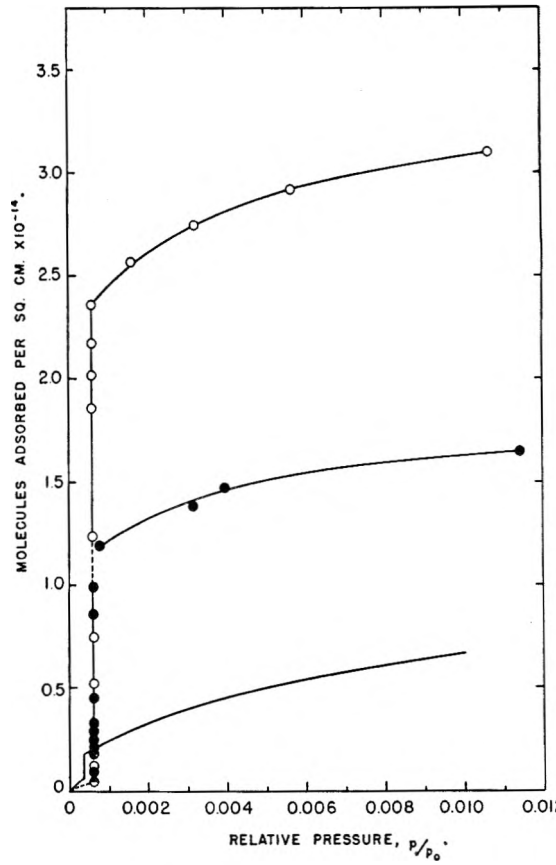

Fig. 2.—Low pressure isotherms at 25°: -○-, *n*-propyl alcohol on Fe_2O_3; -●-, *n*-propyl alcohol on Fe_3O_4; —, *n*-heptane on Fe_2O_3.

rection was determined. The reversibility of these isotherms was not tested as was done in an earlier investigation.[6] However, in several of the systems reported here a large sample of adsorbent was used to determine the extremely low pressure region and a smaller one to determine the remainder of the isotherm. The fact that the curves overlapped in the discontinuous portion indicates the reproducibility but not necessarily the reversibility of the isotherms.

The *n*-propyl alcohol was obtained from the Coleman and Bell Company and was purified by the method of Lund and Bjerrum.[7] The liquid was thoroughly degassed by repeated solidification and ebullition in a vacuum maintained at 10^{-5} mm. The vapor tension of the *n*-propyl alcohol determined at 25° was 20.86 mm.

The iron was 325-mesh electrolytic powder (annealed) and was obtained from Charles Hardy, Inc., of New York. It was guaranteed to be 99.4+ % iron and iron oxide. The existence of an oxide film, formed on the surface of iron exposed to air, is well established. The thickness of the oxide film on this sample, calculated from the amount of water formed on reduction, is about 60 Å. Untreated iron is a sample of the unreduced iron, which has been cleaned by heating at 200° *in vacuo* for 16 hours. The reduced iron was prepared by passing dry hydrogen through the heated (350°) metal powder for eight hours. The entire process was carried out in the adsorption bulb on the vacuum line and the water formed during the reduction was removed from the reaction zone by means of a liquid N_2 trap. The reduced iron was degassed by heating at 200° *in vacuo* for 36 hours. The Fe_2O_3, of Baker and Adamson reagent grade, was degassed *in vacuo* at 500° for 16 hours. The sample of Fe_3O_4 was a 325-mesh powder containing 0.065% Mn, 0.003% Al, 0.005% Cu + Ni and a trace of Si. The Fe_3O_4 content of this sample at the time of its use is unknown. An X-ray diffraction analysis, run on the sample about two years after its use in these studies, indicated the presence of 60% Fe_3O_4 and 40% Fe_2O_3. It was degassed *in vacuo* at 325° for 16 hours.

Phase Changes in Adsorbed Films.—The low pressure region of the adsorption isotherms exhibited in Fig. 1 indicates the presence of two extensive discontinuities in the curve for n-C_3H_7OH on untreated Fe. If the oxide coating is removed from the iron powder by reduction, the amount of adsorption is decreased and the discontinuities nearly disappear. The curve for *n*-heptane on untreated Fe, shown in Fig. 1 for purposes of comparison, exhibits no discontinuity. The curves in Fig. 2 indicate a single discontinuity in the adsorption isotherms of n-C_3H_7OH on Fe_3O_4 or Fe_2O_3 at 25°. Although the pressure at which the discontinuity occurs is the same for the two oxides, Fe_2O_3 adsorbs approximately twice as many alcohol molecules per unit area before leaving the discontinuous portion of the curve. The length of the discontinuity in the alcohol on Fe_2O_3 curve is many times that in the heptane on Fe_2O_3 curve.

The heterogeneous nature of the solid surfaces makes the interpretation of the experimental data difficult. The discontinuities commonly observed in this study are of the type in which the amount of vapor adsorbed varies without any change in pressure. They may be interpreted as first-order phase transitions in the adsorbed films.[6] The two first-order changes in the film of n-C_3H_7OH on untreated Fe may be due to the presence of two different

(6) G. Jura, E. H. Loeser, P. R. Basford and W. D. Harkins, *J. Chem. Phys.*, **14**, 117 (1946).

(7) H. Lund and J. Bjerrum, *Ber.*, **64**, 210 (1931).

crystal surfaces which act as nuclei for cluster formation. Removal of the oxide coating changes the solid surface since only a very short first-order transition and a second-order change are found in the adsorbed phase of alcohol on reduced iron. It is not known whether the first-order change in the alcohol film on Fe_3O_4 is due to contamination by Fe_2O_3.

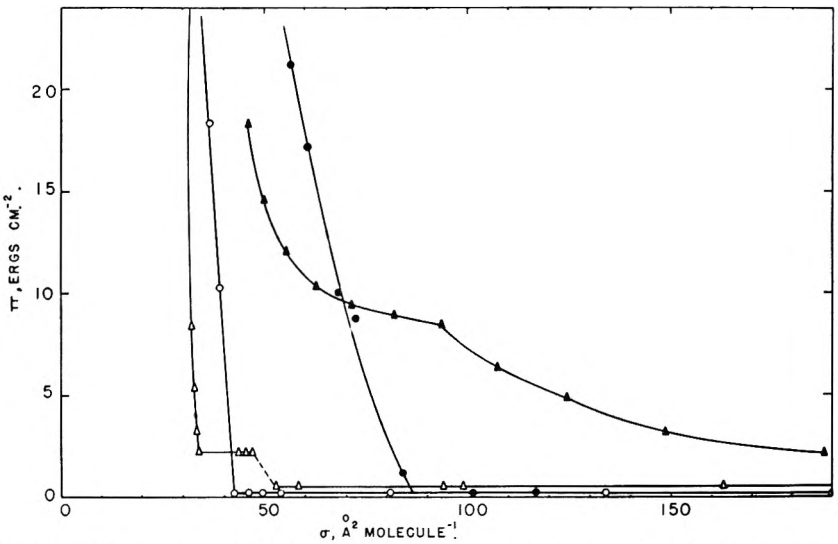

Fig. 3.—The pressure–area relationships in the low pressure region of *n*-propyl alcohol films at 25°: -△-, untreated iron; -▲-, reduced iron; -O-, Fe_2O_3; -●-, Fe_3O_4.

The relation between π, the film pressure and σ, the area per adsorbed molecule, for *n*-C_3H_7OH on untreated Fe and iron oxides is shown in Fig. 3. The low pressure region only is shown. The transitions take place at film pressures ranging from 0.2 to 2 ergs cm.$^{-2}$. The values of π begin to rise again when the area occupied by the molecule is about 33 Å.^{2} on untreated Fe, 42 on Fe_2O_3 and 86 on Fe_3O_4. These values are in reasonable agreement with the area occupied in a completed monolayer, σ_m, as given in Table II.

Free Surface Energy Relations.—The adsorption isotherms at 25° of *n*-propyl alcohol on untreated and reduced iron for the entire pressure range are exhibited in Fig. 4. The presence of the thin coat of oxide on the untreated iron increases the amount of alcohol adsorbed. The curve which represents the adsorption of a hydrocarbon, *n*-heptane, on either untreated or reduced iron is given also in Fig. 4. The number of heptane molecules adsorbed per unit area of solid is less than that of propyl alcohol at all pressures and is unaffected by the presence of the oxide coating on the iron. In Fig. 5 are shown the complete isotherms at 25° of *n*-propyl alcohol on Fe_2O_3 and on Fe_3O_4. For p/p_0 values below 0.5, the number of alcohol molecules adsorbed per unit area on Fe_2O_3 is much larger than adsorbed on Fe_3O_4. The shape of the curve of the alcohol on untreated iron is similar to that of the alcohol on Fe_2O_3. The values of the free surface energy changes were calculated from the adsorption data by the method described by Jura and Harkins.[5] Figure 6 exhibits the curves for the lowering of the free surface energy (π) of the solids as a function of the relative pressure of *n*-propyl alcohol. The alcohol's effectiveness at any p/p_0 value in lowering the free surface energy decreases in the order, Fe_2O_3, untreated Fe, Fe_3O_4 and reduced Fe.

Table I presents the values of π_e, the free energy decrease of the solid caused by the adsorbed film, and W_A, the work of adhesion for the various systems. The π_e and W_A values for *n*-heptane on the untreated iron are

TABLE I

FREE ENERGY OF INTERACTION BETWEEN SOLIDS AND ADSORBED VAPORS AT 25°

Solid	Liquid	π_e, decrease of free surface energy, ergs/cm.$^{-2}$	W_A, work of adhesion, ergs cm.$^{-2}$
Fe (untreated)	*n*-PrOH	102	148
Fe (reduced)	*n*-PrOH	73	119
Fe_3O_4	*n*-PrOH	86	132
Fe_2O_3	*n*-PrOH	122	168
Fe (untreated)	*n*-C_7H_{16}	54[a]	94[a]
Fe (reduced)	*n*-C_7H_{16}	53[a]	93[a]

[a] Reference 2.

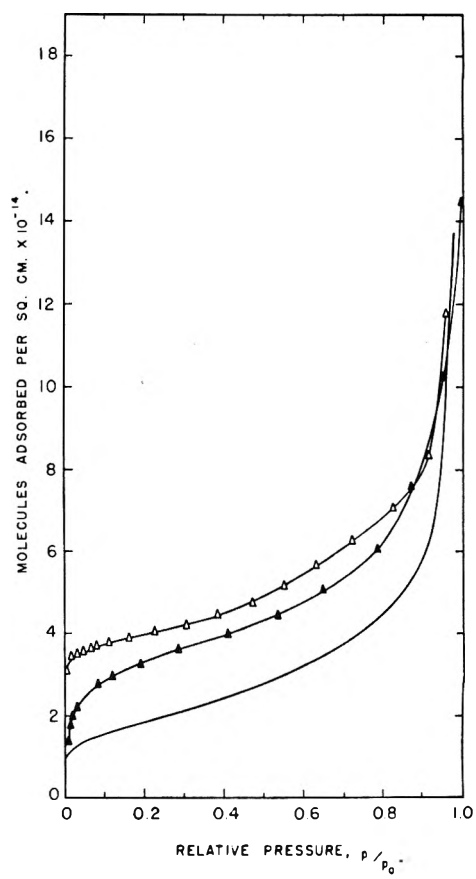

Fig. 4.—Adsorption isotherms at 25°: -△-, *n*-propyl alcohol on untreated iron; -▲-, *n*-propyl alcohol on reduced iron; —, *n*-heptane on untreated or reduced iron.

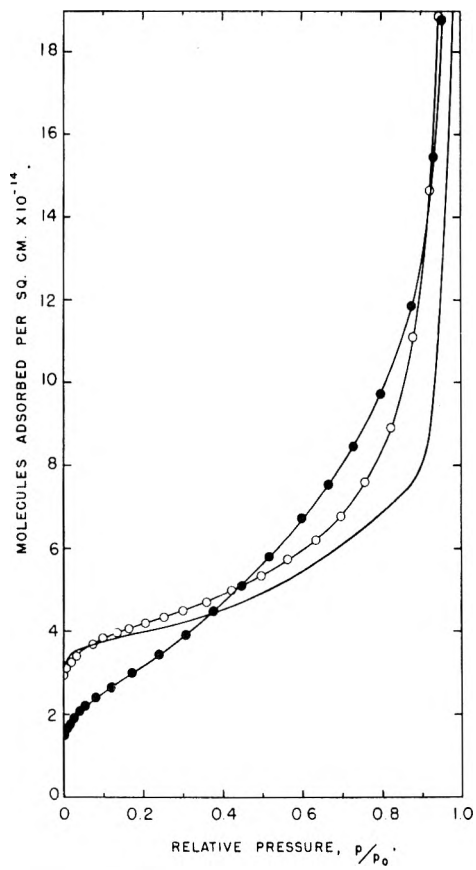

Fig. 5.—Adsorption isotherms at 25°: -O-, *n*-propyl alcohol on Fe_2O_3; -●-, *n*-propyl alcohol on Fe_3O_4; —, *n*-propyl alcohol on untreated iron.

the same as those for heptane on the reduced iron. In the case of the alcohol, however, the oxide film produces a large increase in the π_e and W_A values. These values appear to increase with the percentage of oxygen present in the solid lattice. This is also in agreement with earlier results for polar liquids adsorbed on untreated tin and tin oxide, where π_e and W_A were proportional to concentration of polar sites on the solid surfaces.

Surface Area Relationships.—Several methods have been utilized to calculate the areas of solids from adsorption data. The Langmuir,[8] B.E.T.[9] and Hüttig[10] methods provide the means for the calculation of v_m, the volume of vapor required to form a completed monolayer on the solid. In addition, the average cross-sectional area, σ_m, occupied by the adsorbed molecule is needed for area calculations by these methods. The Harkins-Jura[11] (H.J.) method uses the adsorption data and a constant, k. The value of k for each vapor at a given temperature is evaluated by the use of a solid of known area, anatase. The area of the anatase is 13.8 m.^{2}g.$^{-1}$ as determined by the Harkins and Jura absolute method.

In general, the vapors used for area determinations have been non-polar, *e.g.*, nitrogen or hydrocarbons. The value of σ_m for *n*-heptane on

(8) I. Langmuir, *J. Am. Chem. Soc.*, **40**, 1361 (1918).
(9) S. Brunauer, P. H. Emmett and E. Teller, *ibid.*, **60**, 309 (1938).
(10) S. Ross, THIS JOURNAL, **53**, 383 (1949).
(11) W. D. Harkins and G. Jura, *J. Am. Chem. Soc.*, **66**, 1366 (1944).

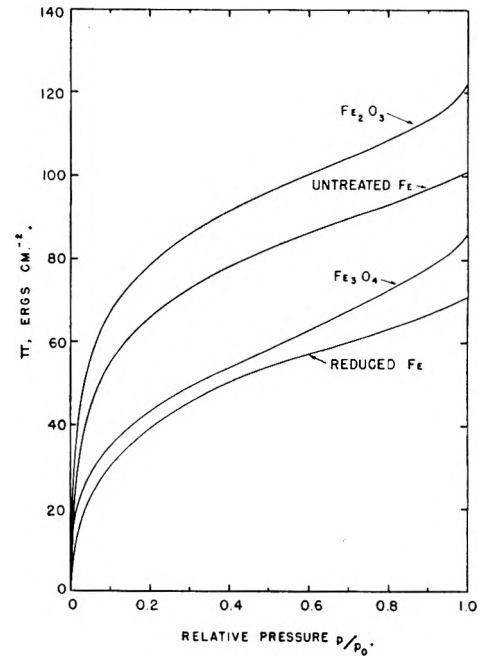

Fig. 6.—Lowering of free surface energy (π) for films of *n*-propyl alcohol on various solids as a function of the relative pressure (p/p_0).

twenty-one non-porous solids was found to be constant.[3] Livingston[12] has assigned "best" values of σ_m for the adsorbed molecules of twenty-three chemical compounds. The applicability of the B.E.T. and Hüttig theories to the *n*-propyl alcohol isotherms presented here may be questioned for two reasons. The first is the presence of discontinuities. According to the B.E.T. and Hüttig theories there are no significant intermolecular forces between the adsorbed molecules in an incomplete monolayer. This would rule out phase changes. Secondly, several of the B.E.T. and one of the Hüttig plots given in Figs. 8 and 9 have intercepts on the abscissa rather than on the ordinate. These are the first such curves to be reported and would yield negative values of the parameter c of the B.E.T. equation.

Because of this anomaly, the experimental procedures used and the calculations made in this investigation were re-examined. The correction for the change in density of mercury with temperature was applied to the pressure readings. A correction for adsorption of propyl alcohol on the glass surface of the apparatus was not made. It was probably negligible since the largest area of glass, the bulbs of the buret, was not used until a p/p_0 value of 0.7 was reached. The perfect gas law was assumed to hold for *n*-propyl alcohol at 25°. To test this, the data for *n*-propyl alcohol on anatase was recalculated using the Berthelot equation

$$pv = RT\left[1 + \frac{9}{128}\frac{pT_c}{p_cT}\left(1 - \frac{6T^2_c}{T^2}\right)\right]$$

where the critical temperature and pressure, T_c and p_c, are the constants in the equation. The recalculated values indicate a very slight deviation from the perfect gas law and no change in the negative intercept of the B.E.T. plot. In spite of the ob-

(12) H. K. Livingston, *J. Colloid Sci.*, **4**, 447 (1949).

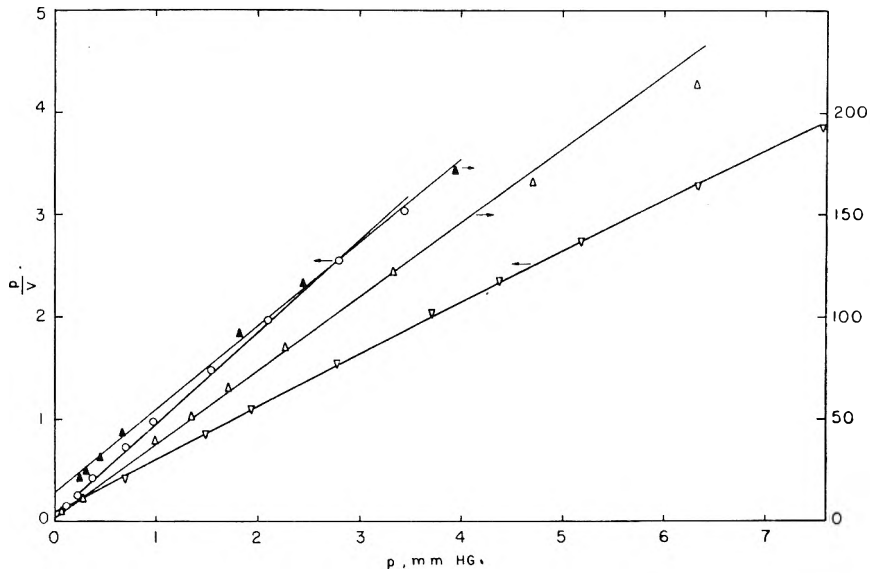

Fig. 7.—Langmuir plots for *n*-propyl alcohol at 25°: -△-, untreated iron; -▲-, reduced iron; -O-, Fe_2O_3; -▽-, TiO_2.

jections to the use of the B.E.T. and Hüttig theories, the results obtained by these methods were included in the correlations between σ_m and Σ values obtained by various methods.

In Tables IIA, B and C are listed the v_m values calculated by the Langmuir, B.E.T. and Hüttig methods from the adsorption data of *n*-propyl alcohol on five non-porous solids. The results for anatase were calculated from unpublished data obtained in this Laboratory. The p/p_0 ranges over which the linear relationships hold and σ_m values are also given. The latter were calculated from the equation, $\sigma_m = \Sigma/N$, where Σ is the surface area of the solid, determined in this case from n-C_7H_{16} or N_2 adsorption data, and N is the number of adsorbate molecules necessary to complete the monolayer. N may be calculated from v_m. The results indicate that the value of σ_m for the alcohol is not constant but varies from solid to solid. The Langmuir value is less variable than the B.E.T. or Hüttig values. The σ_m value calculated by Langmuir's method is approximately the same as that calculated for closely packed liquid molecules while the B.E.T. and Hüttig values are about 1.4 times larger. The p/p_0 ranges over which the Hüttig relation holds are more extensive than obtained by the other methods. Figures 7, 8 and 9 show the Langmuir, B.E.T. and Hüttig plots for *n*-propyl alcohol on TiO_2, Fe_2O_3, untreated iron and reduced iron. The plots for Fe_3O_4 were omitted from Figs. 7, 8 and 9 because they

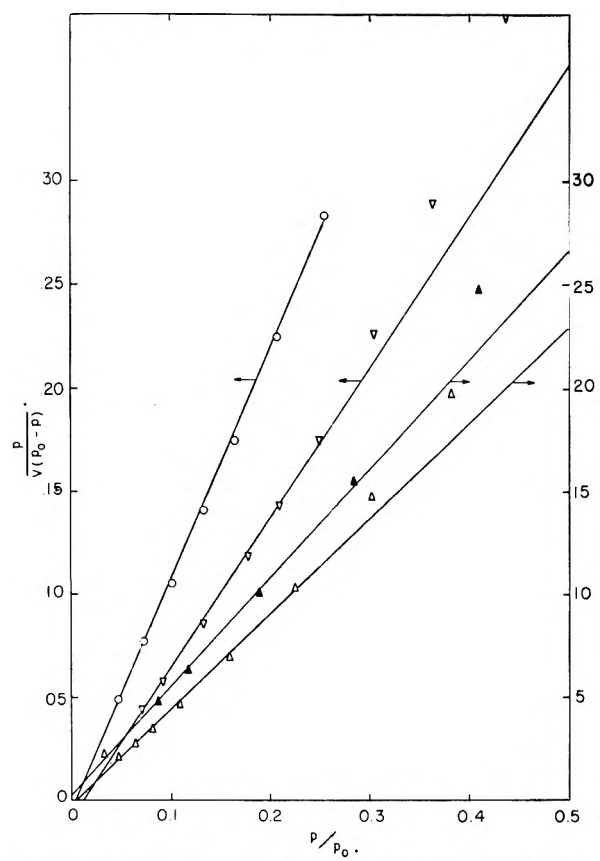

Fig. 8.—B.E.T. plots for *n*-propyl alcohol at 25°: -△- untreated iron; -▲-, reduced iron; -O-, Fe_2O_3; -▽-, TiO_2.

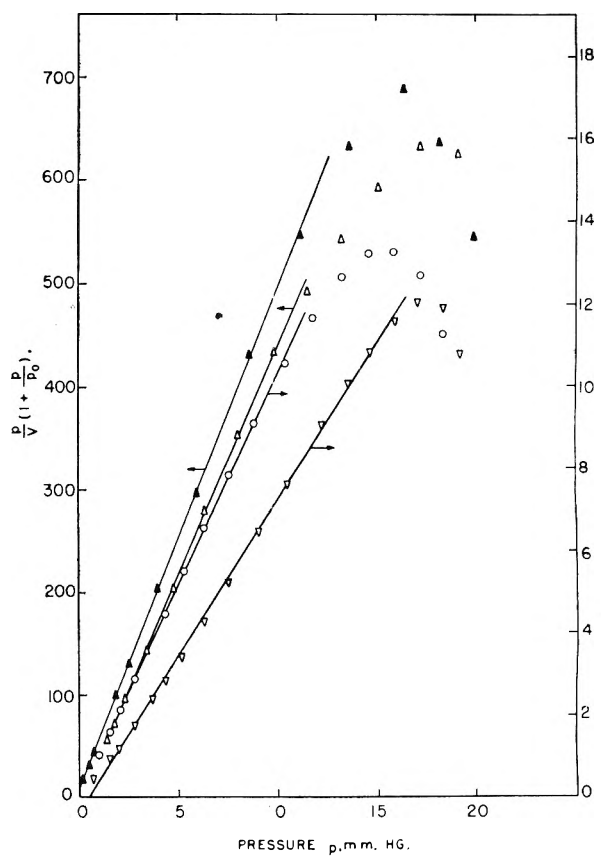

Fig. 9.—Hüttig plots for *n*-propyl alcohol at 25°: -△-, untreated iron; -▲-, reduced iron; -O-, Fe_2O_3; -▽-, TiO_2.

TABLES IIA, B AND C

CALCULATED VALUES OF σ FOR n-C_3H_7OH AT 25° AS OBTAINED FROM VARIOUS THEORIES

Solid	Area,[a] m.²g.⁻¹	v_m, cc. g.⁻¹ (S.T.P.)	Range of validity, p/p_0	Calcd. σ_m, Å.²
	A. Langmuir			
TiO_2	13.8	2.006	0.03 to 0.36	25.6
Fe_2O_3	7.51	1.136	.003 to .17	24.6
Fe_3O_4	1.83	[b]	.....	..
Fe (untreated)	0.187	0.02874	.01 to .23	21.2
Fe (reduced)	.182	.02439	.004 to .19	27.8
	B. B.E.T.			
TiO_2	13.8	1.3809	0.07 to 0.25	37.2
Fe_2O_3	7.51	0.8976	.05 to .25	30.9
Fe_3O_4	1.83	.1816	.04 to .24	36.9
Fe (untreated)	0.187	.02161	.05 to .23	32.6
Fe (reduced)	.182	.01870	.03 to .28	38.2
	C. Hüttig			
TiO_2	13.8	1.3176	0.09 to 0.76	39.1
Fe_2O_3	7.51	0.9684	.05 to .50	28.9
Fe_3O_4	1.83	.1733	.01 to .17	39.3
Fe (untreated)	0.187	.02253	.06 to .55	30.9
Fe (reduced)	.182	.02053	.005 to .55	33.0

[a] Area values calculated by B.E.T. and H.J. methods using N_2 or n-C_7H_{16} data. [b] No linear relationship found.

TABLE IV

HARKINS–JURA k VALUES FOR n-C_3H_7OH AT 25°

Solid	Area, Σ, m.²g.⁻¹	k Value	Range of validity, p/p_0
TiO_2	13.8	k_1 = 4.31	0.03 to 0.18
		k_2 = 5.13	.18 to .43
		k_3 = 8.93	.58 to .76
Fe_2O_3	7.51	k_2 = 5.14	.01 to .30
		k_3 = 8.79	.42 to .88
Fe_3O_4	1.83	k_5 = 12.82	.01 to .04
		k_4 = 11.51	.06 to .52
		k_3 = 8.42	.52 to .92
Fe (untreated)	0.187	k_1 = 4.14	.05 to .23
		k_3 = 8.59	.47 to .82
Fe (reduced)	.182	k_3 = 8.21	.09 to .54
		k_4 = 11.7	.75 to .87

TABLE V

AREAS OF SOLIDS CALCULATED BY H.J. METHOD, k = 8.93

Solid	Correct area, Σ_c, m.² g.⁻¹	H.J. area, $\Sigma_{H.J.}$, using k = 8.93 for n-C_3H_7OH	% Difference, $\frac{(\Sigma_c - \Sigma_{H.J.})100}{\Sigma_c}$
TiO_2	13.8	13.8	.....
Fe_2O_3	7.51	7.57	−0.8
Fe_3O_4	1.83	1.91	−4.4
Fe (untreated)	0.187	0.199	−6.4
Fe (reduced)	0.182	0.206	−13.2

TABLE III

AREAS OF SOLIDS CALCULATED BY LANGMUIR, B.E.T. AND HÜTTIG METHODS

Solid	Correct area, Σ_c, m.²g.⁻¹	Langmuir area, Σ_L, using σ_m = 25.6 Å.²	% Difference, $\frac{(\Sigma_c - \Sigma_L)100}{\Sigma_c}$	B.E.T. area, Σ_B, using σ_m = 37.2 Å.²	% Difference, $\frac{(\Sigma_c - \Sigma_B)100}{\Sigma_c}$	Hüttig area, Σ_H, using σ_m = 39.1 Å.²	% Difference, $\frac{(\Sigma_c - \Sigma_H)100}{\Sigma_c}$
TiO_2	13.8[a]	13.8	...	13.8[c]	....	13.8[d]	....
Fe_2O_3	7.51[a]	7.81	−4.0	8.97[c]	−18.8	10.2	−26.1
Fe_3O_4	1.83[b]	....	...	1.82	+ 0.5	1.82	+ 0.5
Fe (untreated)	0.187[b]	0.198	−5.9	0.216[c]	−15.5	0.237	−26.7
Fe (reduced)	.182[b]	.168	+7.7	.187	− 2.7	.216	−18.7

[a] Area calculated from N_2 data using B.E.T. or H.J. methods. [b] Area calculated from n-C_7H_{16} data using B.E.T. or H.J. methods. [c] Plots give negative values of constant "c"; therefore B.E.T. theory may not apply. [d] Plot gives a negative value of "c"; therefore Hüttig theory may not apply.

would necessitate using a third ordinate scale. In actual practice the process is reversed; the area, Σ, is calculated from v_m and σ_m. The value of σ_m is usually approximated. However, since σ_m is not constant, the calculated area values may deviate from the true values. This is shown in Table III. The area values obtained from the alcohol data by the Langmuir method are more self consistent and are closer to the probable values determined by nitrogen adsorption; the B.E.T. and Hüttig values show deviations from values determined by nitrogen adsorption, which we consider to give the most probable value of the area.

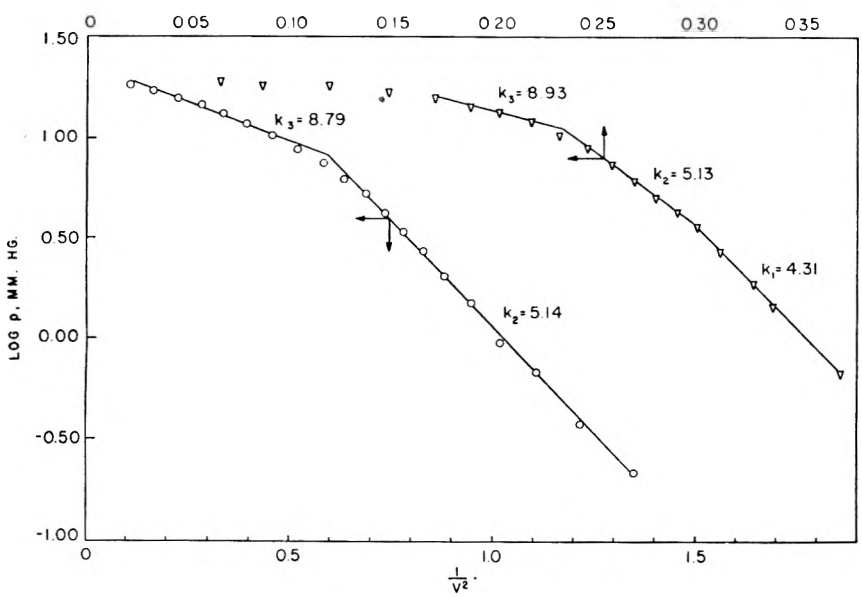

Fig. 10.—H.J. plots for n-propyl alcohol at 25°: -▽-, TiO_2; -O-, Fe_2O_3.

If the adsorption data are plotted with log p *vs.* $1/v^2$, one or more linear sections are obtained. According to the H.J. method, the square root of the slope, A, of these linear plots is proportional to the area of the solid. The equation for this relation is $\Sigma = kA^{1/2}$, where k is the constant for a given adsorbed vapor at a

specified temperature. The value of k for n-C_3H_7OH was determined from the slopes of these H.J. lines for the vapor adsorbed on solids of known areas. Figure 10 exhibits the H.J. plots for n-C_3H_7OH on TiO_2 and Fe_2O_3. It is apparent from these plots and the values given in Table IV that several k values may be calculated for each isotherm. Although the k values appear to fall into groups of approximately the same magnitude, the p/p_0 range of applicability of each is not the same for the various solids. The areas of four solids: Fe_2O_3, Fe_3O_4, Fe (untreated) and Fe (reduced) were calculated using $k_3 = 8.93$, which was one of the values obtained for n-C_3H_7OH on TiO_2. The results given in Table V show fairly good self consistency. The determination of area by the H.J. relative method using n-C_3H_7OH data is not recommended since there appears to be no means of determining the p/p_0 region of the isotherm over which a given k value is valid.

It is apparent from the lack of agreement between these methods for calculating area, and the divergent results obtained with the polar vapor, *n*-propyl alcohol, as compared with the non-polar vapors, nitrogen and *n*-heptane, that the safest procedure is to use non-polar gases for accurate area measurements. This becomes increasingly important when polar solids are involved, such as the iron oxides used in this study.

A STUDY OF THE SYSTEM *cis*- AND *trans*-CYCLOHEXANEDIOL-1,2

BY W. J. SVIRBELY AND SAMUEL GOLDHAGEN[1,2]

Contribution from the Department of Chemistry, University of Maryland, College Park, Md.

Received December 5, 1952

A phase study of the *cis*- and *trans*-cyclohexanediol-1,2 system was made using a micro hot stage in conjunction with a chemical microscope. X-Ray diffraction patterns were determined for the *cis*-diol, *trans*-diol and several solutions ranging from 5% to 25% *trans*-diol in order to help establish the phase diagram. The resulting diagram shows: (1) a eutectic, melting at 71.9°, at 56.6% *trans*-diol; (2) a solid solution field for mixtures containing more than 55% *cis*-diol; (3) three different crystalline forms for the pure *cis*-diol.

The use of the *cis*- and *trans*-cyclohexanediols in determining mechanism has been widespread. In two of the instances,[3,4] data have been obtained from which the temperature–composition curve of the *cis*- and *trans*-cyclohexanediol-1,2 system could be constructed. The diagrams obtained from those studies are not in agreement.

In the present work, temperature–composition data have been obtained chiefly from experiments carried out on a "hot stage" in conjunction with a polarizing microscope. The results have been used to construct the phase diagram of the *cis*- and *trans*-cyclohexanediol-1,2 system.

Experimental Procedure

***cis*- and *trans*-Cyclohexanediol-1,2.**—The crude mixture of isomers was prepared by hydrogenating catechol in ethanol over Raney nickel at 195–200°. The isomers were separated from the crude mixture by use of various procedures. The m. p. of the *cis*-diol and the *trans*-diol were 98.5–99.5° (uncor.) and 103–104° (uncor.), respectively. Mixed melting points of the *cis*- and *trans*-diols with each other and with catechol (m.p. 104°) showed a marked lowering.

Apparatus and Method.—At the start of this work, the classical, cooling curve technique was attempted. The results obtained could not be interpreted; therefore, a procedure involving a chemical microscope with a micro hot stage was used. Crossed nicols were used to make observations when anisotropic crystals on a fused slide were not easily discernible. Isotropic substances were observed directly. If some doubt existed, for a particular sample, as to whether an isotropic or an anisotropic solid resulted, then a first-order red plate was used. The temperature of the hot stage was raised slowly so that the temperature at which the last crystal disappeared could be determined. If cooling were then started immediately by decreasing the heat input, super-cooling was avoided in most cases.

The samples were prepared as follows: weighed amounts of *cis*- and *trans*-diols, usually amounting to 0.4 g. for the mixture, except when the mixture approached one of the pure components in composition, were placed in a vial. The mixture was melted and the melt stirred thoroughly with a wire stirrer. After cooling, the solid mixture was pulverized and again mixed thoroughly. A small portion of the powder, 10–20 mg., was placed on a 1″ × 1.5″ microscope slide, covered with a cover glass and slowly melted over a low flame. The cover glass was then squeezed tightly against the slide to decrease the amount of the solid to a minimum. The excess solid was removed and the slide wiped clean. The slide was placed on the hot stage and the microscope was focused on an interior portion of the material. Actual observations as to the changes taking place during the slow heating and slow cooling were thus easily obtainable.

In the above work, a Leitz petrographic microscope with a 16-mm. objective and a 10× eyepiece was used. The light source was a Spencer Type 370 lamp with a blue, frosted glass. The hot stage was an electrically heated, Kofler micro unit. The current input was controlled with a variable rheostat supplied with the hot stage. The thermometer belonging to the hot stage was calibrated using fused slides containing pure compounds whose true melting points were in turn obtained by standard cooling curve technique. In the latter case, Anschütz thermometers calibrated in 0.2° and checked against similar thermometers calibrated by the Bureau of Standards were used.

Experimental Results

Temperature data were gathered for the disappearance of the last crystal (f′p′) and the appearance of the first crystal (fp). Anywhere from three to eight determinations involving new slides and used slides were made on each mixture or pure compound. In two cases, namely, pure *trans*-diol and 77.6% *trans*-diol, supercooling prevented the obtaining of (fp) data. Otherwise, the disappearance of the last crystal and its reappearance were found to be reproducible. All data obtained for

(1) Abstracted in part from the M.S. Thesis of S. Goldhagen.

(2) Presented at the Atlantic City Meeting of the American Chemical Society, September, 1949.

(3) B. Rothstein, *Ann. Chem.*, **14**, 461 (1930).

(4) S. Winstein and R. E. Buckles *J. Am. Chem. Soc.*, **64**, 2780 (1942).

each mixture or compound were averaged with an average deviation of the mean of about ±0.1°. The results are listed in the second column of Table I.

Using new slides of some of the mixtures, observations which help to fix portions of the phase diagram other than the disappearance of the last crystal were made. We have summarized these data in the third column of Table I.

TABLE I

SUMMARY OF DATA USING MICROSCOPIC TECHNIQUE

Composition in % *trans*-diol	Cor. temp., °C.	Cor. temp., °C. for other observations
100.00	102.8	
90.80	98.4	71.7 ± 0.3[a]
84.30	94.7	
77.67	90.0	
70.05	84.6	
65.05	79.7	72.1[a]
58.80	73.5	
56.95	72.8	71.8[a]
52.62	73.8	73.1 ± 0.4[a]
49.26	74.9	
39.52	78.6	76.1 ± 0.4[a]
31.59	80.9	77.4[a]
24.99	83.5	82.3 ± 0.1[b]
22.00	84.7	
20.04	86.5	80.4 ± 0.2[a]
13.92	90.2	
10.29	92.7[c]	
4.99	95.7[c]	82.2 ± 0.4[a]
0.00	99.2[c]	

[a] First appearance of liquid. [b] Sharp increase in the amount of liquid. [c] Birefringence disappears in each of these cases on raising the temperature at about 86–88°.

Derx,[5] from cooling curves and from observations made using a micro hot stage, determined the freezing point and two transition temperatures for the *cis*-diol, namely, 94, 78.1 and 75.2°. However, the melting point that he used to identify the *cis*-diol was 98°. As reference to Table I shows, there is a loss of birefringence for the *cis*-diol between 86–88°. Two runs made on pure *cis*-diol using a cooling curve technique[6] indicate phase changes in pure *cis*-diol at 99.60, 87.34 and 80.5 ± 0.2°.

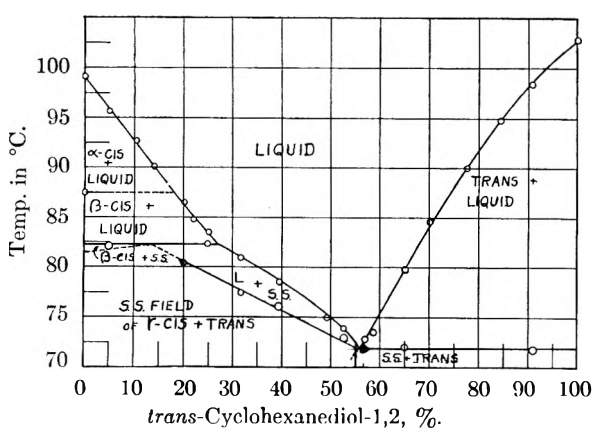

Fig. 1.—Phase diagram of *cis*- and *trans*-cyclohexanediol-1,2.

(5) H. Derx, *Rec. trav. chim.*, **41**, 312 (1922).

(6) Procedure.—About 2 g. of the *cis*-diol was placed in a small test-tube A. Tube A was suspended by means of a cork in the neck of a large test-tube, B. An Anschütz thermometer calibrated in 0.2° was placed in tube A. The exposed stem of the thermometer was covered with a tube to protect it from air currents. Tube B with its contents was supported by a cork in the neck of a one-pint dewar flask containing oil preheated to about 101°. Cooling occurred at the rate of about 0.08° per minute. The first arrest corresponding to the solidification of the diol, lasted about five minutes. The second arrest, corresponding to a transition of one solid form to another, as indicated by the change in optical properties, lasted about 30 minutes. The third discontinuity consisted of a marked change in the slope of the cooling curve.

Discussion

Figure 1 shows the phase diagram for the system based upon the experimental observations.

The intersection of the freezing point curves for the mixtures containing more than 30% *trans*-diol indicates that the eutectic composition and temperature are 56.6% *trans*-diol and 71.9°, respectively. This eutectic temperature is in fairly good agreement with the experimental values obtained for *trans*-rich mixtures.

Although the reproducibility of the temperature data for the appearance of liquid richer in *cis*-diol than the eutectic was not as good as the data used in establishing the freezing point curves, nevertheless, it is definite that the data lead to the postulation of a solid solution.

There are two transition temperatures for pure *cis*-diol, one at 87.34° and the other at 80.5 ± 0.2°. The latter transition temperature was not as reproducible as the higher transition temperature. However, its existence leads to the conclusion that there is a γ-*cis*-diol and that the γ-*cis* form dissolves the *trans* form to the extent indicated by the solidus.

X-Ray diffraction patterns were also determined[7] for pure *cis*-diol, pure *trans*-diol and for five mixtures from 5 to 25% *trans*-diol. *d*-Values were calculated using Bragg's law. While this procedure does not give a true interplanar distance, *d*, it gives definitive values for each compound or mixture. An examination of the *d* and intensity values indicated: (1) with the exception of two weak lines, the remainder of the lines could be traced to either pure *cis*- or pure *trans*-diol; (2) changes occurred in the intensity value for most of the spacings in going from pure *cis*-diol to mixtures with increasing amounts of the *trans*-diol and also in going from pure *trans*-diol to mixtures with increasing amounts of the *cis*-diol, (3) the spacing of the pure *trans*-diol with the greatest intensity value did not occur in any of the mixtures. We have no explanation for this.

The results of the X-ray studies are compatible with the phase diagram shown in Fig. 1. A solid solution phase continuous with γ-*cis*-diol would have the same (or very nearly the same) crystal structure as the pure *cis*-diol even with increasing concentrations of *trans*-diol. Changes in intensity

(7) We acknowledge our indebtedness to Dr. John J. Lander of the Naval Research Laboratories for making the X-ray studies. The instrument was a North American Philips X-ray spectrophotometer. The details of calibration and application to solids are described in Naval Research Laboratory Report No. C-3262. The samples were the unused portions of the mixtures prepared for the studies on the micro hot stage. The crystals were ground and the resulting powder was pressed into a disc one inch in diameter and about 1/8 in. thick at a pressure of about five thousand pounds per square inch. The discs were mounted on glass slides and the diffraction patterns were determined at room temperature.

of the spacings for the pure *cis*-diol would be expected (and were obtained) as the amounts of *trans*-diol increased in the solid solution phase.

The absence of spacings in the mixtures not traceable to either pure *cis*- or pure *trans*-diol eliminates the possibility of existence of either a new compound or of a solid solution which is not continuous with pure *cis*-diol.

SIMPLE GENERAL NOTATIONS FOR SYSTEMS OF SIMULTANEOUS REACTIONS

By F. Halla

Association pour les Etudes Texturales, 4, rue Montoyer, Brussels, Belgium

Received December 8, 1952

With the aid of a simplified notation the general conditions for the kinetics in a system of simultaneous reactions are derived.

For a general treatment of the kinetic laws governing simultaneous reactions[1] it may sometimes be useful to have a more consistent and adequate notation than any employed till now. In an earlier paper of Wegscheider[2] such a notation is already alluded to but no further pursued. It consists in writing the stoichiometric equations in such a way that all s reactants M_σ appear on both sides in each equation. The latter are marked by a line index ρ ("reaction"), the substances by the column index σ. The terms on the right sides are distinguished by a bar on top.

The system of r stoichiometric equations

$$\sum_{\sigma=1}^{s} n_{\rho\sigma} M_\sigma = \sum_{\sigma=1}^{s} \bar{n}_{\rho\sigma} M_\sigma \qquad (1)$$

must be completed by the matrices of the coefficients $(n_{\rho\sigma})_{rs}$ and $(\bar{n}_{\rho\sigma})_{rs}$ which allow for the fact that some of the $n_{\rho\sigma}$ and $\bar{n}_{\rho\sigma}$ must disappear.

By putting

$$m_{\rho\sigma} \equiv n_{\rho\sigma} - \bar{n}_{\rho\sigma} \qquad (2)$$

(1) may also be written[3]

$$\sum_{\sigma=1}^{s} m_\sigma M_\sigma = 0 \qquad (3)$$

The matrices will in general not be quadratic, for s must exceed r at least by 1 (except in cases where the stoichiometric equations are not linearly independent; they will not be considered for the moment).

Each of the partial reactions (1) has in the time interval from t_0 to t brought about a certain exchange $\xi_{\rho\sigma}$ for each reactant M_σ

$$\xi_{\rho\sigma} = m_{\rho\sigma} x_\rho \qquad (4)$$

where x_ρ is the "normal exchange" of the reaction (1), *i.e.*, the decrease in concentration of a reactant whose $m_{\rho\sigma}$ would be unity.

The total exchange ξ_σ for a certain reactant

$$\xi_\sigma = \sum_{\rho=1}^{r} \xi_{\rho\sigma} = \sum_{\rho=1}^{r} m_{\rho\sigma} x_\rho \qquad (5)$$

The aim is to obtain the x_ρ by solving the differential equations given by the law of kinetic mass action

$$\frac{dx_\rho}{dt} \equiv x_\rho' = k_\rho \prod_{\sigma=1}^{s} c_\sigma^{n_{\rho\sigma}} - \bar{k}_\rho \prod_{\sigma=1}^{s} c_\sigma^{\bar{n}_{\rho\sigma}} \qquad (6)$$

k_ρ, $\bar{k}_\rho$ are the velocity coefficients.

The concentrations c_σ occurring in these equations are connected with the exchanges by the s relations

$$c_\sigma = A_\sigma - \xi_\sigma = A_\sigma - \sum_{\rho=1}^{r} m_{\rho\sigma} x_\rho \qquad (7)$$

in which the A_σ mean the initial concentrations.

Eliminating the r quantities x_ρ from the system (7), we obtain s − r ≡ t independent linear relations between the c_σ and the A_σ

$$f_\tau(c_1 \ldots c_s;\ A_1 \ldots A_s) = 0 \quad (\tau = 1, 2, \ldots) \qquad (8)$$

They are equivalent to (7) and especially useful for simplifying the equations (6).

Substituting in (6) the c_σ from (7) or (8) we get

$$x_\rho' = k_\rho \prod_{\sigma=1}^{s} \left(A_\sigma - \sum_{\rho=1}^{r} m_{\rho\sigma} x_\rho\right)^{n_{\rho\sigma}} - \bar{k}_\rho \prod_{\sigma=1}^{s} \left(A_\sigma - \sum_{\rho=1}^{r} m_{\rho\sigma} x_\rho\right)^{\bar{n}_{\rho\sigma}} \qquad (9)$$

Expanding the products in (9), r integer rational functions R_ρ of the x_ρ

$$x_\rho' = R_\rho(x_1 \ldots x_r;\ A_1 \ldots A_s;\ n_{\rho\sigma} \ldots;\ \bar{n}_{\rho\sigma} \ldots;\ k_\rho, \bar{k}_\rho) \qquad (10)$$

are obtained.

The solution of the r equations (9) is possible in principle and must give by reasons of physical continuity, s unique solutions $c_\sigma(t)$ which are mutually related by the s-r equations (8). But it cannot be practically executed because of mathematical difficulties in cases where the order of the reaction exceeds 1. Suppose we had obtained these r solutions $x_\rho(t)$, the concentrations as functions of time are then found from (7)

$$c_\sigma = A_\sigma - \sum_{\rho=1}^{r} m_{\rho\sigma} x_\rho(t;\ A_1 \ldots A_s;\ k_1 \ldots k_r) \qquad (11)$$

Therewith the principal object of simultaneous kinetics would be achieved.

The task becomes simpler if we have to deal only with an *equilibrium* state (*i.e.*, the final state in kinetic sense, for $t = \infty$) of the whole system of

(1) See for instance, C. A. Hollingworth, *J. Chem. Phys.*, **20**, 921 1649 (1952).

(2) R. Wegscheider, *Sitzungsber. Akad. Wissensch. Wien*, **110**, IIa, 561 (1901); *Z. physik. Chem.*, **39**, 266 (1902).

(3) See for instance, J. Prigogine and R. Defay, "Thermodynamique Chimique," Vol. I, Editions Desoer, Liege, 1944, p. 17.

reactions. This state is characterized by the c_σ of all reactants remaining constant. Therefore by differentiating (7) we obtain the s conditions

$$c_\sigma' = -\xi_\sigma' = -\sum_{\rho=1}^{r} m_{\rho\sigma} x_\rho' = 0 \qquad (12)$$

from now on we have to replace in all expressions the concentrations c_σ and the normal exchanges x_ρ by their *stationary* values C_σ and X_ρ. (12) then gives s equations

$$\sum_{\rho=1}^{r} m_{\rho\sigma} \lim\,[x_\rho']_{t=\infty} = 0 \qquad (7')$$

where, according to (10), we have to put

$$\lim[x_\rho']_{t=\infty} = R_\rho(X_1, \ldots;\ A_1, \ldots \bar{k}_r) = 0 \quad (10')$$

Thereby (7′) changes into the s relations

$$\sum_{\rho=1}^{r} m_{\rho\sigma} R_\rho(X_1, \ldots \bar{k}_r) = 0 \qquad (7'')$$

Because the s stationary concentrations must have definite values and because we have from (7″) only r solutions $X_\rho(k_1 \ldots k_r;\ \bar{k}_1 \ldots \bar{k}_r;\ A_1 \ldots A_s)$ the $C_\sigma(k_1 \ldots k_r;\ \bar{k}_1 \ldots \bar{k}_r;\ A_1 \ldots A_s)$ must be connected with the A_σ by $s - r$ independent linear relations.

We may put the problem in another way too, requiring that in the equilibrium state all $\lim[x_\rho']_{t=\infty}$ disappear. This means, we require the existence of (thermodynamical) equilibrium constants, independent of all the A_σ

$$K_\rho \equiv \bar{k}_\rho/k_\rho = \prod_{\sigma=1}^{s} C_\sigma^{m_{\rho\sigma}} \qquad (13)$$

for the single partial reactions. If they exist, the equations (7′) and (7″) are identically satisfied.

Now, each further condition imposed upon the system must lead to a relation between the parameters k_ρ, $\bar{k}_\rho$ only, because the parameters A_σ may be arbitrarily chosen *a priori* and can therefore not be affected.

Let us take as an example Wegscheider's[2] treatment of the mutual conversion of 3 isomers,

$$M_1 \rightleftarrows M_2 \qquad (a)$$
$$M_2 \rightleftarrows M_3 \qquad (b)$$
$$M_3 \rightleftarrows M_1 \qquad (c)$$

The first two equations correspond together to the case $r = 2$, $s = 3$ with $c_1 + c_2 + c_3 = A_1 + A_2 + A_3$ as a secondary condition according to (8), and give unique solutions X_1, X_2, X_3.[4] But if we include equation (c) which is not linearly independent of (a) + (b), we impose upon the system a further condition and this must lead to a relation between the k_ρ, $\bar{k}_\rho$, *viz.*

$$k_1 k_2 k_3 = \bar{k}_1 \bar{k}_2 \bar{k}_3$$

as already shown by Wegscheider.[2] This topic in connection with Wegscheider's paradox has been treated in another paper.[5]

(4) F. Halla, *Monatsh.*, **84**, 1448 (1952).
(5) F. Halla, *ibid.*, **84**, 162 (1953).

THE VAPOR PRESSURE, ASSOCIATION, AND HEAT OF VAPORIZATION OF HYDROGEN FLUORIDE[1a,1b]

BY ROGER L. JARRY AND WALLACE DAVIS, JR.

Research Laboratories, K-25 Plant, Carbide and Carbon Chemicals Company, Union Carbide and Carbon Corporation, Oak Ridge, Tennessee

Received December 11, 1952

The vapor pressure of hydrogen fluoride has been measured, in a dynamic system, over the temperature range 0 to 105°. Data have been fitted to two equations:

$$\log_{10} P_{mm} = 8.38036 - \frac{1952.55}{335.52 + t} \quad (1) \quad \text{and} \quad \log_{10} P_{mm} = -1.91173 - \frac{918.24}{T} + 3.21542 \log_{10} T \qquad (2)$$

The utility of these normal vapor pressure equations is surprising when examined in light of the association of hydrogen fluoride which varies with temperature. Of interest is the value of 335.52 in equation (1) which is greater, rather than less than 273.16, and the fact that the first constant in equation (2) is negative. Association factors for the saturated vapor have been calculated from vapor density measurements; heats of vaporization have been calculated, by use of the Clapeyron equation, for a formula weight, 20.01 g., of material.

Vapor pressure data in the literature on hydrogen fluoride are restricted to temperatures near the normal boiling point (19.4°) and lower. Such data as given by Kelley[2] at higher temperatures are derived from extrapolation of low temperature measurements. The present report deals partially with vapor pressures at temperatures from 0 to 105°. Density measurements of the saturated vapor have been run in the temperature interval 23 to 105°. These data have been used to calculate the degree of association in the saturated vapor.

Experimental

Apparatus.—Apparatus used for obtaining vapor pressures and vapor densities is shown schematically in Fig. 1. Principal components were the pot, A, containing liquid hydrogen fluoride; a vapor volume, B, that could be isolated from the rest of the circulation system; a vapor pump,[3] C, to force the vapor through the liquid, at point D; and a Booth–

(1) (a) This document is based on work performed for the Atomic Energy Commission by Carbide and Carbon Chemicals Company, Union Carbide and Carbon Corporation, at Oak Ridge, Tennessee. (b) For original data order document, from American Documentation Institute, 1719 N Street, N. W., Washington 6, D. C., remitting $1.00 for microfilm (images 1 inch high on standard 35-mm. motion picture film) or $1.50 for photocopies (6 × 8 inches) readable without optical aid.

(2) K. K. Kelley, U. S. Department of the Interior, Bureau of Mines, Bulletin 383.

(3) F. D. Rosen, *Rev. Sci. Instruments*, in press.

Cromer pressure transmitter,[4] BC-1, for measuring vapor pressures. These components were mounted, as indicated in Fig. 1, in one side of a two-section air thermostat, each side being heated independently. Expansion ballasts and the sampling manifold were located in the other side of the air thermostat so that the vapor circulation system would not be affected by temperature changes produced while the weighing flask was being connected to or removed from the system.

Construction materials were as follows: heavy walled, $^3/_8$-inch nickel tubing was used for connection lines; the pot was made from $^1/_4$-inch wall, 4-inch diameter nickel pipe, with $^3/_8$-inch plate nickel ends; the pump, except for monel tubing around the nickel plunger, was made of nickel. Booth–Cromer pressure transmitter BC-1 was enclosed in a steel pressure cylinder having $^1/_4$-inch walls and $^3/_8$-inch thick ends. Electrical contact was made through a 14-mm. aircraft-type spark plug.

Valves V-1 through V-5 were Hoke type M-342; the barrel containing the needle was silver-soldered to the body. The usual packing was replaced with Teflon. Valves V-6 through V-10 were Hoke, monel body, diaphragm valves, with replaceable diaphragms. The vapor bubbler, D, was made from a $^3/_8$-inch nickel sweat cap perforated with a number of $^1/_{16}$-inch diameter holes. All joints were made by welding except where otherwise noted.

The weighing flask was made from spun-nickel to reduce the weight to about 200 g. Replacement of the brass gasket in a $^1/_4$-inch compression fitting by one machined from Teflon made it possible to obtain a vacuum tight seal with finger tip pressure on the ears soldered to the compression nut (Fig. 1).

Materials.—Hydrogen fluoride was obtained from a commercial tank that had been partially emptied and, therefore, depleted of most of the impurities other than traces of water. Further purification was accomplished by first distilling hydrogen fluoride onto sodium fluoride and then onto cobalt trifluoride. In the first step hydrogen fluoride was added until the approximate ratio was 6 moles of hydrogen fluoride to 1 mole of sodium fluoride. This combination exhibits a vapor pressure of about 4 p.s.i.a. at room temperature. Hydrogen fluoride removed from such a mixture had been checked by thermal analysis and shown to be about 99.74 mole % pure. Cobaltic fluoride served to remove any final traces of water. Hydrogen fluoride after such treatment was 99.9 mole % pure. A portion of the hydrogen fluoride used in this work was removed from the equilibrium apparatus during the course of the measurements and was found to be 99.75 mole % pure, with a melting point at −83.76°. Sodium fluoride was C.P. material dried by extensive pumping while heating. Commercial grade cobaltic fluoride was first heated and pumped and then treated with fluorine at about 100° for several hours.

Temperature and Pressure Measurements.—Temperatures in the air thermostat were controlled by mercury regulators operated in conjunction with appropriate electronic relays. Measurement of solution temperature was accomplished by use of a copper–constantan thermocouple, as indicated in Fig. 1, in a well below the liquid surface. Vapor and liquid temperatures were the same within 0.1 to 0.2°. The thermocouple was calibrated at 0° (ice), about 25° (room temperature as determined by a calibrated Beckmann thermometer), 64.02° (melting point of pure uranium hexafluoride[5] by the calorimetric fractional melting point method), and 122.353° (Bureau of Standards certified benzoic acid melting point standard).

Most pressures were measured by means of a Bourdon gage that had been calibrated with nitrogen against a dead weight gage.[6] This Bourdon gage had a 7-inch diameter scale of 0 to 160 p.s.i.g. graduated in 2-pound increments; it was used to measure pressures above 1400 mm. Pressures below this value were observed on a mercury manometer.

Procedure.—The pot (A, Fig. 1) of the equilibrium apparatus was charged with hydrogen fluoride and the system heated to one of the 9 different temperatures above zero degrees used in this work. (For the 0 and −80° determinations of the vapor pressure the hydrogen fluoride was transferred to a ballast flask on the sampling manifold, where a water ice or Dry Ice bath served to maintain a constant temperature.) Vapor was circulated through the liquid while the material was heated and until constant temperature and pressure had been achieved. Pumping was then stopped, valve V-4 (Fig. 1) of the vapor flask, B, was closed, and the system was allowed to remain in this condition for 5 minutes. This delay was to allow drainage of any traces of liquid spray from the vapor flask back into the liquid flask. Valve V-3 was closed following which the entire sample in B was condensed, by means of liquid nitrogen, into the weighing flask. The flask and counterpoise were then removed from the air thermostat and allowed to reach room temperature and the sample weight taken. The tare weight of the flask was determined just prior to taking the sample and also after the sample weight was obtained. In addition, the counterpoise was always simultaneously taken through the same heating and cooling cycles.

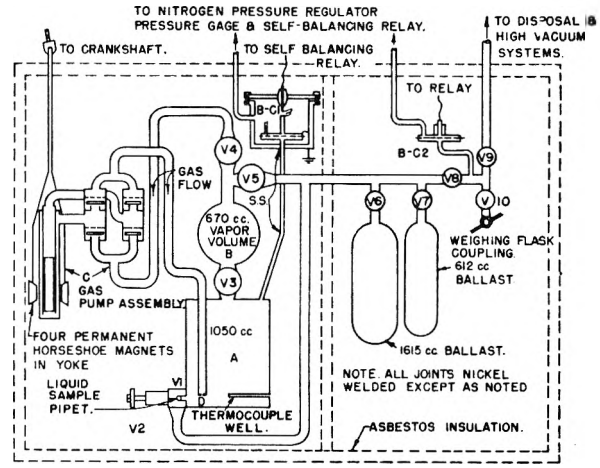

Fig. 1.—Vapor pressure and liquid–vapor equilibrium apparatus.

Results

Vapor pressure data obtained in this work were fitted to the Antoine equation, 1, and the Kirchhoff equation, 2. Constants for each equation have been listed at the 95% confidence level.

$$\log_{10} P_{mm} = A - \frac{B}{C + t} \qquad (1)$$

$A = 8.38036 \pm 0.10896$
$B = 1952.55 \pm 125.85°$
$C = 335.52 \pm 8.15°$

$$\log P_{mm} = a + \frac{b}{T} + c \log T \qquad (2)$$

$a = -1.91173 \pm 1.02000$
$b = -918.24 \pm 48.06°\text{K.}$
$c = 3.21542 \pm 0.34672$
t = Centigrade temp.
T = Kelvin temp.

A priori estimates of precision imposed by the experimental conditions are as follows: temperature, ±0.05°; pressure, ±20 mm. at pressures of 1400 mm. or higher, ±0.2 mm. at pressures below 1400 mm.

Table I gives smoothed values of vapor pressure, from the two equations, saturated vapor density, association number ($Z^v_{sat.} = \bar{M}/20$), heat of vaporization ΔH per formula weight (20.01 g.), and the heat required to vaporize enough liquid to produce 1 mole of saturated vapor ($Z^v_{sat.}\ \Delta H$).

Discussion

Vapor Pressures.—Vapor pressure data[1b] obtained in this research are summarized at convenient temperatures in Table I. Original vapor

(4) S. Cromer, U.S.A.E.C. Declassified Report MDDC-803.

(5) G. D. Oliver, H. T. Milton and J. W. Grisard, *J. Am. Chem. Soc.*, **75**, 2827 (1953).

(6) W. B. Kay *ibid.*, **69**, 1273 (1947).

TABLE I*

* For supplementary Table IA giving the experimental data, order Jarry–Davis Document from the American Documentation Institute, c/o Library of Congress, Washington 25, D.C.

VAPOR PRESSURE, VAPOR DENSITY, ASSOCIATION FACTOR AND HEAT OF VAPORIZATION OF HYDROGEN FLUORIDE

T, °K.	Vapor pressure, mm. Equation 1	Vapor pressure, mm. Equation 2	Vapor density, g./l.	Association factor, $Z^v_{sat.}$	ΔH,[a] cal./20 g.	$Z^v_{sat.}\Delta H$, cal./mole vapor
193.16	5.55	4.84	....	...	..	..
198.16	7.61	6.92	....	...	..	..
223.16	34.82	33.52	....	...	..	..
248.16	123.7	122.5	....	...	..	..
273.16	363.8	363.8	2.015	4.717	1257	5929
278.16	443.0	443.2	2.251	4.407	1354	5967
283.16	536.2	536.7	2.521	4.148	1445	5994
288.16	645.6	646.3	2.826	3.929	1532	6019
293.16	773.2	774.1	3.170	3.743	1616	6049
298.16	921.4	922.5	3.553	3.580	1698	6079
303.16	1093	1094	3.979	3.438	1777	6109
308.16	1290	1291	4.454	3.315	1852	6139
313.16	1516	1517	4.976	3.203	1925	6168
318.16	1776	1775	5.554	3.104	1995	6193
323.16	2069	2069	6.192	3.015	2063	6220
328.16	2403	2401	6.885	2.934	2130	6249
333.16	2778	2777	7.645	2.861	2194	6277
338.16	3201	3199	8.482	2.795	2253	6297
343.16	3677	3674	9.390	2.734	2312	6321
348.16	4208	4205	10.37	2.677	2371	6347
353.16	4801	4797	11.44	2.625	2427	6371
358.16	5460	5457	12.59	2.577	2481	6394
363.16	6191	6189	13.85	2.534	2530	6411
368.16	6999	6999	15.20	2.492	2581	6432
373.16	7891	7894	16.64	2.453	2631	6454
378.16	8872	8880	18.20	2.417	2678	6473

[a] $\Delta H = (H^v - H^l) = T\,(V^v - V^l)\,(dP/dT)$

pressure data were fitted, by methods of least squares, to two normal vapor pressure equations 1 and 2, on the chance that one would yield a better fit than the other. This did not prove to be the case since the variance of data in each equation was about 23,000, equivalent to a precision of ±28 mm. for the 31 measurements made with the Bourdon gage. Either of these equations agrees well with that of Simons[7] in the temperature region −25 to +50°. Above the latter temperature measured pressures show increasingly larger deviations from those calculated from Simons' equation.

The normal boiling point calculated from equation 1 is 19.51 ± 0.05°, as compared to 19.6° given by Simons,[7] 19.9° by Claussen and Hildebrand,[8] 19.4° by Simons and Bouknight,[9] and 19.56° by Fredenhagen.[10] It should be noted that while the normal value of constant C in equation 1 is less than 273.16°K., in this case it is greater, being 335.52°K.

Heat of Vaporization.—Simons and Russell,[11] along with many earlier and later investigators, have considered hydrogen fluoride, liquid and vapor, to be composed of a series of polymers $(HF)_i$, where i is 1, 2, 3,..., m. These authors[11] have stated, however, that obviously it would be incorrect to assume that the liquid is composed of the same species and in the same proportions as the vapor. Whether this statement be correct or not cannot be proved from experimental data now available, at least if the reference vapor is saturated. If such a statement is accepted then the term "heat of vaporization" has a meaning only when expressed on a weight basis; more specifically, the "heat of vaporization per mole" has no meaning. Because of this, heats of vaporization presented in this paper are on a weight basis, the formula weight having been chosen as a convenient one. Heats of vaporization listed in Table I are based on equation 2 (for dP/dT); vapor volumes, of 20.01 g., obtained in this work (for V^v); liquid volumes (V^l) for 20.01 g. reported by Simons[12]; and the rearranged

$$\Delta H_{vap} = (H^v - H^l) = T\,(V^v - V^l)\,(dP/dT) \quad (3)$$

Clapeyron equation 3. H^v and H^l are the enthalpies of formation of 1 formula weight of saturated vapor and liquid, respectively. To provide a ready comparison of data of this work, ΔH_{vap} has been multiplied by $Z^v_{sat.}$ (the saturated vapor association factor) and listed in Table I. This quantity ($Z^v_{sat.}\Delta H_{vap}$) is the heat necessary to vaporize enough liquid to produce one mole of saturated vapor. At the normal boiling point of 19.51°, $Z^v_{sat.}\Delta H_{vap}$ = 6050 cal./75.2 g.; values reported in the literature are essentially the same as this, one[12] being 6025 cal./g. mole of vapor. Calorimetric values reported by Fredenhagen[10] provide an additional comparison of the heat of

(7) J. Simons, *J. Am. Chem. Soc.*, **46**, 2179 (1924).
(8) W. H. Claussen and J. H. Hildebrand, *ibid.*, **56**, 1820 (1934).
(9) J. Simons and W. K. Bouknight, *ibid.*, **54**, 129 (1932).
(10) K. Fredenhagen, *Z. anorg. allgem. Chem.*, **210**, 210 (1933).
(11) J. H. Simons and A. S. Russell, THIS JOURNAL, **43**, 901 (1939).
(12) J. H. Simons, "Fluorine Chemistry," Vol. 1, Academic Press, Inc., New York, N. Y., 1950, p. 228.

vaporization. Specific values so reported are 1704, 1751 and 1780 cal./20 g. at temperatures of 4.40, 17.56 and 19.54°. From data of Table I values at these same temperatures are 1342, 1575 and 1608 cal./20 g. These values are somewhat lower than those of Fredenhagen because of one or both of the following possibilities: (1) values from the present work, below 23°, are dependent on extrapolation of vapor volumes; (2) Fredenhagen's values may contain small contributions from the heat of dissociation.

Saturated Vapor Association.—Association factors listed in Table I are equal to the average molecular weight divided by 20.01. Molecular weights were calculated from vapor density measurements on the assumption that ideal gas laws apply to the mixture of polymers that must be present. Data were fitted to two equations for correlation purposes. These are given below with constants determined by least mean square procedures. Equation 4 summarizes the mathematics that result from a model[13] of equilibrium between $(HF)_1$ and $(HF)_6$ and has been used to indicate a comparison between the present work and that of Long, Hildebrand and Morrell.[14] This comparison is shown in Fig. 2 in which the quantity $-\log K$ is plotted against reciprocal temperature.

$$\log\left\{\left(\frac{5}{P_{mm}}\right)^5\frac{(Z^v_{sat.}-1)}{(6-Z^v_{sat.})^6}\right\} = -42.38089 + \frac{8660.4}{T} \quad (4)$$

$$\log\left\{1-\frac{1}{Z^v_{sat.}}\right\} = -0.56577 + \frac{126.28}{T} \quad (5)$$

$$K = \left(\frac{5}{P_{mm}}\right)^5\frac{(Z^v-1)}{(6-Z^v)^6} \quad (6)$$

In the present paper Z^v of this equation is at the saturated vapor pressure, while data of Long, Hildebrand and Morrell were taken at less than 70% of saturation. Experimental data show very little deviation from the straight line of Fig. 2.

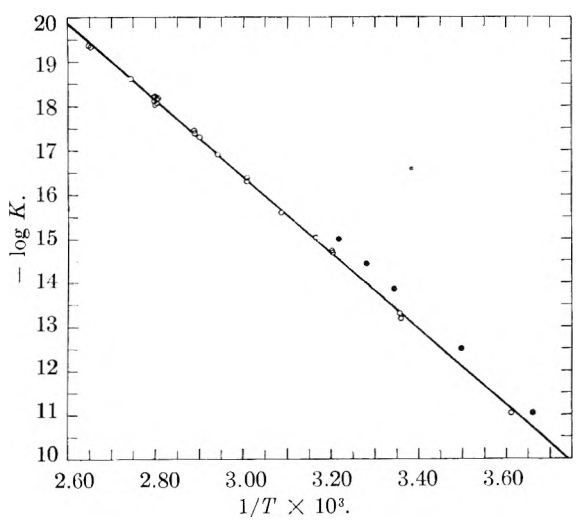

Fig. 2.—Equilibrium constant using monomer–hexamer model: ●, Long, Hildebrand and Morrell[14]; ○, this research.

(13) J. Simons and J. H. Hildebrand, *J. Am. Chem. Soc.*, **46**, 2183 (1924).

(14) R. W. Long, J. H. Hildebrand and W. E. Morrell, *ibid.*, **65**, 182 (1943).

Constants for the linear equation 4 given by Long, Hildebrand and Morrell[14] are −43.65 and 8910°K. as compared with −42.38089 and 8660.4°K. of the present work.

Association data also have been summarized in Fig. 3 in which the quantities $\log\{1-(1/Z^v_{sat.})\}$ have been plotted against reciprocal temperature. With this type of correlation, scatter in the experimental values of $Z^v_{sat.}$ is more realistically shown than is apparent in Fig. 2. Within experimental error the data points in Fig. 3 are best fitted by the linear relation of equation 5, over the temperature range 24 to 105°.

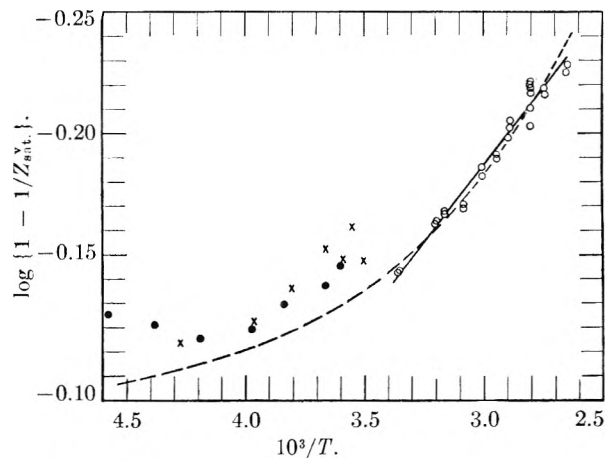

Fig. 3.—Summary of effect of temperature in the function $\log\{1-1/Z^v_{sat.}\}$: ×, Simons and Hildebrand[13]; ●, Fredenhagen[10]; ○, this research.

The function $(1-1/Z^v_{sat.})$ of equation 5 has a definite significance if the saturated vapor is composed only of linear chains. Thus, if we let n^v_1, n^v_2, etc., be the numbers of moles of $(HF)_1$, $(HF)_2$, etc., in 1 formula weight of vapor then the number of polymer bonds n^v_H per formula weight of vapor is

$$\sum_{i=1}^{\infty}(i-1)\,n^v_i = 1-\frac{1}{Z^v_{sat.}} = n^v_H/N \quad (7)$$

where N is Avogadro's number. On this basis Fig. 3 summarizes the effect of temperature on the number of polymer, perhaps "hydrogen," bridges in 20.01 g. of saturated vapor. Oriani and Smyth[15] have found a difference between their values of vapor association factors, determined by dipole moment measurements, and those of Long, Hildebrand and Morrell,[14] which they have interpreted as suggestive of the existence of some symmetrical polymer, *i.e.*, one that has no dipole moment. If this interpretation is correct and if this symmetrical polymer is cyclic, the number of "hydrogen" bridges per formula weight of saturated vapor would not be given by equation 7.

It is interesting to note, however, that if quantities $Z^v_{sat.}$ are calculated by use of equation 4 and these "smoothed" values used to obtain quantities $(1-1/Z^v_{sat.})$, the dashed curve of Fig. 3 is obtained. Although this curve does not fit the data of the present research as well as does the straight line defined by equation 5, it does provide

(15) A. A. Oriani and C. P. Smyth, *ibid.*, **70**, 125 (1948).

a comparison with previous data[10,13] on saturated vapor association factors. Such correlation must be viewed with some caution because it is based on extrapolation of an equation, 4, which markedly tends to minimize differences in data; for example, minor extrapolation of a straight line drawn by Simons and Hildebrand[13] through their data in a plot of molecular weight *versus* temperature (in the range 234 to 289°K.) leads to $Z^{v}_{sat.} = 3.13$ at 20° as compared with a value of 3.74 given in Table I.

It is apparent that extrapolation of either equation 4 or 5 is definitely not justifiable, although equation 4, embodying the monomer–hexamer equilibrium model, does provide a qualitative summary of data obtained by various workers, as is indicated in Figs. 2 and 3.

Acknowledgments.—The authors wish to acknowledge the help of Mr. P. B. Wood in statistical analysis of data, Mr. G. D. Oliver for thermal analysis of samples of hydrogen fluoride and Drs. G. F. Mills and H. A. Smith for many helpful discussions during the course of this work.

POLYMERIZATION OF POLYSILICIC ACID DERIVED FROM 3.3 RATIO SODIUM SILICATE

By R. K. Iler

Contribution from the Grasselli Chemicals Department, Experimental Station, E. I. du Pont de Nemours and Company, Inc.

Received January 22, 1953

Polysilicic acid obtained at *p*H 1.7 by treating with acid sodium silicate having an $SiO_2:Na_2O$ molar ratio of 3.3:1.0, has an initial number-average molecular weight of 200, based on extrapolation of curves relating silica concentration and molecular weight at a fixed sol age, to zero concentration where the polymerization rate must be very slow. This compares favorably with a weight-average molecular weight of 325 found by Debye and Nauman by light scattering, for a sodium silicate solution of this ratio. Further polymerization of this polysilicic acid to higher molecular weight species, at *p*H 1.7, occurs in such a way that (a) the number-average molecular weight increases in proportion to the square root of time, (b) the rate of polymerization is proportional to the square of silica concentration, and (c) the gel point is reached as the extrapolated number-average molecular weight approaches the order of 6,000, regardless of the silica concentration within the range of 2 to 6% SiO_2. This behavior is consistent with the hypothesis that the dense polysilicic acid units, postulated by Debye and Nauman as being present in this type of sodium silicate, combine in some unknown manner to form a three-dimensional network structure. This network becomes infinite at the gel point, even before all units have joined the structure, thus explaining the relatively low number-average molecular weight at the gel point. The strength of the gel network appears to increase with silica concentration, suggesting that the strength of the network increases as the network becomes more compact.

As pointed out by Vail,[1] a large amount of work had been done to determine the mechanism of the aggregation of silica in sols, its transition into solid hydrated gels, and the chemical nature of the silica–water system. It was first shown by Mylius and Groschuff[2] that silicic acid of low molecular weight was obtained by neutralizing a solution of sodium silicate with acid. Subsequently, Willstätter and Kraut[3] found that monosilicic acid could be prepared by adding sodium metasilicate to a solution of acid in such proportion to give a final *p*H of 3.2 at which the monomer is most stable. Since Debye and Nauman[4–6] have shown by light scattering studies that in a highly purified solution of sodium metasilicate there is essentially no aggregation of silicate ions, it appears that the method of Willstätter and Kraut makes possible the conversion of sodium silicate directly to silicic acid in a state of aggregation corresponding to that in the original alkaline silicate solution. Debye and Nauman[6] further have shown that in a solution of sodium silicate of higher SiO_2/Na_2O ratio, the silica is in a higher state of polymerization; in a solution having a molar ratio of SiO_2/Na_2O of 3.3:1.0, a molecular weight of the order of 325 was found.

It is therefore of interest to report the molecular weight of polysilicic acid prepared from 3.3 ratio silicate, as measured by the freezing point method, and also to describe some of the observations which have been made in regard to factors affecting its polymerization.

Experimental

Preparation of Silicic Acid.—In order to form silicic acid from the sodium silicate with as little polymerization as possible, the method described by Iler and Pinkney[7] was employed; Grasselli No. 20 WW grade sodium silicate (28.4% SiO_2, 8.75% Na_2O) and Grasselli C.P. hydrochloric acid were the materials used. The resulting solution, containing 6.34% SiO_2, having a *p*H of 1.7, was stored at 25°.

Molecular Weight by Freezing Point.—The number-average molecular weight of the silicic acid was followed as the solution was aged, using a conventional freezing point apparatus with a Beckmann thermometer. Considerable difficulty was encountered due to supercooling. Instead of following the customary procedure of cooling the sample until it began to freeze and then noting the freezing point, it was found necessary to supercool the sol several degrees by immersing it in a bath at −5° and stirring it vigorously until ice crystals suddenly formed. The container was then placed in the freezing point apparatus which was at 0°; under these conditions the temperature increased slowly at a constant rate, under uniform conditions of agitation, until the last trace of ice disappeared, then increased more rapidly. By plotting the time-temperature curve and extrapolating the two straight portions of the curves to a point of intersection, the freezing point was determined.

(1) J. G. Vail, "Soluble Silicates," Vol. 1, Reinhold Publ. Corp., New York, N. Y., 1952, p. 173.

(2) F. Mylius and E. Groschuff, *Ber.*, **39**, 116 (1906).

(3) R. Willstätter and H. Kraut, *ibid.*, **64B**, 1709 (1931).

(4) P. Debye, This Journal, **53**, 1 (1949).

(5) P. Debye and R. Nauman, *J. Chem. Phys.*, **17**, 664 (1948).

(6) P. J. Debye and R. V. Nauman, This Journal, **55**, 1 (1951).

(7) R. K. Iler and P. S. Pinkney, *Ind. Eng. Chem.*, **39**, 1379 (1947).

In order to calculate the depression of the freezing point due to the silicic acid, it was necessary to determine the freezing point of the same solution after the silicic acid had polymerized until no silica remained in solution. The following procedure was adopted: A sample of the sol was sealed in a Pyrex tube and heated at 100° for 24 hours; this polymerizes and gels the silicic acid. The tube was then enclosed in a still larger tube and frozen by placing it in Dry Ice for 24 hours; freezing invariably cracks the sealed container. The frozen sample was then permitted to melt, forming a slush of finely divided silica upon which the freezing point was then run. After filtering off the precipitate, it was found that less than 0.02% SiO_2 remained in solution.

The number average molecular weight was calculated from the formula

$$M = \frac{1000Kg}{G(\Delta T)}$$

where

M = molecular weight of silicic acid
g = weight of SiO_2
G = weight of solute
ΔT = depression of f.p. due to silicic acid
K = molal freezing point constant

It was assumed that $K = 1.86$, although it is realized that the value of this constant for the solvent which was a dilute solution of a salt, might differ slightly from that of pure water; *e.g.*, for a solution containing 6.34% SiO_2, 3.74% NaCl and 0.06% HCl and 89.86% H_2O

$$N = \frac{1000(1.86)(6.34)}{(60)(89.86)(\Delta T)} = \frac{2.18}{(\Delta T)}$$

where

N = the degree of polymerization, which is the number of SiO_2 units per molecule of polysilicic acid, based on the number-average molecular weight

Titration Procedure for Following Changes in Molecular Weight.—In order to follow changes in molecular weight more conveniently, an empirical titration procedure previously described by Iler and Pinkney[7] was employed. In this procedure the amount of a hydrogen-bonding agent, carbide and carbon diethyl "Carbitol" solvent, required to prevent precipitation of the polysilicic acid by gelation under specified conditions, gives an empirical figure, the "X-value," which has been correlated with the number-average molecular weight as determined by the freezing point method. As the solution of silicic acid polymerized, samples were taken for simultaneous determination of the "X-value," and of the molecular weight by the cryoscopic method. The results on two separately prepared and aged sols are given in Table I. The linear relationship between the "X-value" and the square root of N, is shown in Fig. 1. (No explanation for this relationship can be offered at present.)

In a separate experiment, the increase in molecular weight of a solution of silicic acid was followed carefully over a 50-hour period, by the titration procedure. As shown in Fig. 2, the number-average molecular weight appears to increase

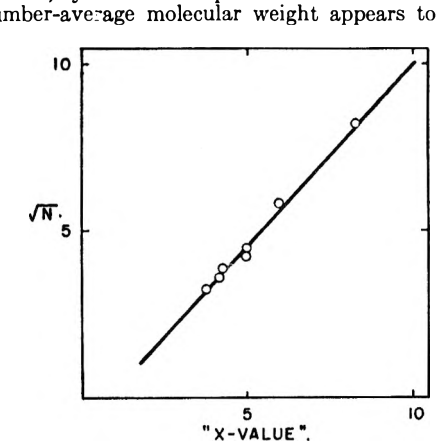

Fig. 1.—Relationship between X-value and degree of polymerization (N).

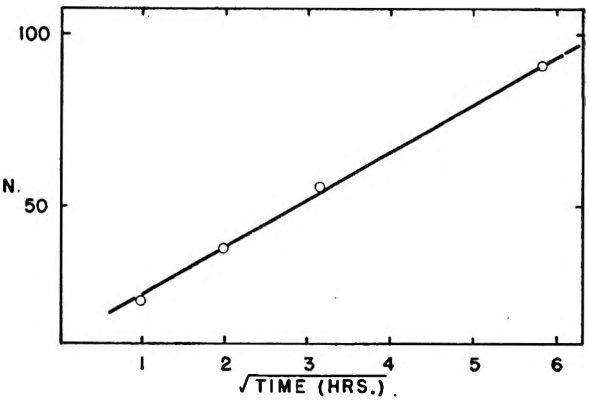

Fig. 2.—Degree of polymerization (N) *versus* square root of time; *p*H 1.7; temp., 25°; SiO_2, 6.25%.

TABLE I

SILICIC ACID SOLUTION: SiO_2, 6.34%; *p*H 1.7; TEMP., 25°

Age, hours	Beckmann f.p.	ΔT	N	"X-Value"
	Sol 1			
0.5	2.937	0.206	10.6	3.8
2.0	2.985	.168	13.0	4.2
2.75	2.991	.153	14.3	4.3
6.0	3.022	.121	18.1	5.0
31.0	3.110	.033	66.0	8.3
Heated 100°, 24 hr. and frozen	3.143			
	Sol 2			
0.1	2.984	0.211	10.4	3.8
3.25	3.084	.110	19.9	5.1
10.5	3.130	.065	33.6	6.0
Heated 100°, 24 hr. and frozen	3.195			

with the square-root of time. However, from this particular curve it is not possible to extrapolate accurately back to zero-time and thus to estimate the initial molecular weight of the silicic acid.

Factors Affecting the Rate of Polymerization.—Using the titration method, the changes in molecular weight of silicic acid were followed under a variety of conditions.

(a) **Effect of *p*H.**—It was of interest to determine whether the effect of *p*H on the rate of polymerization was the same when determined by the titration method, as when determined by observation of the time required for the sol to gel. As previously reported,[8] the time required for a sol made with H_2SO_4 to gel, reaches a maximum at about *p*H 1.5. Using the titration procedure, the time required for the silicic acid solution to reach an arbitrarily selected X-value corresponding to $N = 28$, was observed over a range of *p*H values, as shown in Fig. 3.

A maximum time required, corresponding to a minimum rate of polymerization, was observed at *p*H 1.7. It is concluded that the effect of *p*H on the rate of polymerization, as determined by the titration procedure, parallels the rate of gelling and that the two phenomena are closely related, if not identical.

(b) **Effect of Silica Concentration.**—In another series of experiments, aliquots of the silicic acid solution, freshly prepared in accordance with the standardized procedure, were diluted to 4, 3 and 2% SiO_2. The titration method was then employed to follow the "X-value," plotting curves of this value *vs.* time, from which the "X-values" at 1, 4 and 16 hours were then interpolated and plotted *vs.* silica concentration, giving a linear relationship, as shown in Fig. 4.

Three significant observations were made in this series of experiments:

(i) Regardless of the silica concentration, the silicic acid

(8) R. K. Iler, THIS JOURNAL, **56**, 678 (1952).

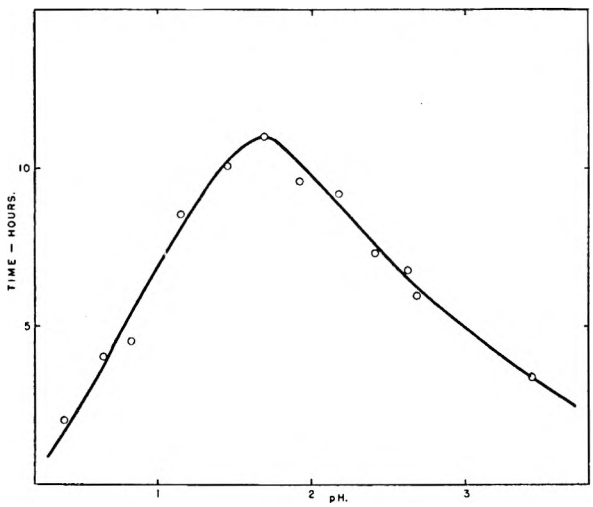

Fig. 3.—Effect of pH on time required for silicic acid to polymerize to a number-average of 28 silicon atoms per molecule; SiO_2 concn., 1.0 M; temp., 25°.

solution gelled when the "X-value" reached about 10, corresponding to a number-average molecular weight of the order of 6000. At the gel point, the 6% gel was hard and brittle, whereas the more dilute solutions gave gels which were increasingly soft, the 2% gel being extremely soft and weak. Nevertheless, in all cases the gel point was readily observable, and there is little doubt that the gel point corresponded to the same degree of polymerization, regardless of concentration.

(ii) The rate of polymerization per unit amount of silica (inverse of the time) was approximately proportional to the square of the silica concentration. Thus, as shown in Fig. 4 by the dotted line A, doubling of the silica concentration reduced the required time by a factor of four.

(iii) Perhaps of greatest significance, from the standpoint of the molecular weight of the original sodium silicate, is the fact that extrapolations to zero silica concentration, where polymerization would be very slow, give an "X-value" of about 2.5. This must represent the molecular weight of polysilicic acid initially formed from 3.3 ratio sodium silicate. As shown in Fig. 1, this would correspond to $\sqrt{N} = 1.8$, or a degree of polymerization of 3.25, corresponding to a number-average molecular weight of 200 based on SiO_2. This is a reasonable value, in view of Debye and Nauman's[6] figure of 325 for the weight-average molecular weight of the particles in 3.3 ratio sodium silicate.

Changes in Viscosity during Polymerization.—The following viscosity data were obtained on a 6% SiO_2 solution of polysilicic acid at pH 1.7 as polymerization progressed.

"X-Value"	Estimated N	Specific viscosity (H_2O = 1.00)
2.6	4	1.18
2.9	5	1.18
4.1	13	1.18
4.4	15	1.18
4.7	18	1.20
5.3	23	1.22
8.8	72	1.62
9.0	78	4.23

As the "X-Value" exceeded about 9.0, the viscosity increased very rapidly and gelling occurred soon thereafter.

Discussion

Debye and Nauman[6] have shown from viscosity data that in solutions of sodium silicate the ultimate particles must be relatively dense. One might therefore visualize a solution of 3.3 ratio sodium silicate as consisting of a dispersion of dense polysilicate ions containing about 3 SiO_2 units each on a number-average basis, or up to 5 units each

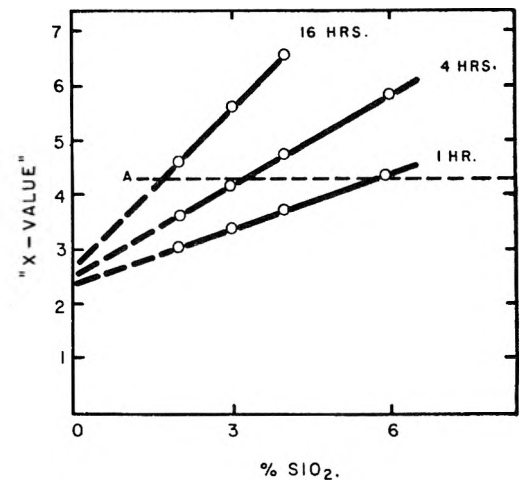

Fig. 4.—Relationship between silica concentration and rate of polymerization.

on a weight-average basis. The corresponding polysilicic acid may be a polymer such as the cyclic trimer $Si_3O_3(OH)_6$, or $(SiO_2 \cdot H_2O)_3$.

It is of interest to note that the viscosity of the freshly prepared polysilicic acid is of the order that would be predicted for a 6% suspension of $(SiO_2 \cdot H_2O)_3$ in a solution of sodium sulfate. The viscosity of a silica-free solution of sodium sulfate at a concentration equivalent to that in the sol (0.3 M), relative to water, is 1.062. The dispersion of 6% by weight of SiO_2 plus 1.8 g. of chemically bound water corresponds to a volume fraction of about 0.05, assuming normal densities for amorphous SiO_2 and water. The viscosity of this suspension relative to the sodium sulfate solution can be estimated from the Einstein equation

$$\text{Relative viscosity} = 1 + 2.5c$$

where c is the volume fraction of dispersed phase. Then the viscosity of the solution of polysilicic acid, relative to the sodium sulfate solution, would be 1.125 and the viscosity, relative to water, would be 1.125 × 1.062, or 1.19. This is close to the observed value of 1.18.

The following mechanism of polymerization of polysilicic acid was postulated in 1925 by Vail[9]:

"If we assume that these phenomena are the result of a tendency on the part of very small particles of colloidal silica to gather together into clusters or masses until they become large enough and sufficiently immobile to produce first a viscous liquid and then a solid gel structure, we shall have a concept which.....fits in with a large number of observed facts."

The observations herein reported are consistent with Vail's picture of gel formation, but give a further insight into the progressive formation of the gel network. This network probably extends through the medium and forms a rigid structure before all the polysilicic acid units become attached. These unattached units may explain the relatively low number-average degree of polymerization observed at the gel point, even though the weight-average molecular weight must be infinite.

(9) James G. Vail, *J. Soc. Chem. Ind.*, **44**, T 214 (1925).

The linking together of the dense polysilicic acid units must occur in about the same way, whether this occurs in dilute or in concentrated sols, since the same degree of polymerization is reached in each case at the gel point. However, the gel formed in the more concentrated solution appears to have a more compact, stronger network structure.

THE VAPOR PRESSURE OF ACETYLATED AMINO ACID ETHYL ESTERS[1]

By Edward F. Mellon, Samuel J. Viola and Sam R. Hoover

Eastern Regional Research Laboratory,[2] Philadelphia 18, Pa.

Received February 6, 1953

A semimicro ebulliometer was used in conjunction with a manostat and mercury Zimmerli gage to determine the vapor pressure–temperature curves of a number of acetylated amino acid ethyl esters over the pressure range of 2 to 90 mm. The amino acids whose derivatives have been studied are glycine, alanine, valine, leucine, isoleucine, phenylalanine, methionine, tyrosine, aspartic acid and pyrrolidonecarboxylic acid.

Although most of the acetylated amino acid ethyl esters have been prepared and distilled, the amount of information available on their boiling points and vapor pressures is very limited. Usually only the boiling points found during their preparation are available and these may be expressed as a range of temperature at a pressure known only to one significant figure. The best collection of such data has been reported by Cherbuliez and Plattner[3] who made boiling point readings at one or two pressures for eleven of the compounds.

More accurate vapor pressure data over a wider range of pressure were desired to study the possibilities of separating these compounds by distillation techniques. The vapor pressure–temperature curves over the range of 2 to 90 mm. pressure were, therefore, determined on purified materials using a regulated pressure system and a semimicro ebulliometer.

Experimental

The acetylated amino acid ethyl esters were prepared by various standard methods of acetylation and esterification of the amino acids and their derivatives. The nitrogen analysis[4] of each derivative agreed with the theoretical value.

Since the preparation of the N-acetylmethionine ethyl ester has not been described previously, the details of its synthesis are as follows: Methionine was esterified with alcoholic hydrogen chloride. The ester hydrochloride crystals were mixed with an equal weight of fused sodium acetate and double their weight of acetic anhydride, and heated on a steam-bath for one hour. The reaction mixture was extracted with chloroform. The extract was evaporated *in vacuo* and the residue was Claisen distilled at 1.3 mm. and 163–164°.

Anal. Calcd. for $C_9H_{17}O_3NS$: C, 49.3; H, 7.8; N, 6.4; S, 14.6. Found: C, 49.6; H, 7.6; N, 6.4; S, 14.8.

The vapor pressure measurements were made in the semimicro ebulliometer of Hoover, John and Mellon.[5] Pressure was regulated by means of a Ratchford and Fein manostat[6] and measured with a mercury Zimmerli gage.[7] A series of determinations at increasing pressures was made for each compound. A 10–15 minute period of refluxing was used to assure stable pressure and temperature readings for each point. The thermometer was calibrated in the apparatus by determining the boiling points at atmospheric pressure of pure compounds which are accepted standards for thermometer calibration. The temperatures reported are, therefore, corrected temperatures.

Results

The numerous vapor pressure measurements obtained have been consolidated by calculating, according to the least squares method, the equations for the straight lines obtained by plotting the log of the vapor pressure against the reciprocal of the absolute temperature. The relationship of the lines for the various *n*-acetylated amino acid ethyl esters is shown in Fig. 1. The experimental points are shown on the alanine and methionine curves to give a visible representation of the closeness of the fit of the calculated line. The constants, A and B, for the equation of these lines, $\log P = A - B/T$, are given in Table I. The pressure is in mm. and the temperature, T, is in degrees Kelvin. The standard error of the estimate, $S_p = \sqrt{\Sigma d^2/n}$, is given in the third column of figures. From S_p

Table I

Constants for Vapor Pressure Equations for N$^{\alpha}$-Acetylamino Acid Ethyl Esters

Amino acid	A	B	S_p	70% limit, %	Points
Glycine	9.7488	3627	0.0090	2.4	11
DL-Alanine	9.3647	3408	.0140	3.5	9
DL-Valine	9.5313	3535	.0125	3.2	8
DL-Methionine	10.1663	4264	.0053	1.4	10
L-Leucine	10.1594	3906	.0092	2.4	16
L-Isoleucine	9.5376	3610	.0054	1.4	17
DL-Phenylalanine	10.1199	4306	.0023	0.8	6
L-Aspartic acid	9.7816	3970	.0139	3.8	6
L-Glutamic acid	8.9254	3509	.0087	2.5	6
DL-Pyrrolidone-2-carboxylic acid[a]	9.4941	3849	0106	2.7	9

[a] The pyrolidone-2-carboxylic acid was esterified but not acetylated.

(1) This paper is part of a talk presented before the Meeting-in-Miniature of the Philadelphia Section of the American Chemical Society, January 29, 1953. Article not copyrighted.

(2) One of the laboratories of the Bureau of Agricultural and Industrial Chemistry, Agricultural Research Administration, U. S. Department of Agriculture.

(3) E. Cherbuliez and Pl. Plattner, *Helv. Chim. Acta*, **12**, 317 (1929).

(4) The authors are indebted to Dr. C. L. Ogg for the analysis of the compounds.

(5) S. R. Hoover, H. John and E. F. Mellon, *Anal. Chem.*, in press.

(6) W. P. Ratchford and M. L. Fein, *ibid.*, **22**, 838 (1950).

(7) A. Zimmerli, *Ind. Eng. Chem., Anal. Ed.*, **10**, 283 (1938).

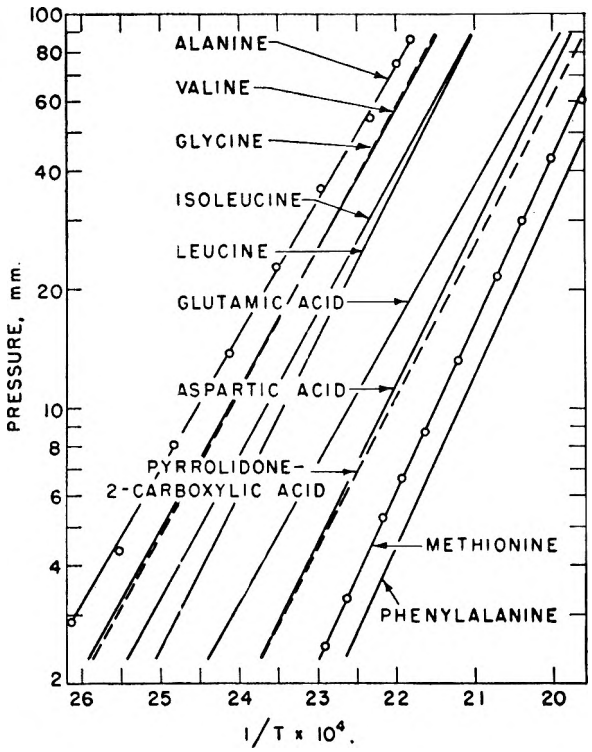

Fig. 1.—Vapor pressure-temperature relationships for the acetylated amino acid ethyl esters.

one can calculate the limits within which a certain percentage of the experimental points will agree with the values given by the curve. This limit calculated to include 70% of the experimental points is reported in column 4 as a percentage of the pressure value represented by the corresponding point on the curve. The average for this limit over all the data is about 2.5%. The number of observations on which each curve is based is given in column 5. The fewer number of points used for the aspartic and glutamic acid calculations was a reflection of their tendency to decompose slowly at elevated temperatures. An independent determination of six points on a second sample of the glutamic acid derivative gave the same curve as the original sample used.

A sample of N-acetyltyrosine ethyl ester melting at 80° was boiled in the micro-ebulliometer at 2.3 mm. and a temperature of 244.4°. There was no decomposition but only one point was obtained because the maximum temperature limit of the apparatus had been reached.

The data obtained from our experiments do not agree very closely with the corresponding points obtained by Cherbuliez and Plattner[3] but the differences are what might be expected between boiling points obtained during a Claisen distillation during preparation and the equilibrium boiling points of previously distilled material obtained in an ebulliometer. The acetylated methionine ethyl ester reported on here also shows a difference in boiling point between the first purification distillation and the equilibrium value.

One of the more important observations was that of the lowered vapor pressure of the glycine derivative. Instead of being the most volatile of the derivatives because of its lower molecular weight and simplest structure, it has a vapor pressure which is very close to that of the valine derivative which is the third member of the homologous series; and considerably less than the vapor pressure of the alanine derivative which is the second member of the series.

A similar inversion phenomenon appears with the aspartic and glutamic acid derivatives. The lower molecular weight homolog—the aspartic acid derivative—actually has a lower vapor pressure than the higher homolog—the glutamic acid derivative. The pyrrolidonecarboxylic acid ethyl ester which can be formed by heating the acetylated diethyl glutamate also shows a vapor pressure which is lower than the glutamic acid derivative.

These differences are also reflected in the heats of vaporization which can easily be calculated as calories per mole by multiplying the slope constant "B" by the factor $2.3R = 4.577$. They can, therefore, probably be attributed to differences in the polar binding forces between the individual molecules with the molecules of the glycine and aspartic acid derivatives being held to each other more strongly than the molecules of the alanine and glutamic acid derivatives are held to each other. This effect of interaction between molecules is shown clearly with the leucine and isoleucine derivatives. These two compounds differ only in the location of a branching methyl group on the amino acid side chain. This methyl group on the beta carbon as in isoleucine, interferes with the polar activities of the amino group on the alpha carbon and gives this compound a lower heat of vaporization than when the methyl group is on the gamma carbon as in leucine.

The vapor pressure curves show that with only a few exceptions the vapor pressures of these acetylated amino acid ethyl esters are sufficiently different from each other to make possible their separation by distillation in an efficient fractionating column. The pressure best suited for a particular separation can also be predicted from the curves. One noteworthy separation—the separation of the leucine derivative from the isoleucine derivative—has been shown to occur very sharply at several millimeters pressure but no separation should be expected at 100 mm. pressure. This separation and the separation of other mixtures of these acetylated amino acid esters will be described in a subsequent publication.

PAMPHLETS

Available for distribution from the office of
CHEMICAL ABSTRACTS

New Titles

ACS COMMITTEE REPORTS

Arene and Arylene ..... Free

Halogenated Derivatives of Hydrocarbons ..... 10¢

The Use of "Per" in Naming Halogenated Organic Compounds ... 10¢

The Use of "H" to Designate the Positions of Hydrogens in Almost Completely Fluorinated Organic Compounds ..... 10¢

Organic Compounds Containing Phosphorus ..... 25¢

Organosilicon Compounds Revised (1952) ..... 10¢

Nomenclature of Natural Amino Acids and Related Substances ... 25¢

Avogram. An ACS committee report ..... Free

The Naming of Geometric Isomers of Polyalkyl Monocycloalkanes. An ACS committee report ..... Free

Commission de Nomenclature de Chimie Inorganique. This relates to the names of the elements Beryllium, Aluminum, Niobium, Technetium, Promethium, Lutetium, Hafnium, Tungsten, Astatine, Francium, Protactinium, Neptunium, Plutonium, Americium, and Curium. In English ..... .10

Commission de Nomenclature de Chimie Biologique. Includes Rules for the Nomenclature of Natural Amino Acids and Related Substances (in English) and Nomenclature de Vitamines (in French) ..... .10

Commission de Nomenclature de Chimie Organique. This includes: Nomenclature of Organosilicon Compounds, Changes and Additions to the Definitive Report, Extended Examples of Radical Names, and List of Radical Names. All in English ..... .50

Definitive Report of the Commission on the Reform of the Nomenclature of Organic Chemistry. Translation with comment and index by Austin M. Patterson ..... .20

Rules for Naming Inorganic Compounds. Report of the Committee of the International Union of Chemistry for the Reform of Inorganic Chemical Nomenclature, 1940. The committee has provided an American version of the rules. .20

The Pronunciation of Chemical Words. An ACS Nomenclature Committee Report ..... .05

Directions for Assistant Editors and Abstractors of Chemical Abstracts. Much concentrated information on chemical nomenclature, symbols, forms, and abbreviations is assembled in this booklet in form convenient for use ..... .25

The Naming and Indexing of Chemical Compounds by Chemical Abstracts. Introduction to the 1945 Subject Index .... .75

Carbohydrate Nomenclature. A report of the Committee on Nomenclature, Spelling and Pronunciation ..... .10

Nomenclature of the Hydrogen Isotopes and Their Compounds. A committee report ..... Free

The Standardization of Chemical Nomenclature. This reprint of an article by the committee chairman contains a list of references to sources of information on chemical literature. Free

The Nomenclature of the Carotenoid Pigments. A report of the Committee on Biochemical Nomenclature of the National Research Council, accepted by the Nomenclature, Spelling, and Pronunciation Committee of the American Chemical Society ..... Free

The Naming of Cis and Trans Isomers of Hydrocarbons Containing Olefin Double Bonds ..... Free

The Designation of "Extra" Hydrogen in Naming Cyclic Compounds. An ACS committee report ..... Free

Address all orders to

CHEMICAL ABSTRACTS

Ohio State University, Columbus 10, Ohio

"75 EVENTFUL YEARS"

By CHARLES ALBERT BROWNE
and MARY ELVIRA WEEKS

A History of the
AMERICAN CHEMICAL SOCIETY

526 pages . . . cloth bound illustrated with portraits. Price, $5.00. Order from: American Chemical Society 1155 Sixteenth St., N.W. Washington 6, D. C.

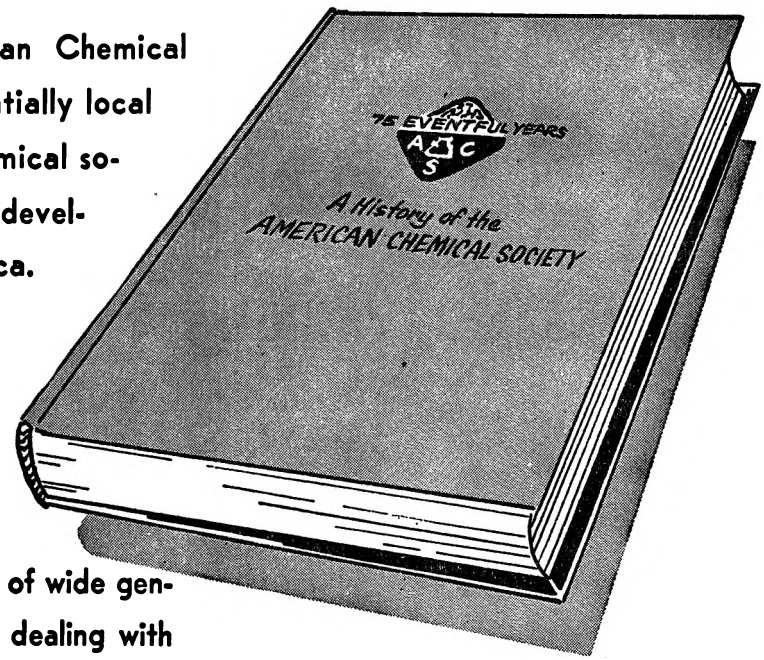

The evolution of the American Chemical Society from a small and essentially local organization to the largest chemical society in the world parallels the development of chemistry in America. Therefore the record of events described in this book is of value to all concerned with the science, the profession and the industry.

Topics treated in detail which are of wide general interest include the chapters dealing with the beginning and subsequent development of industrial chemistry as exemplified by the stories of the ACS Divisions: the activities of the Society in both World Wars, treating of the increasingly important role of the scientist in wartime: the account of the outstanding contributions of the Society toward better standards of training and the campaigns for professional recognition.

The student of ACS history also will be interested in the accounts of the various reorganizations, in the story of the granting of the Federal Charter and in the growth of the publications. A detailed chronology provides a compact record of the notable events of the 75 eventful years.

CONTENTS

xi